Resource Allocation Schemes for Multiuser Wireless Communication Systems Powered by Renewable Energy Sources

by

Dan Zhao

Doctor of Philosophy

School of Electronic Engineering and Computer Science
Queen Mary University of London
United Kingdom

September 2015

Abstract

In the future cyber-physical systems, such as smart grids, a large amount of sensors will be distributively deployed in different locations throughout the systems for the purpose of monitoring and control. Conventionally, sensors are powered by fixed energy supplies, e.g., regular batteries, which can provide stable energy output. However, such energy sources require periodical recharging or replacement, which incurs high maintenance cost and may become impractical in hazardous environments. Self-sustaining devices powered by energy harvesting (EH) sources are thus highly desirable. However, energy provided by energy harvesters is fluctuating over time and thus introduces the EH constraints to the systems, i.e., the total energy consumed until an arbitrary time cannot be larger than the harvested amount up to this time, which invokes the need of advanced power control and scheduling schemes. This thesis studies both the offline and online resource allocation strategies for wireless communication systems empowered by EH sources.

First, the resource allocation problems for a Gaussian multiple access channel (MAC), where the two transmitters are powered by a shared energy harvester, are studied. For both infinite and finite battery capacity cases, the optimal offline resource allocation schemes for maximising the weighted sum throughput over a finite time horizon are derived. It is proved that there exists a capping rate for the user with stronger channel gain. Moreover, the duality property between the MAC with a shared energy harvester and its dual broadcast channel powered is demonstrated. Numerical results are presented to compare the performance of several online schemes. Moreover, the utility of a greedy scheme against the optimal offline one is measured by using competitive analysis technique, where the competitive ratios of the online greedy scheme, i.e., the maximum ratios between the profits obtained by the offline and online schemes over arbitrary energy arrival profiles, are derived.

Then, the resource allocation schemes for the Gaussian MAC with conferencing links, where the two transmitters could talk to each other via some wired rate-limited channels and share a common EH source, are studied. The optimal offline resource allocations are developed for both infinite and finite battery cases. It is shown that the optimal resource allocation in this scenario is more complicated than in the traditional MAC scenario and there exists a capping rate at one of the two transmitters, depending on the weighting factors. Online resource allocation strategies are also examined. Numerical results are used to illustrate the performance comparison of the online schemes. Furthermore, the competitive ratios of the online greedy scheme are derived under different weighting factors.

Acknowledgments

First and foremost, I would like to express my great gratitude to my supervisor Dr Yue Chen. I appreciate her priceless guidance and advices throughout these years. Without her help and support this thesis would not have been possible. Her enthusiasm towards research and life is motivational and contagious for me. I would also like to thank her for the excellent role model she has provided as a successful woman in both career and life.

I would also like to take this opportunity to thank my parents and my boyfriend. They gave me enormous support and courage during my Ph.d. stage. They are always there for me and have always been my strength especially during hardships. 8

I would like to express my special thanks to Prof. Shuguang Cui (Texas A&M University) for inviting me to visit his lab in 2013. I would also like to thank Dr. Chuan Huang (The University of Electronic Science and Technology of China) for his suggestions and advices for my work on both technical development and writing skills.

I would like to thank Prof. Zhiguo Ding (Lancaster University) and Prof. Arumugam Nallanathan (King's College London) for serving as my Ph.D examiners.

I would also like to thank my colleagues and friends, who made my time in London more enjoyable. I treasure every moment I spent with them and I wish all of them the best of luck in the future.

At last, I would like to thank China Scholarship Council (CSC) for their financial supports during my Ph.d. stage.

Table of Contents

List of Figures

List of Abbreviations

AWGN	**A**dditive **W**hite-**G**aussian-**N**oise
BC	**B**roadcast **C**hannel
CSCG	**C**ircularly **S**ymmetric **C**omplex **G**aussian
CSI	**C**hannel **S**tate **I**nformation
DMC	**D**iscrete **M**emoryless **C**hannel
EH	**E**nergy-**H**arvesting
ESI	**E**nergy **S**tate **I**nformation
i.i.d.	**i**ndependently **i**dentically **d**istributed
IoT	**I**nternet **o**f **T**hings
KKT	**K**arush-**K**uhn-**T**ucker
MAC	**M**ultiple **A**ccess **C**hannel
RHS	**R**ight **H**and **S**ide
SNR	**S**ignal-to-**N**oise **R**atio
IEEE	**I**nstitute of **E**lectrical and **E**lectronics **E**ngineers

Chapter 1

Introduction

1.1 Background

In the future cyber-physical systems, such as smart grids, a large amount of sensors will be distributively deployed in different locations throughout the systems for the purpose of monitoring and control. Conventionally, sensors are powered by fixed energy supplies, e.g., regular batteries, which can provide stable energy output. However, such energy sources require periodical recharging or replacement, which incurs high maintenance cost and may become impractical in hazardous environments. Moreover, the energy source for conventional wireless sensor networks consumes non-renewable energy resources, such as coal, petroleum, and natural gas. Estimates from international organisations suggested that if the world's demand for energy from fossil fuels continues at the present rate, oil and gas reserves may run out within some of our lifetimes [ST09, ST08, SS12].

The recent hardware development in energy harvesting devices, i.e., the energy harvesters, makes them viable substitutions to conventional energy supplies. Energy harvesters, such as solar cells, water mills, vibration absorption devices, thermoelectric generator, microbial fuel cells [SET09], can harness and convert the otherwise wasted ambient energy from the environment into usable electrical energy, and thus contributes

to the reduction of the overall carbon footprint. Energy harvesters are envisaged to become one of the important components of future networks, such as smart grids and IoT networks [EKM11, MSPC12, PS05, SK11, Rou03, IGMH05, RAS+00].

1.2 Research Motivation

While EH technique can potentially provide unlimited energy, energy provided by harvesters is intermittent over time due to the uncertain nature of the renewable energy resources, which introduces energy harvesting (EH) constrains to wireless communication systems: at any time during the transmission, the energy used by transmitters for transmission is constrained to be no more than the amount of harvested energy available up to that instance. Moreover, if the batteries for the energy harvesters have limited capacities, then the transmitters should also be able to adjust the transmission power so that the upcoming energy will not overflow the battery (any energy that exceeds battery limit will be lost, which is clearly inefficient). Such unique constraints pose new challenges to wireless communication systems and thus invoke the need of properly designed resource allocation schemes that could adjust transmission power/rate adaptively according to the energy harvesting process to maximise the system throughput.

For resource allocation in EH wireless communication systems, both offline and online schemes have attracted considerable attention in recent years.

1. With non-causal information about the energy arrival times and amounts over the whole transmission period, offline schemes determine the transmission powers/rates before transmissions start. The offline schemes provide the performance upper bound or benchmark for all online schemes and can also be directly applied to scenarios where the output of energy harvesters can be predicted with tolerable errors over a certain period, e.g., when harvesting the vibration energy from a washing/drying machine running on a pre-set program.

2. Online schemes, on the other hand, react upon each energy arrival without knowing the realisations of the future energy arrivals, with at most the statistical information of the EH process. Online schemes can be applied to more general and realistic scenarios where the energy harvesting processes are highly dynamic and thus hard to predict precisely.

Motivated by the aforementioned aspects, in this thesis, both the optimal offline schemes and online schemes for multiuser wireless communication systems are investigated. The optimal offline schemes for the considered scenarios are rigorously derived, based on which some online schemes are proposed. Moreover, since the EH processes vary significantly for different types of EH devices, to more comprehensively examine the performance of online schemes, both the numerical results, which provide the average performance measurement given some hypothesized random distributions of the energy arrival processes, and the competitive analysis [BEY98], which provides the theoretical worst-case performance bounds, are adopted.

1.3 Contributions

The contributions of this thesis are summarised as follows:

- The optimal offline resource allocation schemes for the Gaussian multiple access channel (MAC) with two transmitters powered by a shared energy harvester are developed with the assumption of both infinite and finite battery capacities. Particularly, a slot-based energy-harvesting (EH) model is adopted. To develop the optimal offline resource allocation schemes, which assume that the energy arrival amounts are non-causally known before transmissions, optimisation problems that characterise the maximum departure regions over finite time horizon are formulated. By exploiting the convexity of the problems, both the structural properties of the optimal offline sum power profiles and the optimal resource allocation between the two transmitters are obtained. In particular, it is proved that there exists a

capping rate at the stronger transmitter (the transmitter with the higher channel gain). It is also demonstrated that under the same energy arrival profile, MAC with a shared energy harvester achieves the same maximum departure region as its dual broadcast channel (BC). Based on the optimal offline scheme, three online schemes are proposed. The performances of offline and online schemes are compared by numerical results. Furthermore, competitive analysis is carried out for the online greedy scheme to evaluate how well it performs against the optimal offline scheme under the worst input sequence.

- The resource allocation schemes for the Gaussian MAC with conferencing links and a shared energy harvester are developed where the battery capacity is assumed to be either infinite or finite. Via these wired rate-limited channels, the two transmitters could talk to each other, which helps to enlarge the achievable rate region. Similar to the Gaussian MAC without conferencing links scenario, the goals of the schemes are to maximise the system throughput during the transmission period. Both the optimal offline scheme and online schemes are proposed. The numerical results are used to illustrate the performance of the offline and online schemes. Also, the competitive ratios of the online greedy scheme are derived to further measure the utility of the online scheme against the optimal offline scheme.

1.4 Thesis Outline

The rest of the thesis is organised as follows:

- Chapter 2 provides background information about the theory of channel capacity and the capacity regions for relevant wireless channel models. The basic concepts, definitions and techniques in convex optimisation are introduced. Also, the concept and definitions of online/offline problems and competitive analysis are discussed. Furthermore, literature review of state-of-the-art resource allocation schemes for energy harvesters powered wireless communication systems is presented.

- Chapter 3 presents the optimal offline resource allocation scheme in a two-transmitter Gaussian MAC with a shared renewable source. The system/energy model, problem formulation and the detailed development of the optimal offline scheme are described. Moreover, the duality property between the Gaussian MAC and the Gaussian BC powered by EH sources is presented.

- Chapter 4 investigates online resource allocation schemes for the Gaussian MAC with a shared renewable source. The performance comparison between the optimal offline and the online schemes are carried out by both numerical results and competitive analysis.

- Chapter 5 investigates the optimal offline resource allocation schemes in a two-transmitter Gaussian multiple access channel with conferencing links and a shared renewable resource. Similarly, the system/energy model, problem formulation and the detailed proof of the optimal offline scheme are described.

- Chapter 6 studies online resource allocation schemes for the Gaussian MAC with conferencing links. The numerical results show the performance differences between the optimal offline schemes and the online algorithms. The competitive ratio provides the worst-case performance bound of the online scheme.

- Chapter 7 consists of conclusions and future work of this thesis. For future work, both extensions to the current work and some promising future research directions are presented.

1.5 Notation

In this thesis, $(\cdot)^+ = \max(\cdot, 0)$; $\log(\cdot)$ and $\ln(\cdot)$ represent base-2 and natural logarithms, respectively; $\mathcal{C}(x) = \log(1 + x)$.

1.6 Publication List

Journal Papers

1. D. Zhao, C. Huang, Y. Chen, F. Alsaadi, and S. Cui, "Resource Allocation for Multiple Access Channel with Conferencing Links and Shared Renewable Energy Sources", *IEEE Journal of Selected Areas in Communications (JSAC)*, vol.33, no.3, pp. 423-437, March 2015.

Conference Papers

1. D. Zhao, C. Huang, Y. Chen and S. Cui, "Optimal Resource Allocation for Multiple Access Channel with Conferencing Links and a Shared Renewable Energy Source", *IEEE International Conference on Acoustics, Speech, and Signal Processing (ICASSP 2013)*, Vancouver, Canada, May 2013, pp. 4794-4798.

2. D. Zhao, C. Huang, Y. Chen and S. Cui, "Optimal Resource Allocation for Multiple Access Channels with a Shared Renewable Energy Source", *IEEE International Symposium on Personal, Indoor and Mobile Radio Communications (PIMRC 2013)*, London, UK, September, 2013, pp. 522-526.

3. D. Zhao, C. Huang, Y. Chen and S. Cui, "Competitive Analysis of Online Throughput Maximization Schemes for Multiple Access Channels with a Shared Renewable Energy Source", *IEEE Global Conference on Signal and Information Processing (GlobalSIP 2013)*, Austin, USA, December, 2013, pp. 375-378.

Chapter 2

Fundamental Concept and State-of-the-Art

2.1 Overview

In this Chapter, first, the fundamental theory background about channel capacities, convex optimisation technique, and competitive analysis is introduced. Then, recent research results in energy harvester powered wireless communication system are summarised.

2.2 Fundamental Concepts

In this section, the fundamental concepts involved in our research will be explained.

First, the preliminary knowledge about channel capacities is discussed. In this research, the capacities of the considered wireless channels will be used to characterise the relationship between the achievable transmission rates and the allocated power.

Second, the convex optimisation technique is introduced briefly. In this research,

convex optimisation techniques are used when developing the optimal resource allocation schemes.

Third, the online/offline problems and competitive analysis are explained. In this research, both offline and online algorithms are studied to be applied to different application scenarios. Competitive analysis provides a theoretic performance measurement for online schemes against the optimal offline schemes without the need of hypothesising random distributions on input sequences.

2.2.1 Channel Capacities

2.2.1.1 Gaussian Point-to-Point Channel and its Capacity

1. Real AWGN Channel

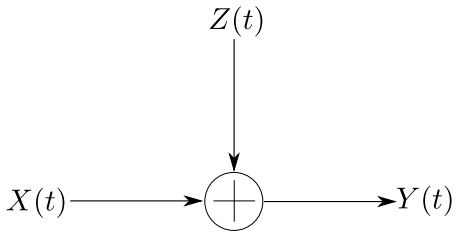

Figure 2.1: Gaussian Channel (Figure 9.1 from [CT06])

As depicted in Figure 2.1, the real Gaussian channel is a time-discrete continuous alphabet channel. At time t, the channel input-output relationship of the Gaussian channel is given as

$$Y(t) = X(t) + Z(t), \qquad Z(t) \sim \mathcal{N}(0, N),$$

where $X(t), Y(t)$ are the real input and output signals, respectively, and $Z(t)$ is the Gaussian noise with zero mean and a variance of N.

With an average power constraint P, the channel capacity of the real Gaussian

channel is given as [CT06]

$$C = \max_{f(x):E\,X^2 \le P} I(X;Y) = \frac{1}{2}\log\left(1+\frac{P}{N}\right) \qquad \text{bits per transmission.} \tag{2.1}$$

Note that the maximum is achieved when $X \sim \mathcal{N}(0,P)$.

2. Complex AWGN Channel

The channel input-output relationship of the complex baseband AWGN channel is given as

$$Y(t) = X(t) + Z(t), \qquad Z(t) \sim \mathcal{CN}(0,N), \tag{2.2}$$

where $X(t), Y(t)$ are the complex input and output signals, respectively, and $Z(t)$ is the circularly symmetric Gaussian complex (CSGC) noise with zero mean and a variance of N.

There is an average power constraint of P per complex input. Each use of the complex channel can be regarded as two uses of a real AWGN channel, with the signal-to-noise ratio SNR $= \frac{P/2}{N/2} = \frac{P}{N}$. Therefore, the capacity of the complex channel is [CT06]

$$\frac{1}{2}\log\left(1+\frac{P}{N}\right) \text{ bits per real dimension,} \tag{2.3}$$

or, equivalently,

$$\log\left(1+\frac{P}{N}\right) \text{ bits per complex dimension.} \tag{2.4}$$

2.2.1.2 Gaussian MAC/BC and Capacities

- Two-user Gaussian MAC

The multiple access channel (MAC) is consists of two transmitters and one receiver,

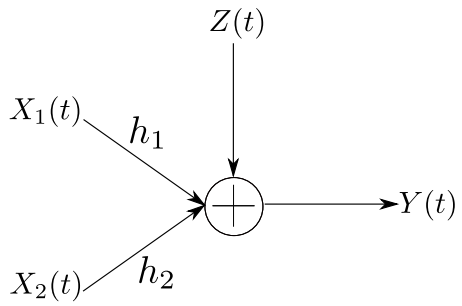

Figure 2.2: Gaussian Multiple Access Channel

as illustrated in Figure 2.2. At time t, the channel input-output relationship of the Gaussian MAC channel is given as

$$Y(t) = \sqrt{h_1(t)}X_1(t) + \sqrt{h_2(t)}X_2(t) + Z(t), \qquad Z(t) \sim \mathcal{N}(0, N),$$

where $X_i(t), i = 1, 2$, are the input signals from transmitter i, respectively, $h_1(t)$ and $h_2(t)$ are the channel gains, $Y(t)$ is the output signal received by the receiver and $Z(t)$ is the Gaussian noise with zero mean and a variance of N.

Let the power constraints on transmitter $i, i = 1, 2$ be P_i. The channel capacity region of the Gaussian MAC is illustrated in Fig. 2.3 and is given as[1] [CT06]

$$\begin{cases} R_1 \leq \frac{1}{2}\log\left(1 + \frac{h_1 P_1}{N}\right) & (2.5) \\ R_2 \leq \frac{1}{2}\log\left(1 + \frac{h_2 P_2}{N}\right) & (2.6) \\ R_1 + R_2 \leq \frac{1}{2}\log\left(1 + \frac{h_1 P_1}{N} + \frac{h_2 P_2}{N}\right). & (2.7) \end{cases}$$

The corner points A and B are achieved by adopting the superposition codes with successive interferencing cancellation. To achieve corner point A, the message of transmitter 1 is decoded first, treating transmitter 2's message noise. The rate achieved for transmitter 1 is therefore given by $R_1 = \frac{1}{2}\log\left(1 + \frac{h_1 P_1}{h_2 P_2 + N}\right)$. Then,

[1] the channel considered here is a real channel therefore there is a coefficient of $\frac{1}{2}$ in the channel capacity. When the channel is complex, this coefficient should be eliminated, similarly hereinafter.

transmitter 1's message is subtracted from the received message. At last, transmitter 2's message is decoded with only the system background noise and therefore achieving the rate $R_2 = \frac{1}{2}\log\left(1+\frac{h_2P_2}{N}\right)$. The corner point B could be achieved by similar scheme only with the reverse decoding order, i.e., decoding transmitter 2's message first and then transmitter 1's. Any point on the segment between points A and B could be achieved by time sharing between the two points.

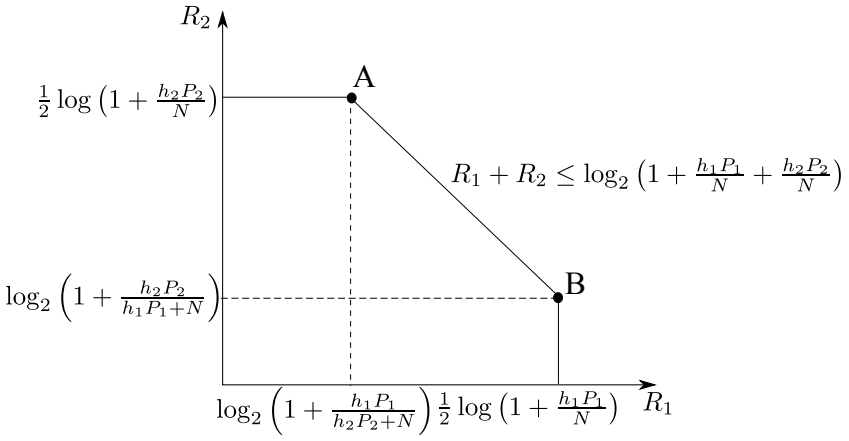

Figure 2.3: The capacity region of the Gaussian MAC channel

- Two-user Gaussian MAC with conferencing links

  On top of the traditional two-user Gaussian MAC described above, certain wired rate-limited two-way conferencing links connecting the two transmitters could be introduced into the system. Via the conferencing links, transmitter 1 can talk to transmitter 2 with a rate up to C_{12}, similar for the opposite direction with a rate up to C_{21}.

  Let the power constraints on transmitter $i, i = 1, 2$ be P_i. For the Gaussian MAC with conferencing links, the coding scheme is described as follows. Transmitter i, $i = 1, 2$, splits its message X_i, into two sub-messages: transmitter i's private message X_i^p and its common message X_i^c. The transmitters exchange their common messages, i.e., X_1^c and X_2^c, with each other by using the conferencing links as in Willem's scheme [Wil83]. As a result of conferencing, transmitter i, $i = 1, 2$, has the

common message $X^c = (X_1^c, X_2^c)$ and its private message X_i^p, which are allocated with the power P_i^c and $P_i^p = P_i - P_i^c$, respectively, and sent over the multiple access channel to the receiver, where P_i^c and P_i^p denote power allocated to the common message of transmitter i and the private message of transmitter i, respectively.

With the above coding scheme, the capacity region of the Gaussian MAC with conferencing links is given as [BLW08]

$$\begin{cases} (R_1 - C_{12})^+ \leq \frac{1}{2}\log\left(1 + \frac{h_1 P_1^p}{N}\right) & (2.8) \\ (R_2 - C_{21})^+ \leq \frac{1}{2}\log\left(1 + \frac{h_2 P_2^p}{N}\right) & (2.9) \\ (R_1 - C_{12})^+ + (R_2 - C_{21})^+ \leq \frac{1}{2}\log\left(1 + \frac{h_1 P_1^p + h_2 P_2^p}{N}\right) & (2.10) \\ R_1 + R_2 \leq \frac{1}{2}\log\left(1 + \frac{h_1 P_1 + h_2 P_2 + 2\sqrt{h_1 P_1^c h_2 P_2^c}}{N}\right). & (2.11) \end{cases}$$

The traditional Gaussian MAC could be regarded as a special case of the Gaussian MAC with conferencing links (both conferencing links of zero capacities, i.e., $C_{12} = 0, C_{21} = 0$). When both conferencing links of zero capacities, there will be no common messages and therefore $P_1^c = 0$ and $P_2^c = 0$. It is worth nothing that in such case, the capacity region defined in (2.8)-(2.11) reduces to the capacity region of the traditional Gaussian MAC defined in (2.5)-(2.7).

- Two-user Gaussian BC

  The broadcast channel (BC) is consists of one transmitter and two receivers, as illustrated in Figure 2.4. At time t, the channel input-output relationship of the Gaussian BC channel is given as

$$Y_i(t) = \sqrt{h_1}X(t) + Z_i(t), \qquad Z_i(t) \sim \mathcal{N}(0, N_i), i = 1, 2,$$

where $X(t)$ is the input signal from the transmitter, $Y_i(t), i = 1, 2$, are the output signals received by receiver i, respectively, h_1 and h_2 are the channel gains,

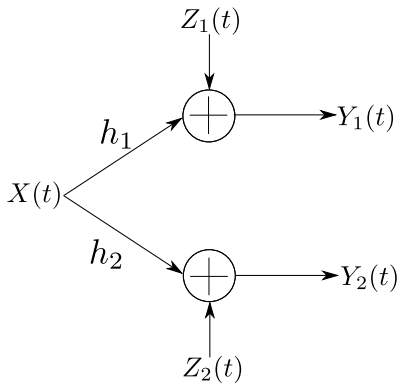

Figure 2.4: Gaussian Broadcast Channel

$Z_1(t)$ and $Z_2(t)$ are arbitrarily correlated Gaussian noises both with zero mean and variances of N. Without loss of generality, it is assumed $h_1 \geq h_2$.

Let the power constraints on transmitter be P. The channel capacity region of the Gaussian BC is illustrated in Fig. 2.5 and is given as [CT06]

$$\begin{cases} R_1 \leq \frac{1}{2}\log\left(1+\frac{\alpha h_1 P}{N}\right) & (2.12) \\ R_2 \leq \frac{1}{2}\log\left(1+\frac{(1-\alpha)h_2 P}{\alpha h_1 P+N}\right), & (2.13) \end{cases}$$

where $\alpha \in [0,1]$ represents the percentage of the power P allocated to receiver 1's message .

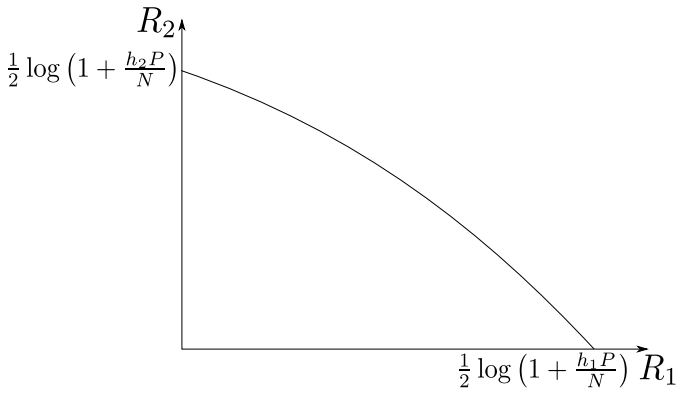

Figure 2.5: The capacity region of the Gaussian Broadcast Channel

The boundary of the capacity region is achieved by using superposition coding with

interference cancellation. The transmitter with the higher channel gain, i.e., transmitter 1, is encoded with fine resolution codes, whereas the other transmitter, transmitter 2, is encoded with coarse resolution codes. When transmitter 1 receives the signal, it firstly decodes the message of transmitter 2, and then decodes its own message after subtracting the message of transmitter 2 out. Therefore, the rate achieved is given as $R_1 = \frac{1}{2}\log\left(1+\frac{\alpha h_1 P}{N}\right)$. When receiver 2 receives the signal, it cannot decodes the message of transmitter 1 because of its inferior channel condition. Therefore, it decodes its own message by treating transmitter 1's message as interference and achieves the rate $R_2 = \frac{1}{2}\log\left(1+\frac{(1-\alpha)h_2 P}{\alpha h_1 P+N}\right)$.

The points on the horizontal and the vertical axes are achieved when $\alpha = 1$ and $\alpha = 0$, respectively.

2.2.2 Convex Optimisation

Convex optimisation is a subset of mathematical optimisation problems. It is widely used in various areas in both research and industry. This technique is adopted extensively in the research of optimal power allocation design in wireless communication systems with energy harvesters.

2.2.2.1 Basic Concepts

- **Convex Set:** For a set C, if for any two elements $x_1, x_2 \in C$ and any $\theta \in [0,1]$,

$$\theta x_1 + (1-\theta)x_2 \in C$$

  is always valid, then C is convex set. Or, in other words, the line segment between any two points in a convex set also lies in this set [BV04].

- **Convex Function:** Define a function $f : R_n \to R$ with domain **dom** f which is a convex set. It is convex if for all $x, y \in$ **dom** f and $\theta \in [0,1]$, the following

inequality always holds:

$$f(\theta x + (1-\theta)y) \leq \theta f(x) + (1-\theta)f(y). \tag{2.14}$$

The inequality in (2.14) is also called **Jensen's Inequality**.

From the perspective of geometry, the above inequality reveals that for convex function, the segment between any $(x, f(x))$ and $(y, f(y))$ lies above the graph of f as shown in Figure 2.6.

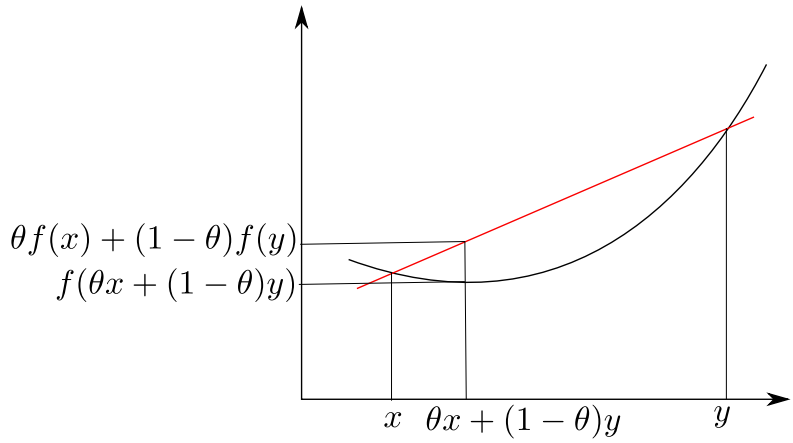

Figure 2.6: An illustration of a convex function

A function is strictly convex when strict inequality holds for (2.14).

- **Optimisation Problem:** The standard form of an optimisation problem which consists m inequality constraints and p equality constraints is as follows

$$\begin{aligned} \min_{x} \quad & f_0(x) \\ \text{s.t.} \quad & f_i(x) \leq 0, \quad i = 1, ..., m \\ & h_i(x) = 0, \quad i = 1, ..., p \end{aligned} \tag{2.15}$$

The problem can be described as minimising the objective function $f_0(x)$ among

all the values of x that satisfy both the inequality constraints $f_i(x) \leq 0$ and equality constraints $h_i(x) = 0$. The domain of the problem (2.15) is defined as $\mathcal{D} = \bigcap_{i=0}^{m} \mathbf{dom}\ f_i \cap \bigcap_{i=1}^{p} \mathbf{dom}\ h_i$.

- **Convex Optimisation Problem:**

  An optimisation problem becomes a convex optimisation problem when it has the following form:

$$\begin{aligned} \min_{x} \quad & f_0(x) \\ \text{s.t.} \quad & f_i(x) \leq 0, \quad i = 1, ..., m \\ & a_i^T x = b_i, \quad i = 1, ..., p \end{aligned} \tag{2.16}$$

  where $f_0, ..., f_m$ are convex functions and ^{T} represents transpose operation. Note that in convex optimisation problems, the objective function and all the constraints are convex.

2.2.2.2 Duality

- **The Lagrange dual function**: Consider the standard form optimisation problem (2.15) with variable $x \in R^n$. Denote its optimal value by p^*.

  Associated with this problem, the *Lagrangian* $L : R^n \times R^m \times R^p \to R$ is defined as

$$L(x, \lambda, \nu) = f_0(x) + \sum_{i=1}^{m} \lambda_i f_i(x) + \sum_{i=1}^{p} \nu_i h_i(x),$$

  with $\mathbf{dom}\ L = \mathcal{D} \times R^m \times R^p$ where the vectors λ and ν are referred as the *Lagrange multiplier vectors.*

  The Lagrange dual function $g : R^m \times R^p \to R$ is defined as the minimum value can

be achieved by the Lagrangian over x:

$$g(\lambda,\nu) = \inf_{x\in\mathcal{D}} L(x,\lambda,\nu) = \inf_{x\in\mathcal{D}} \left(f_0(x) + \sum_{i=1}^{m} \lambda_i f_i(x) + \sum_{i=1}^{p} \nu_i h_i(x) \right).$$

Note that the dual function is always concave even though the problem (2.15) is not necessarily convex.

For each (λ,ν) with $\lambda \geq 0$ pair, the Lagrange dual function provides a lower bound on the value of optimal p^* of problem (2.15), that is, for any $\lambda \geq 0$ and any ν, we always have

$$g(\lambda,\nu) \leq p^*.$$

- **The Lagrange Dual Problem**: The Lagrange dual problem is defined as

$$\begin{aligned} \max_{\lambda,\nu} \quad & g(\lambda,\nu) \\ \text{s.t.} \quad & \lambda \geq 0. \end{aligned} \tag{2.17}$$

The optimal value d^* of the problem (2.17) gives the best (or largest) lower bound on p^*. Problem (2.15) is also called the primal problem.

The optimal (λ^*,ν^*) for problem (2.17) is referred as dual optimal or optimal Lagrange multipliers.

The difference $p^* - d^*$ is defined as **optimal duality gap**.

Strong duality means that the optimal duality gap is 0.

- ***Karush-Kuhn-Tucker* (KKT) conditions** is defined as:

$$f_i(x^*) \leq 0, \quad i = 1, ...m \tag{2.18}$$

$$h_i(x^*) = 0, \quad i = 1, ...p \tag{2.19}$$

$$\lambda_i^* \geq 0, \quad i = 1, ...m \tag{2.20}$$

$$\lambda_i^* f_i(x^*) = 0, \quad i = 1, ...m \tag{2.21}$$

$$\nabla f_0(x^*) + \sum_{i=1}^{m} \lambda_i^* \nabla f_i(x^*) + \sum_{i=1}^{p} \nu_i^* \nabla h_i(x^*) = 0. \tag{2.22}$$

If strong duality holds for any optimisation problem (both convex and nonconvex), then any pair of primal and dual optimal points must satisfy the KKT conditions (2.18)-(2.22).

In addition to above facts, for **convex primal problem**, the KKT conditions are also sufficient for the points to be primal and dual optimal (necessary and sufficient condition).

Therefore, for convex optimisation, if KKT conditions are satisfied, the optimal x^* can be found through solving the KKT conditions and the optimal value of the problem can subsequently be found.

2.2.3 Online/Offline Problems and Competitive Analysis

2.2.3.1 Online Problems and Offline Problems

Online problems are the optimisation problems in which the input and the output is produced in a serial fashion, i.e., the output must be produced in an online manner without knowing the entire input sequence in advance. In online algorithms, each online output have influences on the performance of the overall solution. On the other hand, offline problems are the optimisation problems in which the whole problem input is given

from the beginning, i.e., the output is produced with the full knowledge of the input.

Many problems, such as the selection sort problem [BEY98], are intrinsically offline. There are also many problems that are intrinsically online, such as investment planning and telephone circuit switching. Interestingly, for some other problems, both the offline and online versions are naturally meaningful, such as bin packing and job scheduling.

2.2.3.2 Competitive Analysis

Competitive analysis is widely used in various areas for analyzing online algorithms. In the following, the basic ideas and terminology in competitive analysis will be introduced. Consider an optimisation problem, which may be either a profit maximization problem (for example, the throughput maximization problem) or a cost minimization problem (for example, the transmission completion time minimization problem), and denote it as $\mathcal{P}$. A profit maximization problem (cost minimization problem) $\mathcal{P}$ consists of a set $\mathbf{\Omega}$ of input sequences and a profit (cost) function B. Since this thesis focuses on throughput (profit) maximization problem, the discussion here is mainly in terms of profit maximization problems.

Denote an online algorithm for solving the problem $\mathcal{P}$ as $\mathcal{A}$ and the optimal offline algorithm as $\mathcal{O}$. For any input sequence $\boldsymbol{\omega} \in \mathbf{\Omega}$, let $B^{\mathcal{A}}(\boldsymbol{\omega})$ and $B^{\mathcal{O}}(\boldsymbol{\omega})$ denote the profits earned by $\mathcal{A}$ and $\mathcal{O}$ for serving $\boldsymbol{\omega}$. An online algorithm $\mathcal{A}$ is ρ-competitive [BEY98] if for all feasible input sequences $\boldsymbol{\omega} \in \mathbf{\Omega}$,

$$B^{\mathcal{A}}(\boldsymbol{\omega}) \geq \frac{B^{\mathcal{O}}(\boldsymbol{\omega})}{\rho}. \tag{2.23}$$

Note that the competitive ratio ρ is at least 1. The competitive ratio serves as a worst-case performance bound of the online algorithm against the optimal offline algorithm.

2.3 State-of-the-Art in Wireless Communication Systems Powered by Renewable Sources

Due to the intermittent and random energy availability introduced by EH source, protocols/policies in traditional wireless communication systems need to be revised to accommodate the new challenges. In the physical layer, throughput maximising transmission policies for various channel models were studied in [YU12b, HZ12, YU12a, TY12a, TY12b, YOU12, OYU12a, AUBE11, OYU12b, OYU13]; joint energy transfer and transmission scheduling policies were investigated in [LZC13, PC13, ZZH13, GOJU13a, GOJU12, GOJU13b, TY13, PFS13, DPEP14, DZN$^+$15]. Multiple access control policies for energy harvester powered wireless communication systems were considered in [ISS10, ISPS12, ISS12]. References [LSS07, CSSJ14, JSMK09] focused on the networking layer of wireless communication systems powered by EH and studied several routing protocols. In this section, literatures on throughput maximising transmission schemes, which are the main focuses of this thesis, will be summarised.

2.3.1 Point-to-Point Channel with Energy Harvester

2.3.1.1 AWGN point-to-point channel with energy harvester

The optimal offline resource allocation schemes for maximising the throughout over a finite time horizon in the single-user additive white Gaussian noise (AWGN) channel was investigated in [YU12b] (assuming infinite battery capacity) and [TY12a] (assuming finite battery capacity).

For a point-to-point AWGN channel, the relationship between the transmission rate r and the power P is given as $r = g(P) = \frac{1}{2}\log(1+P)$.

A deterministic energy model was adopted in both papers, which assumes energy arrival instants, i.e., $0, s_1, s_2, \cdots, s_n, \cdots$, and amounts $E_0, E_1, E_2, \cdots, E_n, \cdots$ are known

to the system before the transmissions start.

The optimal offline resource allocation scheme assuming infinite battery capacity was investigated in [YU12b]. It was proved that the optimal power/rate allocation satisfies the following structural properties: 1) the rate/power keeps constant between energy arrivals; 2) the rate/power is non-decreasing over time; 3) whenever the rate/power changes, the energy stored in the battery must be depleted. Based on these properties, the optimal power/rate allocation could be obtained, as indicated in Fig. 2.7. As shown in Fig. 2.7, the staircase curve represents the amount of accumulated harvested energy and the red piecewise linear curve is the accumulated amount of consumed energy, whose slopes indicate the power level.

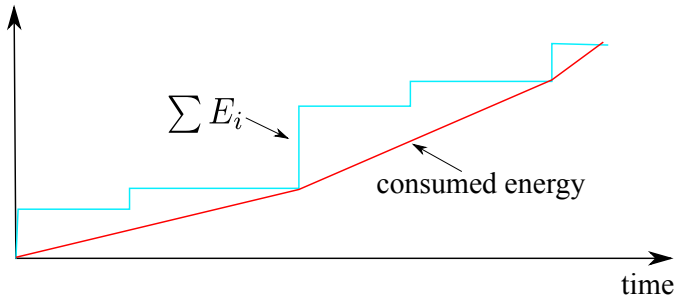

Figure 2.7: Optimal power allocation in point-to-point channel with energy harvester (infinite battery capacity case).

In [TY12a], the optimal offline resource allocation for finite battery capacity case was studied. It was proved that the rate/power should satisfy the following structural properties: 1) the rate/power keeps constant between energy arrivals; 2) whenever the rate/power changes, the battery is either full or depleted; 3) the rate/power only increases when the battery is depleted while only decreases when the battery is full. Based on these properties, the optimal rate/power could be obtained by the algorithm proposed in [TY12a]. As illustrated in Fig. 2.8, unlike the infinite battery capacity case where the power level only increases with time, in finite battery case, the power level may both increase and decrease, depends on the battery status.

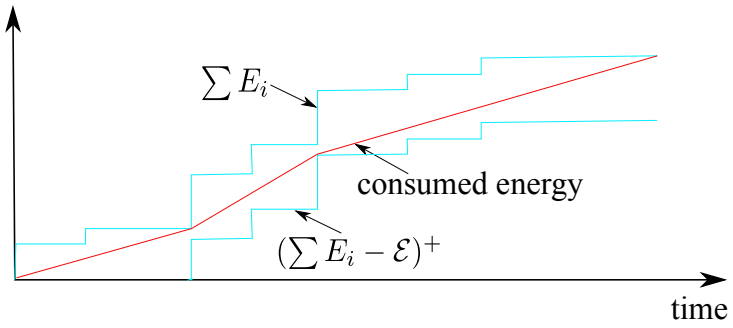

Figure 2.8: Optimal power allocation in point-to-point channel with energy harvester (finite battery capacity case).

2.3.1.2 Fading channel with energy harvester

In [HZ12], the authors studied the throughput maximisation problem for point-to-point channel with varying channel conditions over a finite horizon of K time slots. Assuming causal side information at the transmitter, i.e., only information about channel conditions and energy amount of the past and presents slots is known, and modelling both the channel condition and energy profiles as first-order Markov processes, the optimal solution to maximise the summation of the expected mutual information over K slots can be obtained by dynamic programming. With full causal side information at the transmitter, i.e., information about channel conditions and harvested energy amount of the K slots is known before transmission starts, the authors obtained: 1) the closed-form optimal solution was when $K = 2$; 2) the structure of the optimal solution for arbitrary K which has a water-filling interpretation where there are multiple non-decreasing water levels, based on which an algorithm was proposed that uses both forward-search and backward-search.

In [OTY+11], the throughput maximisation problem was considered in a point-to-point wireless fading channel with finite battery capacity. In this paper, a continuous system model was adopted, where the arrival times of harvested energy and the changing points of the channel gains are uneven over time. With the assumption of non-causal channel state information (CSI) and energy state information (ESI), the problem of max-

imising the throughput given the deadline T was investigated. Based on KKT condition analysis, a directional water-filling algorithm was proposed. The water level keeps constant between two adjacent energy arrivals and there may exist multiple water levels during the whole transmission process. Right permeable water taps are used at the points of energy arrival which only allows energy to flow to the right. Similar to the classic water filling algorithms, the water level is used to make sure that the higher power level is granted when the channel gain is high where as lower power level (or even zero power) is used when the channel condition is poor.

2.3.2 Multiuser Wireless Communication Systems with Energy Harvesters

2.3.2.1 Broadcast Channel with Energy Harvester

In [YOU12], [AUBE11] and [OYU12a], the Gaussian BC where the transmitter is powered by an energy harvester, as shown in Figure 2.9, was studied. They adopted the same energy model as in [YU12b]. The data packages are assumed to be ready before transmissions start.

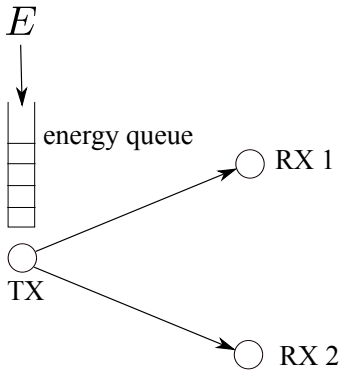

Figure 2.9: Broadcast channel with energy harvester

As indicated by (2.12), the channel capacity region of the BC shown in Figure 2.9 is

given as

$$r_1 \leq \frac{1}{2}\log\left(1+\frac{\alpha P}{\sigma_1^2}\right), \tag{2.24}$$

$$r_2 \leq \frac{1}{2}\log\left(1+\frac{(1-\alpha)P}{\alpha P+\sigma_2^2}\right), \tag{2.25}$$

where α represents the portion of the total power P that is allocated for the message for receiver 1 and σ_1^2, σ_2^2 are the variance of the zero mean Gaussian noise experienced by receiver 1 and receiver 2, respectively. Without loss of generality, it is assumed that $\sigma_1^2 \leq \sigma_2^2$, which indicates receiver 1 experiences weaker noise interference than receiver 2.

It was proved that the smallest sum power needed to support data rates r_1 and r_2 in this BC is given as

$$g(r_1, r_2) \triangleq \sigma_1^2 2^{2(r_1+r_2)} + (\sigma_2^2 - \sigma_1^2)2^{2r_2} - \sigma_2^2. \tag{2.26}$$

The optimal offline resource allocation with infinite battery capacity assumption was studied in the parallel work in [YOU12] and [AUBE11].

In [YOU12], by analysing the KKT conditions of the optimisation problem, it was proved that the sum power allocation has the same structural properties as that in the point-to-point channel [YU12b] and thus could be obtained similarly. It is worth noting that the proof process only applies to the specific expression of $g(r_1, r_2)$ in (2.26). Then, it was proved that there exists a cut-off power for the stronger user: 1) if the sum power is smaller than the cut-off power, all the sum power will be allocated to the data for the stronger user; and 2) if the sum power is larger than cut-off power, then the amount of power allocated to the stronger user equals the cut-off power level while all the remaining power will be allocated to the weaker user.

Similar result was obtained in [AUBE11] by an iterative algorithm, i.e., the modified

FlowRight algorithm.

The optimal offline resource allocation with finite battery capacity assumption was investigated in [OYU12a]. It was proved that the optimal sum power allocation has the same structure as that in the point-to-point channel with finite battery capacity [TY12a], and thus could be obtained by adopting the algorithm in [TY12a]. Note that, however, the above conclusion is proved by KKT conditions which involves the derivatives of $g(r_1, r_2)$. Therefore, their proof process only applies to the specific expression of $g(r_1, r_2)$ in (2.26). The optimal way of splitting the sum power for the two users is the same as that in the BC channel with infinite battery capacity [YOU12].

2.3.2.2 Multiple Access Channel with Energy Harvesters

Reference [YU12a] studied the resource allocation problem for maximising the weighted sum throughput in a two-transmitter Guassian MAC, where each transmitter is powered by an energy harvester, as illustrated in Fig. 2.10. Considering infinite battery capacities, the optimal offline generalised iterative backward water-filling scheme was proposed, which was based on the generalized iterative water-filling algorithm in [KU06]. Note that however, the optimal solution proposed in this paper is not an analytic solution and therefore has relatively high computational burden.

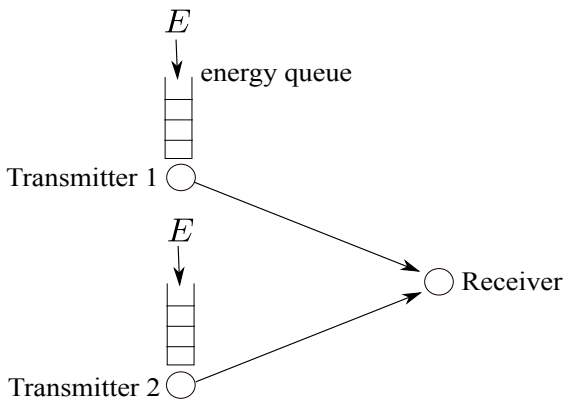

Figure 2.10: Multiple access channel with energy harvesters

2.3.2.3 Relay Channel with Energy Harvester

In [HZC13], the classic decode-and-forward Gaussian relay channel where the source and relay nodes are both powered by energy harvesting sources was investigated. With a slotted energy arrival model where the harvested energy arrives at the beginning of each slot, the optimal offline resource allocation algorithm to maximise the throughput over a finite horizon of N slots for two traffic types, i.e., the delay-constrained traffic and the no-delay constrained traffic, were studied. With delay-constrained traffic, by examining the KKT conditions of the optimisation problem, it was proved that the resource allocation at the transmitter and relays should be jointly optimised. A forward search algorithm was proposed which gives the optimal offline power profiles. For the no-delay constrained traffic case, a two-stage offline resource allocation algorithm, which separately computes the optimal power profiles for the source and relay nodes, was proposed.

Reference [OE13] and [LZL13] studied the resource allocation problems in half-duplex decode-and-forward relay channel with no direct link between the source and the destination, assuming the relay is powered by energy harvester and the source is powered by an energy harvester, respectively. Assuming infinite battery capacity, the optimal offline resource allocation schemes were developed in [OE13] and [LZL13] for their respective problems.

Chapter 3

Optimal Offline Resource Allocation Schemes for Multiple Access Channels with a Shared Renewable Energy Source

3.1 Overview

In this Chapter, the optimal offline resource allocation for the Gaussian multiple access channel (MAC) with two transmitters powered by a shared energy harvester is investigated. The aim of the resource allocation schemes are to maximise the weighted sum throughput over a finite time horizon. Packets of both transmitters are assumed to be ready before transmissions start. Moreover, both infinite battery capacity and finite battery capacity cases are considered. The optimal offline resource allocation schemes for both cases are developed based on the assumption that the energy arrival amounts are non-causally known before transmissions.

To develop the optimal offline schemes, first, the resource allocation problems that characterises the maximum departure regions over a finite time horizon is formulated. The structural properties of the optimal offline sum power profiles are investigated by exploiting the convexity of the sum power function. Then, the optimal offline resource allocation between the two transmitters, in which there exists a capping rate at the stronger transmitter, is obtained. It is also demonstrated that under the same energy arrival profile, the Gaussian MAC with a shared energy harvester achieves the same maximum departure region as its dual broadcast channel (BC).

3.2 System Model and Problem Formulation

3.2.1 System Model

As illustrated in Fig. 3.1, a two-user Gaussian multiple access channel is considered. The constant channel power gains from transmitter 1 and transmitter 2 to the receiver are denoted by h_1 and h_2, respectively. The assumption of constant channel gains can be validated by the practical scenario where the locations and the wireless medium between the transmitters and the receiver are relatively fixed and thus the channel gains are quasi-static over the considered transmission period. Such assumption has been widely adopted in several other papers in the same line of work, e.g., [YU12b], [TY12a], [GP13], [YOU12], [AUBE11], and [YU12a]. Without loss of generality, it is assumed $h_1 > h_2$, which indicates that the link from transmitter 1 to the receiver is stronger than that from transmitter 2 to the receiver. The transmitter with the higher (lower) channel gain is called the stronger (weaker) transmitter.

Consider a finite time horizon of N slots, each with a duration of T. It is assumed that at the beginning of the n-th slot, $n = 1, \cdots, N$, the EH source receives harvested energy with an amount of $E_n \in [0, E_{\max}]$, where $E_{\max}$ denotes the maximum amount of the harvested energy and is assumed to be known. Denote the sequence of the N energy

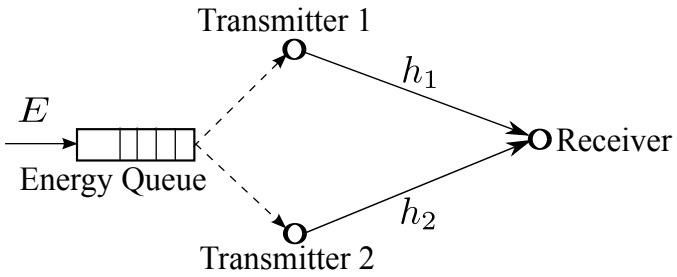

Figure 3.1: Gaussian MAC with a shared energy harvester

arrivals as $\boldsymbol{\omega} = (E_1, \cdots, E_N)$ (which is also called the energy input sequence) and the set of all possible energy input sequences as $\boldsymbol{\Omega} = \{\boldsymbol{\omega} | 0 \leq E_n \leq E_{\max}, n = 1, \cdots, N\}$.

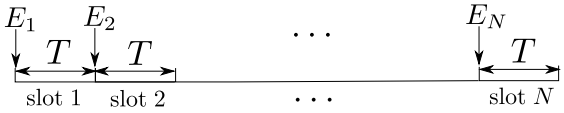

Figure 3.2: The slot-based energy arrival model

Denote the power and rate of transmitter i, $i = 1, 2$, in the n-th slot, $n = 1, \cdots, N$, as $P_{i,n}$ and $r_{i,n}$, respectively. The channel input/output relationship of the Gaussian MAC in the n-th slot is given as [CT06]

$$Y_n = \sqrt{h_1 P_{1,n}} X_{1,n} + \sqrt{h_2 P_{2,n}} X_{2,n} + Z_n, \tag{3.1}$$

where $X_{i,n}$, $i = 1, 2$, is the unit-power transmitted signals at transmitter i, Y_n is the received signal at the receiver and Z_n is the additive circularly symmetric complex Gaussian (CSCG) noise with zero mean and unit variance.

As indicated in Fig. 3.2, the energy provided by the energy harvester is intermittent and discrete over time. As a result, the transmission scheme adopted by the EH system must guarantee that the total amount of energy consumed by the two transmitters during the first j slots must be smaller than or equal to the total amount of energy harvested in the first j slots, $\forall j \in [1, \cdots, N]$. This constraint is called the EH constraint and is

mathematically modeled as:

$$T\sum_{n=1}^{j}(P_{1,n}+P_{2,n})\leq\sum_{n=1}^{j}E_n, j=1,\cdots N. \tag{3.2}$$

3.2.2 Problem Formulation

In this subsection, first, the minimum sum power $g(r_{1,n},r_{2,n})$ required to achieve given data rates $(r_{1,n},r_{2,n})$ of the two transmitters in the n-th slot is derived. Then, for both the infinite and finite battery cases, the maximum departure regions are defined and optimisation problems are formulated, whose optimal solutions give the resource allocation schemes that achieve the boundary points of the maximum departure region, respectively. In the sequel, the index n is omitted whenever it causes no confusion.

3.2.2.1 Minimum Sum Power to Achieve Given Rates

First, the minimum sum power $g(r_1,r_2)$ required to achieve given data rates (r_1,r_2) of the two transmitters is derived.

The capacity region of the Gaussian MAC is given by [CT06]

$$\begin{cases} r_1\leq\log(1+h_1P_1) & (3.3)\\ r_2\leq\log(1+h_2P_2) & (3.4)\\ r_1+r_2\leq\log(1+h_1P_1+h_2P_2), & (3.5)\end{cases}$$

which is convex over (r_1,r_2) [BV04].

An illustration of the capacity region of the Gaussian MAC is shown in Figure 3.3.

Given the data rates (r_1,r_2) of the two transmitters, the minimum sum transmit

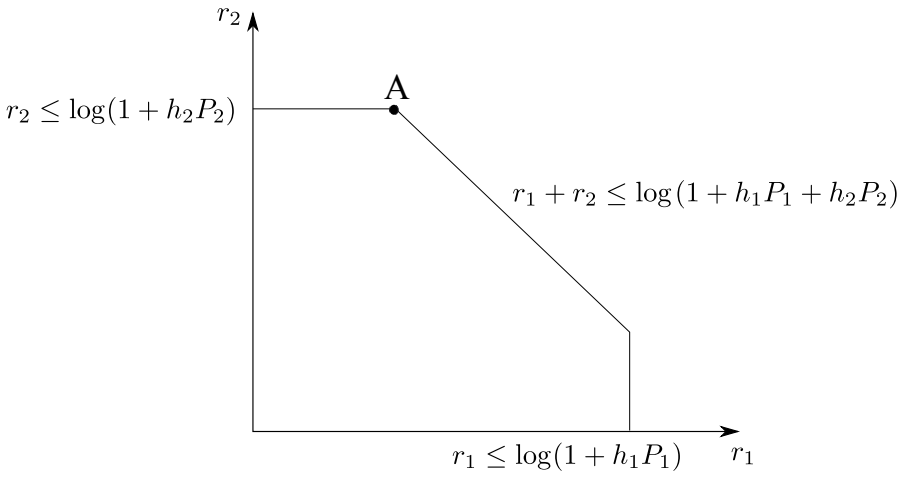

Figure 3.3: The capacity region of the Gaussian MAC

power required can be obtained from the following problem

$$\text{(P3.1)} \quad g\left(r_1, r_2\right) = \min_{\{P_1, P_2\}} P_1 + P_2 \tag{3.6}$$

$$\text{s.t. } (3.3)\text{–}(3.5). \tag{3.7}$$

Proposition 1. *For a given non-negative rate pair (r_1, r_2) and $h_1 > h_2$, the sum minimum transmit power is achieved when equality is achieved for (3.4) and (3.5). The minimum sum power and corresponding power allocation for the two transmitters are*

$$g(r_1, r_2) \triangleq \frac{2^{r_1+r_2} - 2^{r_2}}{h_1} + \frac{2^{r_2} - 1}{h_2}, \tag{3.8}$$

$$P_1 = \frac{2^{r_1+r_2} - 2^{r_2}}{h_1}, \tag{3.9}$$

$$P_2 = \frac{2^{r_2} - 1}{h_2}. \tag{3.10}$$

Proof. Note that problem (P3.1) is convex and its Lagrangian $\mathcal{L}$ is defined as:

$$\begin{aligned} \mathcal{L}(P_1, P_2, \lambda_1, \lambda_2, \lambda_3) &= \sum_{j=1}^{2} \lambda_j (2^{r_j} - 1 - h_j P_j) \\ &+ \lambda_3 (2^{r_1+r_2} - 1 - h_1 P_1 - h_2 P_2) + P_1 + P_2, \end{aligned} \tag{3.11}$$

where $\lambda_1 \geq 0$, $\lambda_2 \geq 0$, and $\lambda_3 \geq 0$ are the Lagrangian multipliers.

By letting the partial derivatives of $\mathcal{L}$ with respective to P_1 and P_2 be equal to zero, respectively, the first set of optimality conditions is given as

$$1 - \lambda_1 h_1 - \lambda_3 h_1 = 0, \tag{3.12}$$

$$1 - \lambda_2 h_2 - \lambda_3 h_2 = 0. \tag{3.13}$$

Note that the complementary slackness conditions of this problem are:

$$\lambda_1 (2^{r_1} - 1 - h_1 P_1) = 0, \tag{3.14}$$

$$\lambda_2 (2^{r_2} - 1 - h_2 P_2) = 0, \tag{3.15}$$

$$\lambda_3 (2^{r_1 + r_2} - 1 - h_1 P_1 - h_2 P_2) = 0. \tag{3.16}$$

If $\lambda_2 = 0$, solving (3.12) and (3.13) gives $\lambda_3 = \frac{1}{h_2} > 0$ and $\lambda_1 = \frac{1}{h_1} - \frac{1}{h_2} < 0$, which is infeasible as the condition $\lambda_1 \geq 0$ is violated. If $\lambda_3 = 0$, solving (3.12) and (3.13) gives $\lambda_1 = \frac{1}{h_1} > 0$ and $\lambda_2 = \frac{1}{h_2} > 0$, which is also infeasible, since it would imply that constraints (3.3) and (3.4) should be achieved with equality, which violates the constraint (3.5). Thus, it is concluded that $\lambda_2 > 0$ and $\lambda_3 > 0$ both hold.

Therefore, by complementary slackness, we have that the optimal solution of problem (P3.1) is achieved when constraints (3.4) and (3.5) are achieved with equality, while the constraint (3.3) would be inactive since (3.3) and (3.4) cannot be active at the same time as we argued above. Based on this, the power P_1 and P_2 allocated for transmitters 1 and 2, respectively, and the minimum sum power $g(r_1, r_2) = P_1 + P_2$ could be obtained.

□

Remark 1. *The minimum sum power transmission given in Proposition 1 is achieved by adopting the following coding scheme: each transmitter encodes its data with a capacity-*

achieving AWGN channel code. When the receiver receives the data of the two transmitters, it first decodes transmitter 1's data while treating the signal from transmitter 2 as Gaussian interference (the rate transmitter 1 could achieve is $r_1 = \log\left(1 + \frac{h_1 P_1}{1+h_2 P_2}\right)$*; then, after the data from transmitter 1 is decoded, it could be subtracted from the received signal; at last, the signal from transmitter 2 could be decoded with only the system background Gaussian noise and the resulted rate is given as* $r_2 = \log(1 + h_2 P_2)$*. Such scheme corresponds to point A in Fig. 3.3*

By (3.8), the causal EH constraints defined in (3.2) could be rewritten as:

$$T\sum_{n=1}^{j} g\left(r_{1,n}, r_{2,n}\right) \leq \sum_{n=1}^{j} E_n, j = 1, \cdots, N. \tag{3.17}$$

3.2.2.2 Problem Formulation for Infinite Battery Capaticy Case

Based on the definition of the EH constraints in (3.17), the maximum departure region is defined as follows.

Definition 1. *Given an energy input sequence* $\boldsymbol{\omega} \in \boldsymbol{\Omega}$*, within the finite time horizon of* N *slots, the* ***maximum departure region*** $\mathcal{D}(N)$ *of the Gaussian MAC with a shared energy harvester with infinite battery capacity is defined as the union of all achievable bits pair* (B_1, B_2) *under the EH constraint (3.17), i.e.,*

$$\mathcal{D}(N) = \left\{ (B_1, B_2) \middle| B_i = T\sum_{n=1}^{N} r_{i,n}, i = 1, 2, \ (3.17) \right\}, \tag{3.18}$$

where B_i *is the total amount of data transmitted from transmitter* i*,* $i = 1, 2$*.*

Proposition 2. *The maximum departure region* $\mathcal{D}(N)$ *defined in* (3.18) *for the MAC with infinite battery capacity is convex.*

Proof. Let (B_1, B_2) and (B_1', B_2') be two points in $\mathcal{D}(N)$ achieved by the rate profiles $(r_{1,n}, r_{2,n})$ and $\left(r_{1,n}', r_{2,n}'\right)$, $n \in \{1, \cdots, N\}$, respectively. Define another point $\left(\bar{B}_1, \bar{B}_2\right)$

as $\left(\bar{B}_1, \bar{B}_2\right) = \theta\left(B_1, B_2\right) + (1-\theta)\left(B_1', B_2'\right), \theta \in [0,1]$, which is achieved by the rate profile

$$\begin{aligned}\left(\bar{r}_{1,n}, \bar{r}_{2,n}\right) &= \theta\left(r_{1,n}, r_{2,n}\right) + (1-\theta)\left(r_{1,n}', r_{2,n}'\right) \\ &= \left(\theta r_{1,n} + (1-\theta) r_{1,n}', \theta r_{2,n} + (1-\theta) r_{2,n}'\right),\end{aligned}$$

for each $n \in \{1, \cdots, N\}$.

To prove that $\mathcal{D}(N)$ is a convex region, we only need to prove that the point $\left(\bar{B}_1, \bar{B}_2\right)$ is also in $\mathcal{D}(N)$, i.e., the rate profile $\left(\bar{r}_{1,n}, \bar{r}_{2,n}\right)$ is feasible (satisfies the EH constraints), as illustrated in Fig. 3.5.

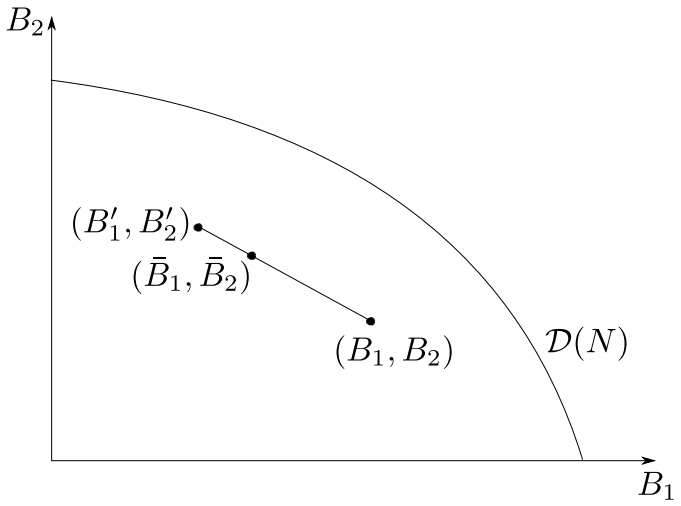

Figure 3.4: Proof of the convexity of the maximum departure region of MAC with a shared energy harvester (infinite battery capacity case)

Due to the convexity of $g\left(r_1, r_2\right)$, we have

$$g\left(\bar{r}_{1,n}, \bar{r}_{2,n}\right) \leq \theta g\left(r_{1,n}, r_{2,n}\right) + (1-\theta)\, g\left(r_{1,n}', r_{2,n}'\right),$$

for all $n \in \{1, \cdots, N\}$. Since (B_1, B_2) and (B_1', B_2') are both in $\mathcal{D}(N)$, we have that for

any $j \in \{1, \cdots, N\}$,

$$T\sum_{n=1}^{j} g\left(r_{1,n}, r_{2,n}\right) \leq \sum_{n=1}^{j} E_n,$$
$$T\sum_{n=1}^{j} g\left(r'_{1,n}, r'_{2,n}\right) \leq \sum_{n=1}^{j} E_n.$$

For $j \in \{1, \cdots, N\}$, we have

$$\begin{aligned} T\sum_{n=1}^{j} g\left(\bar{r}_{1,n}, \bar{r}_{2,n}\right) &\leq T\sum_{n=1}^{j} \left(\theta g\left(r_{1,n}, r_{2,n}\right) + (1-\theta)\, g\left(r'_{1,n}, r'_{2,n}\right)\right) \\ &= \theta T\sum_{n=1}^{j} g\left(r_{1,n}, r_{2,n}\right) + (1-\theta)\, T\sum_{n=1}^{j} g\left(r'_{1,n}, r'_{2,n}\right) \\ &\leq \theta\sum_{n=1}^{j} E_n + (1-\theta)\sum_{n=1}^{j} E_n \\ &= \sum_{n=1}^{j} E_n, \end{aligned}$$

which indicates that the EH constraints are satisfied. Therefore, the point $\left(\bar{B}_1, \bar{B}_2\right)$ can be achieved and is in $\mathcal{D}(N)$.

Hence, we can conclude that $\mathcal{D}(N)$ is a convex region.

□

As illustrated by Fig. 3.5, due to the convexity of this region and its special structure in the first orthant, the boundary of $\mathcal{D}(N)$ can be characterized by solving the following problem,

$$\text{(P3.2)} \quad \max_{\{r_{1,n}, r_{2,n}\}} \quad \mu_1 \sum_{n=1}^{N} r_{1,n} T + \mu_2 \sum_{n=1}^{N} r_{2,n} T \tag{3.19}$$

$$\text{s.t.} \quad \sum_{n=1}^{j} g\left(r_{1,n}, r_{2,n}\right) T \leq \sum_{n=1}^{j} E_n, \quad j = 1, \cdots, N, \tag{3.20}$$

where $\mu_1 + \mu_2 = 1$, $\mu_1 \geq 0$, $\mu_2 \geq 0$. By varying the value of μ_1 and μ_2, different points

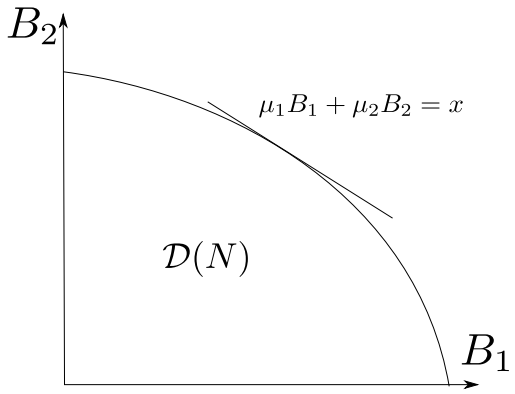

Figure 3.5: An illustration of the maximum departure region of MAC with a shared energy harvester

on the boundary of $\mathcal{D}(N)$ can be achieved.

3.2.2.3 Problem Formulation for Finite Battery Case

Denote the capacity of the battery as $\mathcal{E}$[1]. During the transmission, if the amount of unconsumed energy is larger than the battery capacity, the battery can only store the amount of $\mathcal{E}$ while the rest is discarded because of battery overflow. Notice that battery overflow might only happen at the beginning of each slot when new harvested energy arrives. The battery non-overflow constraints are mathematically modeled as:

$$\left(\sum_{n=1}^{j+1} E_n\right) - \mathcal{E} \leq T \sum_{n=1}^{j} g\left(r_{1,n}, r_{2,n}\right), j = 1, \cdots, N-1. \tag{3.21}$$

Based on the definition of the EH constraints (3.17) and the battery non-overflow constraints (3.21), the maximum departure region for the case of finite battery capacity is defined as follows.

Definition 2. *Given an energy input sequence $\boldsymbol{\omega} \in \boldsymbol{\Omega}$, within the finite time horizon of N slots, the **maximum departure region** $\mathcal{D}(N)$ of the Gaussian MAC with a shared energy harvester with finite battery capacity is defined as the union of all achievable bits*

[1]In the finite battery case, E_n, $n = 1, \cdots, N$, and thus $E_{\max}$ are truncated at $\mathcal{E}$ since any energy exceeding $\mathcal{E}$ cannot be stored in the battery [TY12a].

pair (B_1, B_2) *under the EH constraint (3.17) and the battery non-overflow constraints* (3.21)*, i.e.,*

$$\mathcal{D}(N) = \left\{ (B_1, B_2) \middle| B_i = T \sum_{n=1}^{N} r_{i,n}, i = 1, 2, \ (3.17), (3.21) \right\}. \tag{3.22}$$

Proposition 3. *The maximum departure region* $\mathcal{D}(N)$ *defined in* (3.22) *for the MAC with finite battery capacity is convex.*

Proof. Let (B_1, B_2) and (B_1', B_2') be two points in $\mathcal{D}(N)$ achieved by the rate profiles $(r_{1,n}, r_{2,n})$ and $\left(r_{1,n}', r_{2,n}'\right)$, $n \in \{1, \cdots, N\}$, respectively. Since (B_1, B_2) and (B_1', B_2') are both in $\mathcal{D}(N)$, we have that

$$T \sum_{n=1}^{j} g\left(r_{1,n}, r_{2,n}\right) \leq \sum_{n=1}^{j} E_n, j = 1, \cdots, N, \tag{3.23}$$

$$T \sum_{n=1}^{j} g\left(r_{1,n}', r_{2,n}'\right) \leq \sum_{n=1}^{j} E_n, j = 1, \cdots, N, \tag{3.24}$$

and

$$\left(\sum_{n=1}^{j+1} E_n\right) - \mathcal{E} \leq T \sum_{n=1}^{j} g\left(r_{1,n}, r_{2,n}\right), j = 1, \cdots, N-1, \tag{3.25}$$

$$\left(\sum_{n=1}^{j+1} E_n\right) - \mathcal{E} \leq T \sum_{n=1}^{j} g\left(r_{1,n}', r_{2,n}'\right), j = 1, \cdots, N-1. \tag{3.26}$$

Define another point $\left(\bar{B}_1, \bar{B}_2\right)$ as $\left(\bar{B}_1, \bar{B}_2\right) = \theta\left(B_1, B_2\right) + (1-\theta)\left(B_1', B_2'\right), \theta \in [0, 1]$, which is achieved by the rate profile

$$\begin{aligned}\left(\bar{r}_{1,n}, \bar{r}_{2,n}\right) &= \theta\left(r_{1,n}, r_{2,n}\right) + (1-\theta)\left(r_{1,n}', r_{2,n}'\right) \\ &= \left(\theta r_{1,n} + (1-\theta) r_{1,n}', \theta r_{2,n} + (1-\theta) r_{2,n}'\right), n = 1, \cdots, N.\end{aligned}$$

It is easy to see that the point $\left(\bar{B}_1, \bar{B}_2\right)$ is located on the segment formed by (B_1, B_2) and (B_1', B_2'), as illustrated in Fig. 3.6. Therefore, to prove the convexity of maximum

departure region, we only need to prove that the point $\left(\bar{B}_1, \bar{B}_2\right)$ is in $\mathcal{D}(N)$.

Due to the convexity of $g\left(r_1, r_2\right)$, we have

$$g\left(\bar{r}_{1,n}, \bar{r}_{2,n}\right) \leq \theta g\left(r_{1,n}, r_{2,n}\right) + (1-\theta)\, g\left(r'_{1,n}, r'_{2,n}\right),$$

for all $n \in \{1, \cdots, N\}$.

It is easy to check that for $x_1 > x_2$ and $y_1 > y_2$, we have $g(x_1, y_1) > g(x_2, y_2)$. Also note that $g(r_1, r_2)$ is a continuous function over (r_1, r_2). Therefore, for each $n \in \{1, \cdots, N\}$, we can always find some new rate profile $(\tilde{r}_{1,n}, \tilde{r}_{2,n})$ such that $\tilde{r}_{1,n} > \bar{r}_{1,n}$, $\tilde{r}_{2,n} > \bar{r}_{2,n}$, and $g\left(\tilde{r}_{1,n}, \tilde{r}_{2,n}\right) = \theta g\left(r_{1,n}, r_{2,n}\right) + (1-\theta)\, g\left(r'_{1,n}, r'_{2,n}\right)$.

Denote the point achieved by the new rate profiles $(\tilde{r}_{1,n}, \tilde{r}_{2,n})$ by $\left(\tilde{B}_1, \tilde{B}_2\right)$. Obviously, $\tilde{B}_1 > \bar{B}_1$ and $\tilde{B}_2 > \bar{B}_2$. Clearly, the point $\left(\bar{B}_1, \bar{B}_2\right)$ is dominated by the point $\left(\tilde{B}_1, \tilde{B}_2\right)$, and therefore, if $\left(\tilde{B}_1, \tilde{B}_2\right)$ is in $\mathcal{D}(N)$, so is $\left(\bar{B}_1, \bar{B}_2\right)$.

For $j = 1, \cdots, N$, we have

$$\begin{aligned} T\sum_{n=1}^{j} g\left(\tilde{r}_{1,n}, \tilde{r}_{2,n}\right) &= T\sum_{n=1}^{j} \left(\theta g\left(r_{1,n}, r_{2,n}\right) + (1-\theta)\, g\left(r'_{1,n}, r'_{2,n}\right)\right) \\ &= \theta T\sum_{n=1}^{j} g\left(r_{1,n}, r_{2,n}\right) + (1-\theta)\, T\sum_{n=1}^{j} g\left(r'_{1,n}, r'_{2,n}\right). \end{aligned} \tag{3.27}$$

Based on (3.23)-(3.26), we have

$$T\sum_{n=1}^{j} g\left(r_{1,n}, r_{2,n}\right) \leq \sum_{j=1}^{n} E_n, j = 1, \cdots, N, \tag{3.28}$$

and

$$\left(\sum_{n=1}^{j+1} E_n\right) - \mathcal{E} \leq T\sum_{n=1}^{j} g\left(r_{1,n}, r_{2,n}\right), j = 1, \cdots, N-1, \tag{3.29}$$

which indicates that both the EH constraints and the battery non-overflow constraints are satisfied. Therefore, the point $\left(\tilde{B}_1, \tilde{B}_2\right)$ is in $\mathcal{D}(N)$, so is $\left(\bar{B}_1, \bar{B}_2\right)$.

Hence, we can conclude that $\mathcal{D}(N)$ is a convex region.

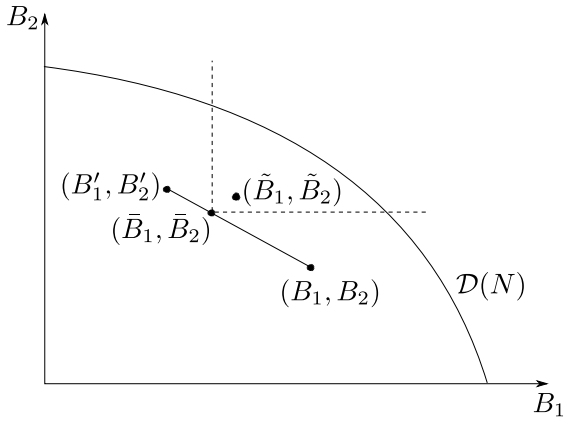

Figure 3.6: Proof of the convexity of the maximum departure region of MAC with a shared energy harvester (finite battery capacity case)

□

Due to the convexity of this region and its special structure in the first orthant, the boundary of $\mathcal{D}(N)$ can be characterized by solving the following problem,

$$\text{(P3.3)} \quad \max_{\{r_{1,n}, r_{2,n}\}} \quad \mu_1 \sum_{n=1}^{N} r_{1,n} T + \mu_2 \sum_{n=1}^{N} r_{2,n} T \tag{3.30}$$

$$\text{s.t.} \quad \sum_{n=1}^{j} g\left(r_{1,n}, r_{2,n}\right) T \leq \sum_{n=1}^{j} E_n, \quad j = 1, \cdots, N, \tag{3.31}$$

$$\left(\sum_{n=1}^{j+1} E_n\right) - \mathcal{E} \leq T \sum_{n=1}^{j} g\left(r_{1,n}, r_{2,n}\right), j = 1, \cdots, N-1. \tag{3.32}$$

3.3 The Optimal Offline Resource Allocation Scheme

In this section, the optimal resource allocation schemes, denoted by $\mathcal{O}$, for solving the Problem (P3.2) and (P3.3) will be described. First, for each problem, the structure of the optimal sum power sequence $g(r_{1,n}, r_{2,n})$, $n = 1, \cdots, N$, is analysed. Then, the optimal rate allocation that achieve the boundary points of the maximum departure region $\mathcal{D}(N)$ is derived.

3.3.1 Optimal Sum Power Allocation

3.3.1.1 Optimal Sum Power Allocation for Infinite Battery Case

This section presents the structural properties of the optimal sum power profile for the optimisation problem (P3.2).

Lemma 1. *The optimal offline solution for Problem (P3.2) satisfies* $g(r_{1,n}, r_{2,n}) \leq g(r_{1,n+1}, r_{2,n+1})$, $\forall n \in \{1, \cdots, N-1\}$, *i.e., the optimal sum power can only stay constant or increase over time.*

Proof. Suppose that in the optimal offline solution, the rates of the two transmitters at some $\dot{n}$-th slot and the $(\dot{n}+1)$-th slot satisfy $g(r_{1,\dot{n}}, r_{2,\dot{n}}) > g(r_{1,\dot{n}+1}, r_{2,\dot{n}+1})$, $\dot{n} \in \{1, \cdots, N-1\}$. The amounts of data sent for the two users over the $\dot{n}$-th slot and the $(\dot{n}+1)$-th under such rate allocation is $(r_{1,\dot{n}} + r_{1,\dot{n}+1}, r_{2,\dot{n}} + r_{2,\dot{n}+1})\, T$.

Define a new rate profile as

$$\begin{aligned}(\tilde{r}_{1,\dot{n}}, \tilde{r}_{2,\dot{n}}) &= (\tilde{r}_{1,\dot{n}+1}, \tilde{r}_{2,\dot{n}+1}) \\ &= \frac{1}{2}(r_{1,\dot{n}}, r_{2,\dot{n}}) + \frac{1}{2}(r_{1,\dot{n}+1}, r_{2,\dot{n}+1}) \\ &= \left(\frac{1}{2}r_{1,\dot{n}} + \frac{1}{2}r_{1,\dot{n}+1}, \frac{1}{2}r_{2,\dot{n}} + \frac{1}{2}r_{2,\dot{n}+1}\right).\end{aligned} \tag{3.33}$$

With the new rate profile, the amounts of data sent for the two users in these two slots are still $(r_{1,\dot{n}} + r_{1,\dot{n}+1}, r_{2,\dot{n}} + r_{2,\dot{n}+1})\, T$. From the convexity of $g(r_1, r_2)$ over r_1 and r_2, we have

$$\begin{aligned}g(\tilde{r}_{1,\dot{n}}, \tilde{r}_{2,\dot{n}}) &= g(\tilde{r}_{1,\dot{n}+1}, \tilde{r}_{2,\dot{n}+1}) \\ &< \frac{1}{2}g(r_{1,\dot{n}}, r_{2,\dot{n}}) + \frac{1}{2}g(r_{1,\dot{n}+1}, r_{2,\dot{n}+1}) \\ &< g(r_{1,\dot{n}}, r_{2,\dot{n}}).\end{aligned} \tag{3.34}$$

The inequality (3.34) indicates that the new rate profile does not violate the causal EH

constraints. The total energy consumed during the $\dot{n}$-th and the $(\dot{n}+1)$-th slots under the new rate profile is smaller than that under the original rate pair, i.e.,

$$(Tg(r_{1,\dot{n}}, r_{2,\dot{n}}) + Tg(r_{1,\dot{n}+1}, r_{2,\dot{n}+1})) - (Tg(\tilde{r}_{1,\dot{n}}, \tilde{r}_{2,\dot{n}}) + Tg(\tilde{r}_{1,\dot{n}+1}, \tilde{r}_{2,\dot{n}+1})) = \Delta > 0. \tag{3.35}$$

Since $g(r_1, r_2)$ is an increasing function over (r_1, r_2), the rate of one transmitter can be increased while the rate of the other one is kept unchanged without violating the EH constraint if the saved energy Δ is spent uniformly in the $(\dot{n}+1)$-th slot, which leads to a larger value of objective function (5.38).

This contradicts the fact that the original rate profile where $g(r_{1,\dot{n}}, r_{2,\dot{n}}) > g(r_{1,\dot{n}+1}, r_{2,\dot{n}+1})$ is the optimal solution of Problem (P3.2). Thus, this proposition is proved. □

Lemma 2. *The optimal offline solution for Problem (P3.2) satisfies that if* $g(r_{1,n}, r_{2,n}) < g(r_{1,n+1}, r_{2,n+1})$, $n \in \{1, \ldots, N-1\}$, *there is no residual energy at the end of the n-th slot, i.e., when the optimal sum power level changes, all harvested energy must be depleted.*

Proof. Suppose that in the optimal offline solution, the rates of the two transmitters at some $\dot{n}$-th slot and the $(\dot{n}+1)$-th slot satisfy $g(r_{1,\dot{n}}, r_{2,\dot{n}}) < g(r_{1,\dot{n}+1}, r_{2,\dot{n}+1})$, $\dot{n} \in \{1, \cdots, N-1\}$ and there is residual energy of amount E_{res} at the end of the $\dot{n}$-th slot. The amounts of data sent for the two users over the $\dot{n}$-th slot and the $(\dot{n}+1)$-th under such solution are $(r_{1,\dot{n}} + r_{1,\dot{n}+1}, r_{2,\dot{n}} + r_{2,\dot{n}+1})\, T$.

Define a new rate profile as

$$(\tilde{r}_{1,\dot{n}}, \tilde{r}_{2,\dot{n}}) = \theta(r_{1,\dot{n}}, r_{2,\dot{n}}) + (1-\theta)(r_{1,\dot{n}+1}, r_{2,\dot{n}+1}), \tag{3.36}$$

$$(\tilde{r}_{1,\dot{n}+1}, \tilde{r}_{2,\dot{n}+1}) = (1-\theta)(r_{1,\dot{n}}, r_{2,\dot{n}}) + \theta(r_{1,\dot{n}+1}, r_{2,\dot{n}+1}), \tag{3.37}$$

where $\theta \in (0, 1)$. With such new rate profile, the amounts of bits sent for the two users over these two slots are still $(r_{1,\dot{n}} + r_{1,\dot{n}+1}, r_{2,\dot{n}} + r_{2,\dot{n}+1})\, T$.

Notice that from the convexity of $g(r_1, r_2)$ over r_1 and r_2, we have

$$g(\tilde{r}_{1,\dot{n}}, \tilde{r}_{2,\dot{n}}) < \theta g(r_{1,\dot{n}}, r_{2,\dot{n}}) + (1-\theta) g(r_{1,\dot{n}+1}, r_{2,\dot{n}+1}), \tag{3.38}$$

$$g(\tilde{r}_{1,\dot{n}+1}, \tilde{r}_{2,\dot{n}+1}) < (1-\theta) g(r_{1,\dot{n}}, r_{2,\dot{n}}) + \theta g(r_{1,\dot{n}+1}, r_{2,\dot{n}+1}). \tag{3.39}$$

The sum power $g(\tilde{r}_{1,\dot{n}}, \tilde{r}_{2,\dot{n}})$ may be larger than $g(r_{1,\dot{n}}, r_{2,\dot{n}})$. However, since the function $g(r_1, r_2)$ is continuous over (r_1, r_2), there must exists some $\theta \in (0, 1)$ such that $(g(\tilde{r}_{1,\dot{n}}, \tilde{r}_{2,\dot{n}}) - g(r_{1,\dot{n}}, r_{2,\dot{n}}))\, T \leq E_{\text{res}}$. With such θ, the new rate profile still satisfies the causal EH constraints. From (3.38) and (3.39), we have

$$(Tg(r_{1,\dot{n}}, r_{2,\dot{n}}) + Tg(r_{1,\dot{n}+1}, r_{2,\dot{n}+1})) - (Tg(\tilde{r}_{1,\dot{n}}, \tilde{r}_{2,\dot{n}}) + Tg(\tilde{r}_{1,\dot{n}+1}, \tilde{r}_{2,\dot{n}+1})) = \Delta > 0, \tag{3.40}$$

which indicates that the total energy consumed over the $\dot{n}$-th and $(\dot{n}+1)$-th slots by the new rate profile is less than the original solution. Since $g(r_1, r_2)$ is an increasing function over (r_1, r_2), we can increase the rate of one transmitter while keep the rate of the other one unchanged without violating the EH constraint if we spend the saved energy Δ uniformly in the $(\dot{n}+1)$-th slot, which leads to a larger value of objective funtion (5.38).

This contradicts the fact that the original rate profile is the optimal solution of Problem (P3.2). Thus, this proposition is proved. □

Remark 2. *In [YOU12] and [AUBE11], properties similar to Lemma 1 and Lemma 2 were proved by KKT conditions, which directly depends on the expression of the sum power function $g(r_1, r_2)$. It is worth noting that our proof of Lemma 1 and Lemma 2 only involves the convexity of the sum power function $g(r_1, r_2)$ and hence can be easily applied to other scenarios/models as long as the sum power function is convex.*

As indicated by Lemma 1 and 2, the optimal sum power sequence for the Problem

(P3.3) has the same structural properties as that for the single-user channel case discussed in [YU12b]. Given an energy input sequence $\boldsymbol{\omega}$, the optimal offline sum power sequence $\mathbf{P}^{\mathcal{O}} = [P_1^{\mathcal{O}}, \cdots, P_N^{\mathcal{O}}]^T$, where $P_n^{\mathcal{O}}, n = 1, \cdots, N$, denotes the optimal sum power in the n-th slot, can be obtained as [YU12b]:

$$n_k = \arg \min_{n_{k-1}<n\leq N} \left\{ \frac{\sum_{j=n_{k-1}+1}^{n} E_j}{(n-n_{k-1})\,T} \right\}, \tag{3.41}$$

$$g(r_{1,n}, r_{2,n}) = \frac{\sum_{j=n_{k-1}+1}^{n_k} E_j}{(n_k-n_{k-1})\,T} \doteq P_n^{\mathcal{O}}, \text{for } n_{k-1} < n \leq n_k, \tag{3.42}$$

where $n_0 = 0$.

3.3.1.2 Optimal Sum Power Allocation for Finite Battery Case

This section presents the structural properties of the optimal sum power profile for the optimisation problem (P3.3).

Lemma 3. *The optimal solution for problem (P3.3) satisfies that if* $g(r_{1,n}, r_{2,n}) \neq g(r_{1,n+1}, r_{2,n+1})$*, either the energy is depleted at the end of the* n*-th slot or the battery is full at the beginning of the* $(n+1)$*-th slot,* $\forall n \in \{1, \cdots, N-1\}$*.*

Proof. Suppose that $g(r_{1,\dot{n}}, r_{2,\dot{n}}) \neq g(r_{1,\dot{n}+1}, r_{2,\dot{n}+1})$ for some $\dot{n} \in \{1, \cdots, N-1\}$, and the battery is neither depleted at the end of the $\dot{n}$-th slot nor full at the beginning of the $(\dot{n}+1)$-th slot.

Denote the residual energy at the end of the $\dot{n}$-th slot as

$$E_{\text{res}} = \sum_{n=1}^{\dot{n}} E_n - T \sum_{n=1}^{\dot{n}} g\left(r_{1,n}, r_{2,n}\right),$$

we have $E_{\text{res}} > 0$ and $E_{\text{res}} + E_{\dot{n}+1} < \mathcal{E}$. The amounts of data sent for the two users over the $\dot{n}$-th and $(\dot{n}+1)$-th slots under such rate allocation are $(r_{1,\dot{n}} + r_{1,\dot{n}+1}, r_{2,\dot{n}} + r_{2,\dot{n}+1})\,T$.

Define a new rate profile as $(\tilde{r}_{1,\dot{n}}, \tilde{r}_{2,\dot{n}}) = \theta(r_{1,\dot{n}}, r_{2,\dot{n}}) + (1-\theta)(r_{1,\dot{n}+1}, r_{2,\dot{n}+1})$ and

$(\tilde{r}_{1,\dot{n}+1}, \tilde{r}_{2,\dot{n}+1}) = (1-\theta)(r_{1,\dot{n}}, r_{2,\dot{n}}) + \theta(r_{1,\dot{n}+1}, r_{2,\dot{n}+1})$, where $\theta \in (0,1)$. By adopting the new rate profile $(\tilde{r}_{1,\dot{n}}, \tilde{r}_{2,\dot{n}})$ and $(\tilde{r}_{1,\dot{n}+1}, \tilde{r}_{2,\dot{n}+1})$, the amounts of data sent for the two users over these two slots are still $(r_{1,\dot{n}} + r_{1,\dot{n}+1}, r_{2,\dot{n}} + r_{2,\dot{n}+1})\, T$.

Note that for any $\theta \in (0,1)$, from the convexity of $g(r_1, r_2)$, we have

$$g(\tilde{r}_{1,\dot{n}}, \tilde{r}_{2,\dot{n}}) < \theta g(r_{1,\dot{n}}, r_{2,\dot{n}}) + (1-\theta) g(r_{1,\dot{n}+1}, r_{2,\dot{n}+1}), \tag{3.43}$$

$$g(\tilde{r}_{1,\dot{n}+1}, \tilde{r}_{2,\dot{n}+1}) < (1-\theta) g(r_{1,\dot{n}}, r_{2,\dot{n}}) + \theta g(r_{1,\dot{n}+1}, r_{2,\dot{n}+1}), \tag{3.44}$$

and hence

$$\left(g\left(\tilde{r}_{1,\dot{n}}, \tilde{r}_{2,\dot{n}}\right) + g\left(\tilde{r}_{1,\dot{n}+1}, \tilde{r}_{2,\dot{n}+1}\right)\right) T < \left(g\left(r_{1,\dot{n}}, r_{2,\dot{n}}\right) + g\left(r_{1,\dot{n}+1}, r_{2,\dot{n}+1}\right)\right) T. \tag{3.45}$$

1. If $g(r_{1,\dot{n}}, r_{2,\dot{n}}) > g(r_{1,\dot{n}+1}, r_{2,\dot{n}+1})$, from (3.43), we have $g(\tilde{r}_{1,\dot{n}}, \tilde{r}_{2,\dot{n}}) < g(r_{1,\dot{n}}, r_{2,\dot{n}})$, which indicates the energy consumed in the $\dot{n}$-th slot is reduced and therefore the causal EH constraints are not violated under the new rate profile, with any $\theta \in (0,1)$. Under the new rate profile, the residual energy at the end of the $\dot{n}$-th slot is $\tilde{E}_{\text{res}} = E_{\text{res}} + (g(r_{1,\dot{n}}, r_{2,\dot{n}}) - g\left(\tilde{r}_{1,\dot{n}}, \tilde{r}_{2,\dot{n}}\right)) T > E_{\text{res}}$. Since $\mathcal{E} - E_{\dot{n}+1} - E_{\text{res}} > 0$ and $g(r_1, r_2)$ is continuous over (r_1, r_2), we can always find a $\theta \in (0,1)$ such that $g\left(r_{1,\dot{n}}, r_{2,\dot{n}}\right) - g(\tilde{r}_{1,\dot{n}}, \tilde{r}_{2,\dot{n}}) \leq \frac{\mathcal{E} - E_{\dot{n}+1} - E_{\text{res}}}{T}$. With such θ, we have $\tilde{E}_{\text{res}} \leq \mathcal{E} - E_{\dot{n}+1}$, which indicates the battery capacity would not be exceeded at the beginning of the $(\dot{n}+1)$-th slot.

   As can be seen from (3.45), the total energy consumed by the new rate profile is less than the original rate profile. The saved energy can be used in the $(\dot{n}+1)$-th slot to increase the value of the objective function. This contradicts the optimality of the original rate profile.

2. If $g(r_{1,\dot{n}}, r_{2,\dot{n}}) < g(r_{1,\dot{n}+1}, r_{2,\dot{n}+1})$, we have $g(\tilde{r}_{1,\dot{n}+1}, \tilde{r}_{2,\dot{n}+1}) < g(r_{1,\dot{n}+1}, r_{2,\dot{n}+1})$, $\forall \theta \in (0,1)$, from (3.44).

   Suppose that there exists some $\theta \in (0,1)$, such that $g(\tilde{r}_{1,\dot{n}}, \tilde{r}_{2,\dot{n}}) \leq g(r_{1,\dot{n}}, r_{2,\dot{n}})$.

Let $\hat{\theta}$ denote the largest θ such that $g(\tilde{r}_{1,\dot{n}}, \tilde{r}_{2,\dot{n}}) \leq g(r_{1,\dot{n}}, r_{2,\dot{n}})$. It is easy to check from the convex and continuous properties of $g(r_1, r_2)$ that $g(\tilde{r}_{1,\dot{n}}, \tilde{r}_{2,\dot{n}}) \leq g(r_{1,\dot{n}}, r_{2,\dot{n}}), \forall \theta \in (0, \hat{\theta}]$. With any $\theta \in (0, \hat{\theta}]$, the causal EH constraints are not violated. Since $g(r_1, r_2)$ is continuous over (r_1, r_2), we can always find a $\theta \in (0, \hat{\theta}]$ such that $g\left(r_{1,\dot{n}}, r_{2,\dot{n}}\right) - g(\tilde{r}_{1,\dot{n}}, \tilde{r}_{2,\dot{n}}) \leq \frac{\mathcal{E} - E_{\dot{n}+1} - E_{\text{res}}}{T}$, which indicates the battery capacity would not be exceeded at the beginning of the $(\dot{n}+1)$-th slot. Since $g(\tilde{r}_{1,\dot{n}+1}, \tilde{r}_{2,\dot{n}+1}) < g(r_{1,\dot{n}+1}, r_{2,\dot{n}+1})$ and $g(\tilde{r}_{1,\dot{n}}, \tilde{r}_{2,\dot{n}}) < g(r_{1,\dot{n}}, r_{2,\dot{n}})$, the energy consumed by the new rate profile is less than that consumed by the original rate profile. The saved energy can be used in the $(\dot{n}+1)$-th slot to increase the value of the objective function. This contradicts the optimality of the original rate allocation.

Suppose that $g(\tilde{r}_{1,\dot{n}}, \tilde{r}_{2,\dot{n}}) > g(r_{1,\dot{n}}, r_{2,\dot{n}})$, $\forall \theta \in (0, 1)$, the battery capacity would not be exceeded at the beginning of the $(\dot{n}+1)$-th slot under the new rate profile. Since $g(r_1, r_2)$ is continuous over (r_1, r_2), there must exist some $\theta \in (0, 1)$ such that $\left(g\left(\tilde{r}_{1,\dot{n}}, \tilde{r}_{2,\dot{n}}\right) - g\left(r_{1,\dot{n}}, r_{2,\dot{n}}\right)\right) T \leq E_{\text{res}}$, which indicates that the causal EH constraints are not violated. According to (3.45), the new rate profile results in less energy consumption, compared with the original rate allocation. The saved energy can be used in the $(\dot{n}+1)$-th slot to increase the value of the objective function. This contradicts the optimality of the original rate allocation.

Thus, this lemma is proved. □

Lemma 4. *The optimal solution for problem (P3.3) satisfies that for* $n = 1, \cdots, N-1$, $g(r_{1,n}, r_{2,n}) \leq g(r_{1,n+1}, r_{2,n+1})$ *if the battery is depleted at the end of the* n*-th slot and* $g(r_{1,n}, r_{2,n}) \geq g(r_{1,n+1}, r_{2,n+1})$ *if the battery is full at the beginning of the* $(n+1)$*-th slot.*

Proof. The proof is similar to that for Lemma 3 and is thus omitted. □

Remark 3. *In [OYU12a], properties similar to Lemma 3 and Lemma 4 were proved by KKT conditions, which directly depends on the expression of the sum power function* $g(r_1, r_2)$*. It is worth noting that our proof of Lemma 3 and Lemma 4 only involves the convexity of the sum power function* $g(r_1, r_2)$ *and hence can be easily applied to other*

scenarios/models as long as the sum power function is convex.

Based on Lemma 3 and Lemma 4, it can be seen that the optimal sum power sequence of problem (P3.3) has the same structural properties as that in the point-to-point channel with limited battery capacity in [TY12a]. Therefore, the optimal sum power sequence can be obtained with similar method as in [TY12a]. The following part will describe how the first constant power level and interval is determined. The rest of the scheme could be obtained similarly with updated problem after obtaining each constant power level and period.

Suppose the sum power level keeps constant at p_1 in the first n_1 slot. Define two sets of powers $\{\check{p}[1], \check{p}[2], \cdots\}$ and $\{\hat{p}[1], \hat{p}[2], \cdots\}$, where $\check{p}[n] = \frac{\sum_{j=1}^{n} E_n}{nT}$ and $\hat{p}[n] = \frac{\sum_{j=1}^{n+1} E_n - \mathcal{E}}{nT}$ denote the constant power levels needed to adopt in the first n slots such that the battery would be empty at the end of the n-th slot or full at the beginning of the $(n+1)$-th slot, respectively. Define $\mathbf{p}[n]$ as the closed interval $\mathbf{p}[n] = [\hat{p}[n], \check{p}[n]]$. Note that the interval $\mathbf{p}[n]$ implicates the range of constant power level that achieve energy-feasibility at the $(n+1)$-th energy arrival (in other words, constant power level inside $\mathbf{p}[n]$ ensure that the battery would be neither depleted by the end of the n-th slot, nor overflowed at the beginning of the $(n+1)$-th slot), though without guaranteeing the feasibility at previous energy arrivals.

From the definition of the power interval $\mathbf{p}[n]$ it could be seen that a constant power has to be inside $\mathbf{p}[n]$, for each $n \in \{1, \cdots, k\}$, to ensure its feasibility in the first k slots. As such, an upper bound $\tilde{n}$ on the duration of the first constant power period n_1 can be calculated as

$$\tilde{n} = \max \left\{ n \left| \bigcap_{j=1}^{n} \mathbf{p}\left[j\right] \neq \emptyset, j = 1, \cdots, N \right. \right\}. \tag{3.46}$$

The first constant power level and interval satisfies $p_1 \in \bigcap_{j=1}^{n_1} \mathbf{p}\left[j\right]$ and it cannot be feasible beyond $\tilde{n}$. With the constant transmission power p_1, the battery will be either depleted at the end of the $(\tilde{n}+1)$-th slot or overflowed at the beginning of the $(\tilde{n}+2)$-th

slot. If the battery is depleted at the end of the $(\tilde{n}+1)$-th slot, the power level needs to decrease from the begining of the (n_1+1)-th slot. Otherwise, it needs to increase. From Lemma 3 and 4, the power level may only increase or decrease when the battery is either depleted or full. This fact indicates that p_1 is either $\check{p}[n_1]$ or $\hat{p}[n_1]$, respectively, for the two cases discussed above. The optimal power level p_1 can thus be decided from whether the power level tends to increase or decrease after n_1-th slot.

Note that after p_1 and n_1 are determined, the parameters could be modified to obtain a shifted problem which starts from the (n_1+1)-th slot. By repeating the process of finding p_1 and n_1, the optimal sum power sequence $\mathbf{P}^{\mathcal{O}} = [P_1^{\mathcal{O}}, \cdots, P_N^{\mathcal{O}}]^T$ could be obtained. The algorithm for calculating the optimal sum power profile for the finite battery capacity case is presented in Algorithm 1.

3.3.2 Optimal Resource Allocation between the two Transmitters

In subsection 3.3.1, the optimal sum power profiles for both the infinite and finite battery capacity cases were obtained.

From (3.41),(3.42) and Algorithm 1, it is observed that the optimal sum power sequence $\mathbf{P}^{\mathcal{O}} = [P_1^{\mathcal{O}}, \cdots, P_N^{\mathcal{O}}]$ only depends on the energy input sequence and is not influenced by the values of μ_1 and μ_2, for both cases. The constraints of Problem (P3.2) and P(3.3) can be rewritten as

$$g\left(r_{1,n}, r_{2,n}\right) = P_n^{\mathcal{O}}, n = 1, \cdots, N \tag{3.47}$$

where $P_n^{\mathcal{O}}$ is the optimal sum power profile obtained by (3.41),(3.42) for the infinite battery capacity case and by Algorithm 1 for the finite battery capacity case.

Therefore, both problem (P3.2) and P(3.3) can be decomposed into N optimisation

Algorithm 1: Calculating the optimal sum power profile for the finite battery capacity case

Initialization $\tilde{n} = 0$;
while $\tilde{n} \neq N$ **do**
  Calculate $\tilde{n}$ by (3.46);
  if $\tilde{n} = N$ **then**
    $n_1 = N$, $p_1 = \frac{\sum_{n=1}^{N} E_n}{NT}$;
  else
    if $P[\tilde{n}+1] > \bigcap_{j=1}^{\tilde{n}} \mathbf{p}[j]$ **then**
      $n_1 = \max\left\{ n \left| \check{p}[n] \in \bigcap_{j=1}^{n} \mathbf{p}[j] \right. \right\}$;
      $p_1 = \check{p}[n_1]$;
    else
      $n_1 = \max\left\{ n \left| \hat{p}[n] \in \bigcap_{j=1}^{n} \mathbf{p}[j] \right. \right\}$;
      $p_1 = \hat{p}[n_1]$;
    end
    Update/shift the problem;
  end
end

problems as follows [YOU12]. For $n = 1, \ldots, N$,

$$\text{(P3.4n)} \quad \max_{\{r_{1,n}, r_{2,n}\}} \quad \mu_1 r_{1,n} + \mu_2 r_{2,n} \tag{3.48}$$

$$\text{s.t.} \quad g(r_{1,n}, r_{2,n}) = P_n^{\mathcal{O}}. \tag{3.49}$$

Denote the curve defined by $g(r_{1,n}, r_{2,n}) = P_n^{\mathcal{O}}$ as $\mathcal{G}_n$ and the power allocated to transmitter $i, i = 1, 2$, in problem (P3.4n) as $P_{i,n}^{\mathcal{O}}$. By first order derivative analysis, it can seen that the optimal solution $\left(r_{1,n}^{\mathcal{O}}, r_{2,n}^{\mathcal{O}}\right)$ should satisfy:

1. $g\left(r_{1,n}^{\mathcal{O}}, r_{2,n}^{\mathcal{O}}\right) = P_n^{\mathcal{O}}$;

2. the tangent line for the curve $\mathcal{G}_n$ at this point equals $-\frac{\mu_1}{\mu_2}$.

From (3.8) we have $r_2 = \log\left(\frac{h_1\left(1+h_2P_n^{\mathcal{O}}\right)}{h_2 2^{r_1}+h_1-h_2}\right)$. The first order derivative $\frac{dr_2}{dr_1}$ is given as

$$\frac{dr_2}{dr_1} = -\frac{h_2 2^{r_1}}{h_2 2^{r_1} + h_1 - h_2} > -1. \tag{3.50}$$

As indicated by (3.50), the derivative $\frac{dr_2}{dr_1}$ decreases as r_1 increases and $\lim_{r_1\to\infty} \frac{dr_2}{dr_1} = -1$.

Lemma 5. *For $-\frac{\mu_1}{\mu_2} \leq -1$, all power is allocated to transmitter 1, that is, $\left(P_{1,n}^{\mathcal{O}}, P_{2,n}^{\mathcal{O}}\right) = \left(P_n^{\mathcal{O}}, 0\right)$ and $\left(r_{1,n}^{\mathcal{O}} r_{2,n}^{\mathcal{O}}\right) = \left(\log\left(1 + h_1 P_n^{\mathcal{O}}\right), 0\right)$. For any given $-\frac{\mu_1}{\mu_2} > -1$, there exists a capping rate $R_c = \left(\log\left(\frac{(h_1-h_2)\mu_1}{h_2(\mu_2-\mu_1)}\right)\right)^+$ at transmitter 1:*

1. *If $P_n^{\mathcal{O}} \leq g\left(R_c, 0\right) = \left(\frac{h_1\mu_1-h_2\mu_2}{h_1h_2(\mu_2-\mu_1)}\right)^+$, all the sum power P_n is allocated to transmitter 1, that is,*

$$\left(P_{1,n}^{\mathcal{O}}, P_{2,n}^{\mathcal{O}}\right) = \left(P_n^{\mathcal{O}}, 0\right), \tag{3.51}$$

$$\left(r_{1,n}^{\mathcal{O}} r_{2,n}^{\mathcal{O}}\right) = \left(\log\left(1 + h_1 P_n^{\mathcal{O}}\right), 0\right). \tag{3.52}$$

2. *If $P_n^{\mathcal{O}} > g\left(R_c, 0\right) = \left(\frac{h_1\mu_1-h_2\mu_2}{h_1h_2(\mu_2-\mu_1)}\right)^+$, the sum power $P_n^{\mathcal{O}}$ is allocated to the two transmitters such that transmitter 1 has the rate $r_{1,n}^{\mathcal{O}} = R_c$, that is,*

$$\left(P_{1,n}^{\mathcal{O}}, P_{2,n}^{\mathcal{O}}\right) = \left(\frac{(2^{R_c}-1)(1+h_2P_n^{\mathcal{O}})}{h_1-h_2+h_2 2^{R_c}}, \frac{1+h_1P_n^{\mathcal{O}}-2^{R_c}}{h_1-h_2+h_2 2^{R_c}}\right), \tag{3.53}$$

$$\left(r_{1,n}^{\mathcal{O}}, r_{2,n}^{\mathcal{O}}\right) = \left(R_c, \log\left(\frac{h_1\left(1+h_2P_n^{\mathcal{O}}\right)}{h_1-h_2+h_2 2^{R_c}}\right)\right). \tag{3.54}$$

Following Lemma 5, the optimal solution $(r_{1,n}^{\mathcal{O}}, r_{2,n}^{\mathcal{O}})$ of problem (P3.3) and the corresponding power for the two transmitters $(P_{1,n}^{\mathcal{O}}, P_{2,n}^{\mathcal{O}})$, can be obtained by solving problems (P3.4n), $\forall n \in \{1, \cdots, N\}$.

Remark 4. *The weighting factors could be interpreted as priorities allocated to transmitters to some extent. When $-\frac{\mu_1}{\mu_2} \leq -1$, i.e., $\mu_1 > \mu_2$, transmitter 1, who enjoys the*

better channel gain, is allocated with higher priority. Therefore, it is natural to allocate all the power to transmitter 1 to fully exploit its advantageous channel gain. When $-\frac{\mu_1}{\mu_2} > -1$*, i.e.,* $\mu_1 < \mu_2$*, higher priority is allocated to transmitter 2. In Lemma 5, the capping rate* R_c *decreases as* μ_2 *increases. In other words, the larger* μ_2 *is, the more likely transmitter 2 will get higher power/rate. This confirms* μ_1 *and* μ_2*'s effect as the weighting factors. The weighting factors can be used to adjust the user fairness between the two transmitters.*

3.4 MAC-BC Throughput Duality with Renewable Source

In the previous section, the optimal offline resource allocation scheme for the MAC with a shared energy harvester was derived. In this section, it will be shown that with the same energy arrivals, the MAC with a shared energy harvester and its dual BC achieve the same maximum departure region within the N slots. In this section, the superscript $^{\mathrm{BC}}$ is used to indicate the optimal offline quantities related to BC, and similarly superscript $^{\mathrm{MAC}}$ is used for MAC (and thus suppress the superscript $^{\mathcal{O}}$).

The dual BC [JVG04] of the MAC in Fig. 3.1 is shown in Fig. 3.7. The constant channel power gains in BC are the same as those in MAC (h_1 and h_2 from the transmitter to receiver 1 and receiver 2, respectively). The received signals at the two users are both corrupted by CSCG noise with zero mean and unit variance. The optimal power allocation scheme to achieve the maximum departure region in BC channel where the transmitter is powered by an energy harvester was investigated in [YOU12] and is summarised here for completeness.

As mentioned in Section 3.3, the optimal sum power profile in the BC with infinite battery case also satisfies Lemma 1 and Lemma 2, and can be obtained by (3.41) and (3.42) (Lemma 3 in [YOU12]). For the BC with finite battery case, the optimal sum power profile also satisfies Lemma 3 and Lemma 4 and thus is obtained by Algorithm. 1. Therefore, for both cases, with the same energy arrival profile, we have $P_n^{\mathrm{BC}} = P_n^{\mathrm{MAC}}, n =$

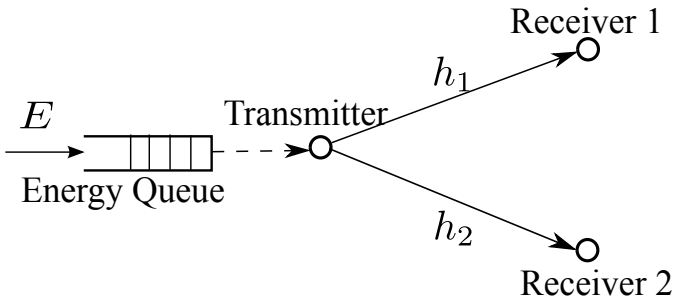

Figure 3.7: The dual BC of the MAC with a shared energy harvester.

$1, \cdots, N$, i.e., the optimal sum power profiles of the MAC and its dual BC are exactly the same, where P_n^{BC} denotes the sum power allocated to the messages for both receiver 1 and receiver 2 in the n-th slot.

In the BC case, there exists a capping power

$$P_c = \left(\frac{h_1\mu_1 - h_2\mu_2}{h_1 h_2(\mu_2 - \mu_1)} \right)^+. \tag{3.55}$$

It is worth noting that $P_c = g\left(R_c, 0\right)$.

For each $n \in \{1, \cdots, N\}$, the optimal rate/power for the messages of the two users can be obtained as follows.

1) If $P_n^{\mathrm{BC}} \leq P_c$, all power is allocated to message for receiver 1, i.e.,

$$\left(P_{1,n}^{\mathrm{BC}}, P_{2,n}^{\mathrm{BC}}\right) = \left(P_n^{\mathrm{BC}}, 0\right), \tag{3.56}$$

$$\left(r_{1,n}^{\mathrm{BC}}, r_{2,n}^{\mathrm{BC}}\right) = \left(\log(1 + h_1 P_n^{\mathrm{BC}}), 0\right), \tag{3.57}$$

where $P_{i,n}^{\mathrm{BC}}$ and $r_{i,n}^{\mathrm{BC}}$ denote the power allocated to the message for receiver i and the rate for receiver i in the n-th slot, $i = 1, 2$.

2) If $P_n^{\mathrm{BC}} > P_c$, the power allocated to message for receiver 1 is exactly P_c, while all

the remaining power is allocated to message for receiver 2, i.e.,

$$\left(P_{1,n}^{\mathrm{BC}}, P_{2,n}^{\mathrm{BC}}\right) = \left(P_c, P_n^{\mathrm{BC}} - P_c\right), \tag{3.58}$$

$$\left(r_{1,n}^{\mathrm{BC}}, r_{2,n}^{\mathrm{BC}}\right) = \left(\log(1+h_1P_c), \log\left(1+\frac{h_2\left(P_n^{\mathrm{BC}}-P_c\right)}{1+h_2P_c}\right)\right). \tag{3.59}$$

Substitute the expression of P_c in (3.55) into (3.59), the optimal rate pair for the case of $P_n^{\mathrm{BC}} > P_c$ can be rewritten as

$$\left(r_{1,n}^{\mathrm{BC}}, r_{2,n}^{\mathrm{BC}}\right) = \left(R_c, \log\left(\frac{h_1(1+h_2P_n)}{h_1-h_2+h_22^{R_c}}\right)\right). \tag{3.60}$$

Compare the optimal rates given in (3.57) and (3.60) for the BC case with those given in (3.52) and (3.54) for the MAC case, we have the following proposition.

Proposition 4. *With the same energy profile and any fixed μ_1 and μ_2, the optimal sum power profiles, the optimal rates profiles, and the total amounts of transmitted data for MAC and its dual BC are the same, i.e., $P_n^{\mathrm{MAC}} = P_n^{\mathrm{BC}}, n = 1, \cdots, N$, $\left(r_{1,n}^{\mathrm{MAC}}, r_{2,n}^{\mathrm{MAC}}\right) = \left(r_{1,n}^{\mathrm{BC}}, r_{2,n}^{\mathrm{BC}}\right), n = 1, \cdots, N$, and $\left(B_1^{\mathrm{MAC}}, B_2^{\mathrm{MAC}}\right) = \left(B_1^{\mathrm{BC}}, B_2^{\mathrm{BC}}\right)$. Therefore, the maximum departure regions of MAC and its dual BC are also the same, i.e., $\mathcal{D}(N)^{\mathrm{MAC}} = \mathcal{D}(N)^{\mathrm{BC}}$.*

It is worth noting that, however, the optimal power profiles $(P_{1,n}^{\mathrm{BC}}, P_{2,n}^{\mathrm{BC}})$ and $(P_{1,n}^{\mathrm{MAC}}, P_{2,n}^{\mathrm{MAC}})$ of the dual BC and MAC, respectively, are different, as indicated by (3.53) and (3.58).

3.5 Numerical Examples

In this section, one energy input sequence is used as an example to illustrate the properties of the optimal offline scheme and the boundary of the maximum departure region.

We adopt $h_1 = 0.8$, $h_2 = 0.7$, $\mathcal{E} = 20$ J, $N = 15$, $T = 10$ s.

There are infinite possible input sequences. Similarly to [YU12b, YU12a, YOU12],

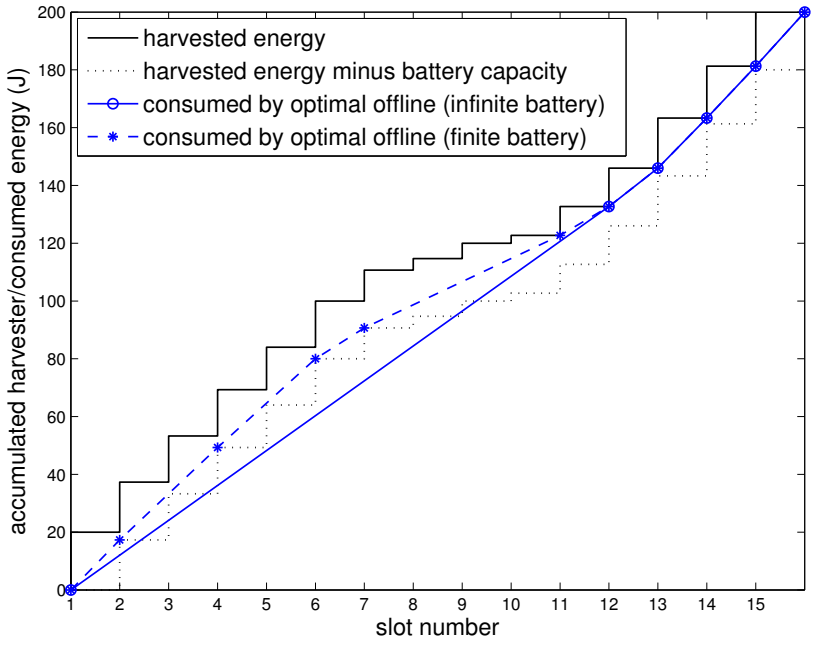

Figure 3.8: The accumulated amounts of harvested energy and the amounts of energy consumed by the optimal offline schemes for $\boldsymbol{\omega}_1$ in the Gaussian MAC with a shared energy harvester.

one random energy input sequence $\boldsymbol{\omega}_1$ is used as an example to demonstrate the properties of the optimal offline schemes:

$$\boldsymbol{\omega}_1 = (20, 17.3, 16, 16, 14.7, 16, 10.7, 4, 5.3, 2.7, 10, 13.3, 17.3, 18, 18.7) \text{ J}.$$

Given $\boldsymbol{\omega}_1$, the sum power sequences obtained by the optimal offline schemes for the infinite battery capacity case and the finite capacity case are given as

$$\mathbf{P}^{\mathcal{O}} = [1.206, 1.206, 1.206, 1.206, 1.206, 1.206, 1.206, 1.206, 1.206, 1.206, 1.206, 1.33, 1.73, 1.8, 1.87]^T \text{ J/s},$$

and

$$\mathbf{P}_{\mathcal{E}}^{\mathcal{O}} = [1.73, 1.6, 1.6, 1.535, 1.535, 1.07, 0.8, 0.8, 0.8, 0.8, 1, 1.33, 1.73, 1.8, 1.87]^T \text{ J/s},$$

respectively.

As shown in Fig. 3.8, the slopes of the blue solid curve and the blue dash curve represent the sum power levels for the optimal offline scheme $\mathcal{O}$ with infinite and finite battery capacities, respectively. The blue curves are both beneath the black solid curve that represents the accumulated amount of harvested energy, which indicates the causal EH constraints are satisfied by both schemes. Moreover, the blue dash curve is above the black dot curve, which represents the accumulated amount of harvested energy minus the battery capacity. This indicates the battery non-overflow constraints are satisfied.

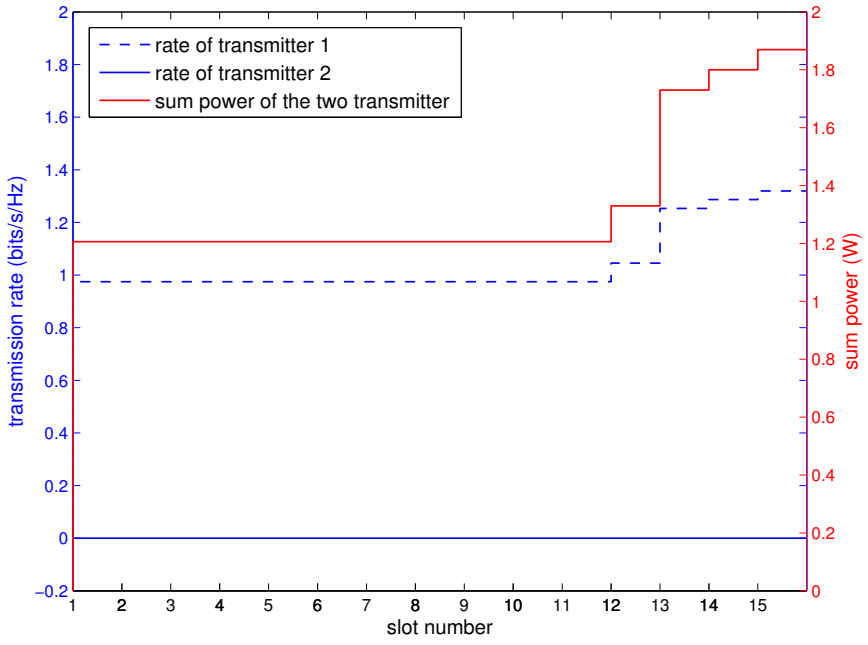

Figure 3.9: Transmission rates of the two transmitters (blue curves, correspond to the left Y axis) when $\mu_1 = 0.7, \mu_2 = 0.3$ and the sum power levels (red curve, corresponds to the right Y axis) during the 15 slots for the Gaussian MAC with a shared energy harvester.

Given the energy input sequence $\boldsymbol{\omega}_1$, the sum power levels (which are independent of μ_1, μ_2) and the transmission rates of the two transmitters for the optimal offline scheme $\mathcal{O}$ (with infinite battery capacity) when $\mu_1 = 0.7$ and $\mu_1 = 0.485$ are illustrated in

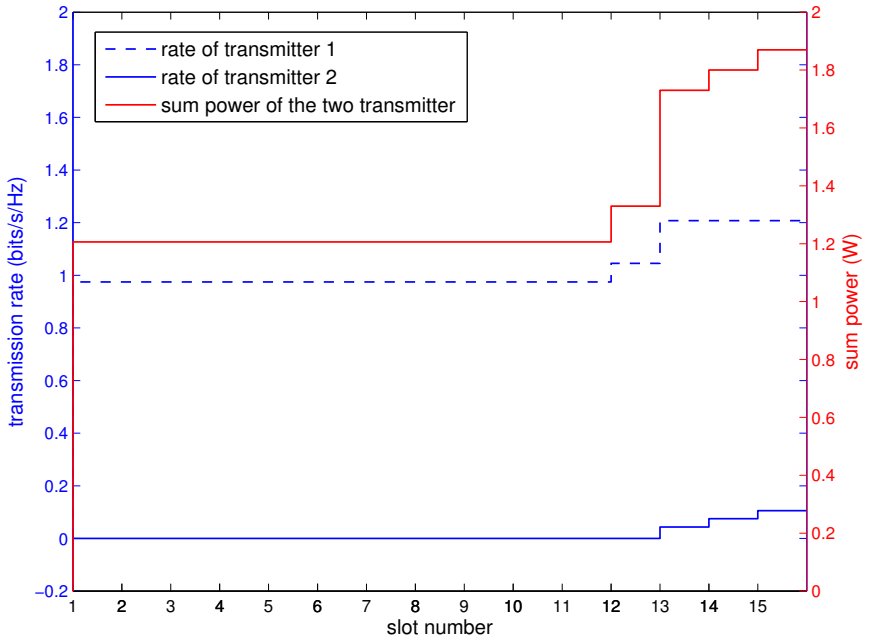

Figure 3.10: Transmission rates of the two transmitters (blue curves, correspond to the left Y axis) when $\mu_1 = 0.485, \mu_2 = 0.515$ and the sum power levels (red curve, corresponds to the right Y axis) during the 15 slots for the Gaussian MAC with a shared energy harvester.

Fig. 3.9 and Fig. 3.10, respectively.

Based on the optimal rate allocation, when $\mu_1 = 0.7$, all power is allocated to transmitter 1 all the time. Therefore, the rate transmitter 2 is always zero whereas the rate of transmitter 1 increases as the sum power increases, as shown in Fig. 3.9.

When $\mu_1 = 0.485$, in the optimal offline scheme, there exists a capping rate at transmitter 1 given by $R_c = \log\left(\frac{(h_1-h_2)\mu_1}{h_2(\mu_2-\mu_1)}\right) = 1.2075$ bits/s. As can be seen from Fig. 3.10, in slot 1 to 12, the sum power is smaller than $g(R_c, 0) = 1.637$ bits/s, therefore all sum power is allocated to transmitter 1 and its rate increases as the sum power increases; in slot 12 to 15, the sum power is larger than $g(R_c, 0) = 1.637$ bits/s, therefore, the rate of transmitter 1 keeps at the capping rate $R_c = 1.2075$ bits/s, and the remaining

power is allocated to transmitter 2, whose rate increases as the sum power increases.

Fig. 3.11 shows the performance achieved by the optimal offline scheme $\mathcal{O}$, i.e., the boundary of the maximum departure region, with both infinite and several different finite battery capacities, i.e., $\mathcal{E} = 20, 15, 10$ J, given $\boldsymbol{\omega}_1$. As expected, the maximum departure region with infinite battery capacity is larger than those with finite battery capacities. Moreover, the smaller the battery capacity, the smaller the maximum departure region.

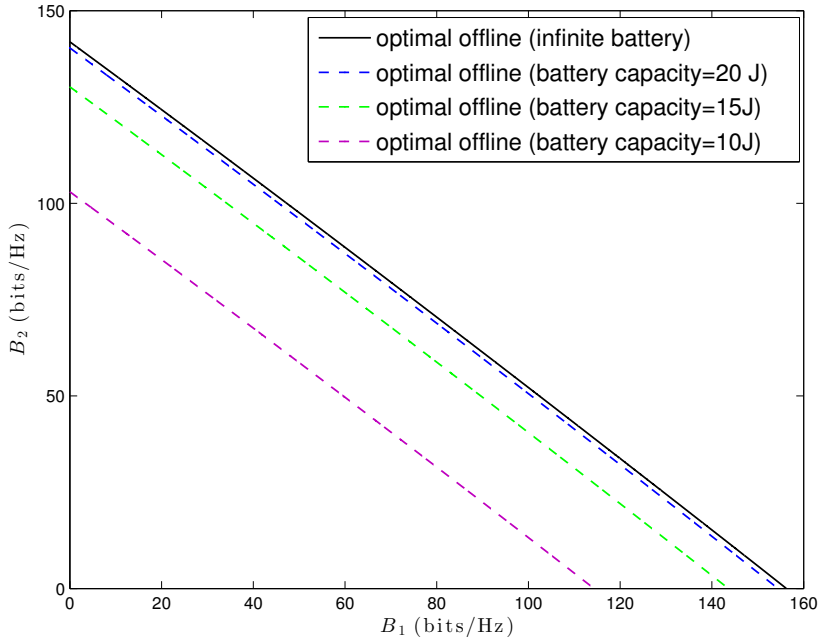

Figure 3.11: The boundaries of $\mathcal{D}(N)$ achieved by the optimal offline schemes for serving $\boldsymbol{\omega}_1$ in the Gaussian MAC with a shared energy harvester with both infinite and finite battery capacites over 15 slots (150s).

3.6 Summary

In this chapter, the optimal offline resource allocation schemes for the two-user Gaussian MAC with a shared energy harvester were studied. Both the infinite battery capacity case and the finite battery capacity case were considered. The structure of the optimal offline sum power profile and the optimal offline rate scheduling over the two transmitters to achieve the boundary points of the maximum departure region were obtained. It is proved that there exists a capping rate at the stronger transmitter; the weaker transmitter can get non-zero rate (power) only when the stronger transmitter reach its capping rate. The fact that the MAC with a shared energy harvester and its dual BC own the same maximum departure regions was also revealed. Numerical examples were shown to illustrate the properties of the optimal offline schemes.

Chapter 4

Online Resource Allocation Schemes for Multiple Access Channels with a Shared Renewable Energy Source

4.1 Overview

In the previous chapter, the optimal offline resource allocation schemes for the Gaussian MAC, where the two transmitters are powered by a shared energy harvester, were investigated, assuming the energy input sequence is known before the transmissions start. In this chapter, the online schemes for the MAC with a shared energy harvester are considered, assuming only causal information of the energy input sequences is known, i.e., at any moment, only the amounts of energy arrival in the previous slots are known. First, several online schemes assuming no/partial statistical information about the EH process are described. Then, numerical results are used to evaluate these schemes' average performance given some stochastic energy arrivals. At last, the worst case performance of

the online greedy scheme is evaluated by competitive analysis.

4.2 The Online Schemes

In this section, three online schemes that require no/partial statistical information about the EH process are proposed.

1. *Online greedy scheme:* Given an arbitrary energy input sequence $\boldsymbol{\omega} \in \boldsymbol{\Omega}$, at the beginning of the n-th slot, the harvested energy of amount E_n becomes available to the system and the system decides to consume as much available energy as possible to maximise the short-term throughput in the n-th slot. Thus, the sum power allocated to slot n, $n = 1, \cdots, N$, is $\frac{E_n}{T}$. The rate scheduling of the two transmitters follows the optimal solution of problem (P3.4).

   This scheme requires no statistical information about the EH process.

2. *Online on-off scheme:* The two transmitters transmit with a sum power of $\frac{\tilde{E}}{T}$, where $\tilde{E}$ is the transmitters' estimation of the average energy arrival amount, whenever there is energy available; otherwise, the transmission is suspended. The rate scheduling of the two transmitters follows the optimal solution of problem (P3.4).

3. *Online passive scheme:* This scheme always passively assume that there would be no future energy arrivals. Therefore, it always allocates the available energy evenly over the remaining time. The sum power allocated in the n-th slot is thus given as $\frac{1}{T}\sum_{i=1}^{n}\frac{E_i}{N+1-i}$. Similarly, the rate scheduling of the two transmitters follows the optimal solution of problem (P3.4).

For the case of finite battery capacity, any energy exceeding the battery capacity will be discarded by the online on-off scheme and the online passive scheme. For online greedy scheme, there will be no energy left by the end of each slot. Therefore, battery

overflow would never happen in the greedy scheme.

Note that both the online greedy scheme and the online passive scheme require no information about the energy harvesting process while the online on-off scheme requires the partial statistical information, i.e., the average energy arrival amount.

4.3 Simulation Results

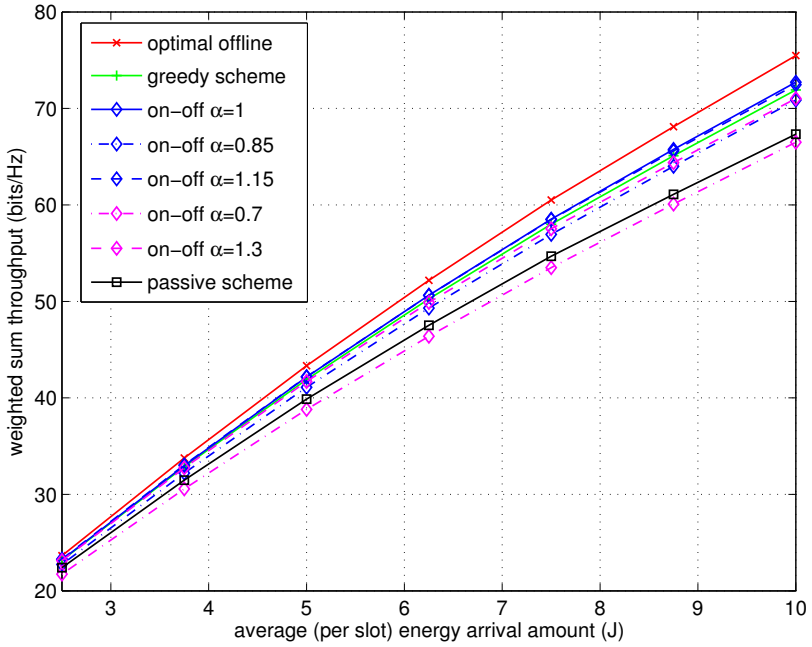

Figure 4.1: Weighted sum throughput versus average energy arrival amounts with infinite battery capacity for Gaussian MAC when $\mu_1 = 0.6, \mu_2 = 0.4$.

In this section, the average performance of the three online schemes described in the previous section are investigated with some stochastic energy arrivals for both the infinite and finite battery cases.

In this section, we adopt $h_1 = 0.8$, $h_2 = 0.7$, $N = 15$, and $T = 10$ s. For the case of finite battery capacity, it is assumed $\mathcal{E} = 20$ J.

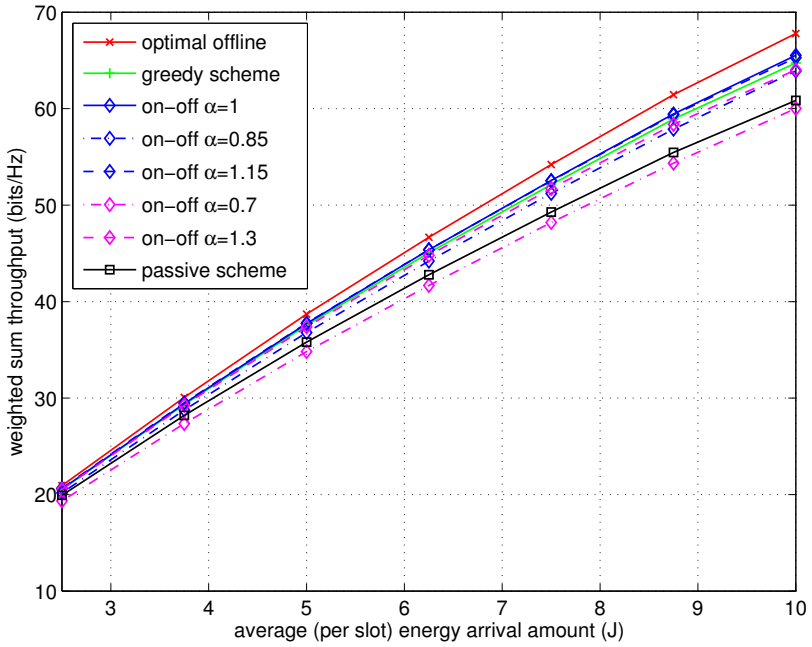

Figure 4.2: Weighted sum throughput versus average energy arrival amounts with infinite battery capacity for Gaussian MAC when $\mu_1 = 0.4, \mu_2 = 0.6$.

For the purpose of exposition, it is assumed that the energy arrival amount, i.e., the amount of harvested energy that arrives at the beginning of a slot, follows a uniform distribution over $[0, E_{\max}]$. The average (per slot) energy arrival amount, denoted by $\bar{E}$, is thus given by $\bar{E} = \frac{E_{\max}}{2}$. For the online on-off scheme, $\alpha = \tilde{E}/\bar{E}$ indicates the estimation accuracy for the average energy arrival amount (i.e., when $\alpha = 1$, the estimation is accurate; otherwise, the average energy arrival amount is either overestimated or underestimated).

Fig. 4.1 and Fig. 4.3 show the performance of the schemes for different average energy arrival amounts with infinite and finite battery capacities, respectively, with weighting factors $\mu_1 = 0.6$ and $\mu_2 = 0.4$. Fig. 4.2 and Fig. 4.4 show the performance of the schemes for different average energy arrival amounts with infinite and finite battery capacities, respectively, with weighting factors $\mu_1 = 0.4$ and $\mu_2 = 0.6$. It is worth noting that the

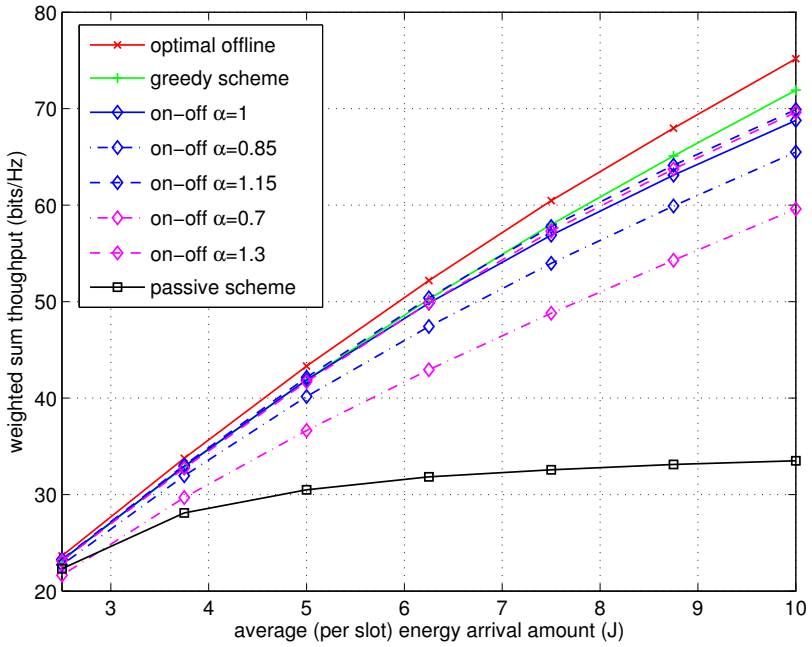

Figure 4.3: Weighted sum throughput versus average energy arrival amounts with finite battery capacity for Gaussian MAC when $\mu_1 = 0.6, \mu_2 = 0.4$.

weighted sum throughputs in Fig. 4.1 and Fig. 4.3 are higher than those in Fig. 4.2 and Fig. 4.4, respectively. This is because that with larger μ_1, higher priority is assigned to transmitter 1, who enjoys better channel conditions.

For the case of infinite battery capacity, as seen from Fig. 4.1 and Fig. 4.2, the greedy scheme, whose (per unit spectrum) weighted sum throughput is around 5% less than that of the optimal offline scheme for different average energy arrival amounts, is outperformed by the on-off scheme with accurate estimation, i.e., $\alpha = 1$. However, the performance of the on-off scheme degrades as the estimation becomes inaccurate. In particular, the performance of the on-off scheme is worse than the greedy scheme when $\alpha = 1.3$ or 0.7. The passive scheme performs the worse than both the online greedy scheme and the on-off scheme with accurate estimation.

For the case of finite battery capacity, it can observed from Fig. 4.3 and Fig. 4.4

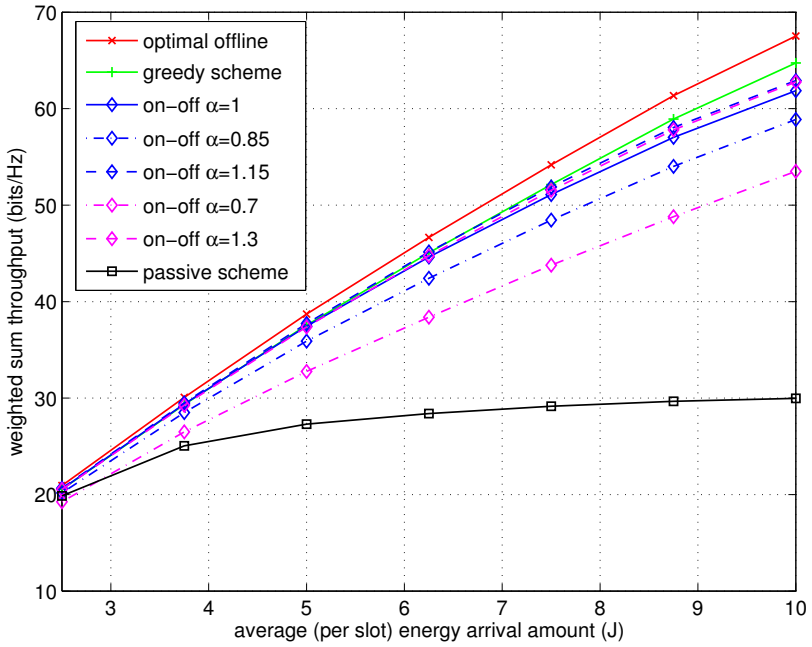

Figure 4.4: Weighted sum throughput versus average energy arrival amounts with finite battery capacity for Gaussian MAC when $\mu_1 = 0.4, \mu_2 = 0.6$.

that the on-off scheme with accurate estimation has comparable performance with the greedy scheme in the low average energy arrival amount regime. However, the greedy scheme performs significantly better than the on-off scheme in the high average energy arrival amount regime. Unlike the greedy scheme that never causes battery overflow, the on-off scheme and the passive scheme may cause battery overflow since the stored energy may not be depleted before the next energy arrival. The passive scheme performs dramatically worse than all other schemes. It is worth noting that the influence of the finite battery capacity on the performance of both the on-off scheme and the passive scheme is more significant in the high average energy arrival amount regime than that in the low average energy arrival amount regime. This is due to the fact that battery overflow is more likely to happen when the energy arrival amount is large.

The greedy scheme is thus recognised to enjoy robustness against the estimation error

of the energy arrival process statistics and the battery capacity limitation compared to other schemes.

4.4 Competitive Analysis

In the previous section, the average performance of several online schemes was studied and it is observed that the online greedy scheme enjoy robustness against the estimation error of the energy arrival process statistics and the battery capacity limitation compared to other considered online schemes. In this section, the performance of the online greedy scheme is further investigated in terms of its worst case performance by using competitive analysis. First, the definition of the competitive ratio is given. Second, two preliminary results are presented. Then, the competitive ratios of the online greedy scheme for various values of μ_1 and μ_2 are obtained.

In the sequel, $\mathcal{A}$ is used to denote the online greedy scheme and superscript $^{\mathcal{A}}$ is used to denote quantities related to the greedy scheme. The infinite battery case is considered first. Later, it will be shown the finite battery case could be solved similarly.

4.4.1 Definition of Competitive Ratios

Given the energy input sequence $\boldsymbol{\omega}$ and weighting factors μ_1, μ_2, the profit obtained by the optimal offline scheme $\mathcal{O}$ and the online greedy scheme $\mathcal{A}$ are defined as

$$B^{\mathcal{O}}(\boldsymbol{\omega}) = \mu_1 \sum_{n=1}^{N} r_{1,n}^{\mathcal{O}} T + \mu_2 \sum_{n=1}^{N} r_{2,n}^{\mathcal{O}} T, \tag{4.1}$$

and

$$B^{\mathcal{A}}(\boldsymbol{\omega}) = \mu_1 \sum_{n=1}^{N} r_{1,n}^{\mathcal{A}} T + \mu_2 \sum_{n=1}^{N} r_{2,n}^{\mathcal{A}} T, \tag{4.2}$$

respectively.

Definition 3. *The online greedy scheme $\mathcal{A}$ for solving the maximisation problem (P3.2)*

is called ρ-competitive or has a competitive ratio of ρ if for all possible energy input sequences $\boldsymbol{\omega} \in \boldsymbol{\Omega}$,

$$\max_{\boldsymbol{\omega}\in\boldsymbol{\Omega}} \frac{B^{\mathcal{O}}(\boldsymbol{\omega})}{B^{\mathcal{A}}(\boldsymbol{\omega})} \leq \rho, \tag{4.3}$$

where ρ is a constant independent of the energy input sequences.

4.4.2 Derivation of the Competitive Ratios

Proposition 5. *For an arbitrary energy input sequence $\boldsymbol{\omega} \in \boldsymbol{\Omega}$, define its corresponding enhanced energy input sequence as $\tilde{\boldsymbol{\omega}} = \left(\sum_{n=1}^{N} E_n, \underbrace{0, \cdots, 0}_{N-1}\right)$. The profit obtained by $\mathcal{O}$ for serving $\boldsymbol{\omega}$ is upper bounded by that for serving $\tilde{\boldsymbol{\omega}}$, i.e., $B^{\mathcal{O}}(\boldsymbol{\omega}) \leq B^{\mathcal{O}}(\tilde{\boldsymbol{\omega}})$.*

Proof. Suppose that the profit earned by $\mathcal{O}$ for serving $\tilde{\boldsymbol{\omega}}$ is smaller than that for serving $\boldsymbol{\omega}$, i.e., $B^{\mathcal{O}}(\boldsymbol{\omega}) > B^{\mathcal{O}}(\tilde{\boldsymbol{\omega}})$. Notice that with $\tilde{\boldsymbol{\omega}}$, the causal EH constraints (3.17) are inactive. Therefore, $\mathcal{O}$ can always serve $\tilde{\boldsymbol{\omega}}$ with the same solution as that for serving $\boldsymbol{\omega}$. The resulting profits for serving the two energy input sequences would be the same, which contradicts with the assumption that $B^{\mathcal{O}}(\boldsymbol{\omega}) > B^{\mathcal{O}}(\tilde{\boldsymbol{\omega}})$. Thus, this lemma is proved. □

Consider a "lazy" version of $\mathcal{A}$ and denote it as $\tilde{\mathcal{A}}$, which does not involve the capping rate/power. For an arbitrary energy input sequence $\boldsymbol{\omega} \in \boldsymbol{\Omega}$, $\tilde{\mathcal{A}}$ determines the sum power allocation $P_n^{\tilde{\mathcal{A}}}$ in slot $n, n = 1, \cdots, N$, as $P_n^{\tilde{\mathcal{A}}} = P_n^{\mathcal{A}} = \frac{E_n}{T}$. In each slot n,

1. for $-\frac{\mu_1}{\mu_2} > -1 + \frac{h_1 - h_2}{h_1 + \frac{h_1 h_2 E_{\max}}{T}}$, regardless of the value of $P_n^{\mathcal{A}}$, always allocate all the sum power to the transmitter 2 only, i.e., $\left(P_{1,n}^{\tilde{\mathcal{A}}}, P_{2,n}^{\tilde{\mathcal{A}}}\right) = \left(0, P_n^{\tilde{\mathcal{A}}}\right)$ and $\left(r_{1,n}^{\tilde{\mathcal{A}}}, r_{2,n}^{\tilde{\mathcal{A}}}\right) = \left(0, \log\left(1 + h_2 P_n^{\tilde{\mathcal{A}}}\right)\right)$;

2. $-1 + \frac{h_1 - h_2}{h_1 + \frac{h_1 h_2 E_{\max}}{T}} \geq -\frac{\mu_1}{\mu_2} > -1$, though transmitter 2 still has higher priority than transmitter 1, to keep close to $\mathcal{A}$, all the sum power is always allocated to the transmitter 1 only regardless of the value of $P_n^{\mathcal{A}}$, i.e., $\left(P_{1,n}^{\tilde{\mathcal{A}}}, P_{2,n}^{\tilde{\mathcal{A}}}\right) = \left(P_n^{\tilde{\mathcal{A}}}, 0\right)$ and $\left(r_{1,n}^{\tilde{\mathcal{A}}}, r_{2,n}^{\tilde{\mathcal{A}}}\right) = \left(\log\left(1 + h_1 P_n^{\tilde{\mathcal{A}}}\right), 0\right)$ (in this case, $\mathcal{A}$ would always allocated to

the transmitter 1 only since the capping rate is so large that $E_n/T \leq E_{\max}/T < g\left(R_c, 0\right), n = 1, \cdots, N$);

3. for $-\frac{\mu_1}{\mu_2} \leq -1$, regardless of the value of $P_n^{\mathcal{A}}$, always allocate all the sum power to the transmitter 1 only, i.e., $\left(P_{1,n}^{\tilde{\mathcal{A}}}, P_{2,n}^{\tilde{\mathcal{A}}}\right) = \left(P_n^{\tilde{\mathcal{A}}}, 0\right)$ and $\left(r_{1,n}^{\tilde{\mathcal{A}}}, r_{2,n}^{\tilde{\mathcal{A}}}\right) = \left(\log\left(1 + h_1 P_n^{\tilde{\mathcal{A}}}\right), 0\right)$.

The profit obtained by $\tilde{\mathcal{A}}$ for a given energy input sequence is given as

1. for $-\frac{\mu_1}{\mu_2} \leq -1$ and $-1 + \frac{h_1 - h_2}{h_1 + \frac{h_1 h_2 E_{\max}}{T}} \geq -\frac{\mu_1}{\mu_2} > -1$,

$$B^{\tilde{\mathcal{A}}}(\boldsymbol{\omega}) = \mu_1 \sum_{n=1}^{N} T \log\left(1 + h_1 P_n^{\tilde{\mathcal{A}}}\right). \tag{4.4}$$

2. for $-\frac{\mu_1}{\mu_2} > -1 + \frac{h_1 - h_2}{h_1 + \frac{h_1 h_2 E_{\max}}{T}}$,

$$B^{\tilde{\mathcal{A}}}(\boldsymbol{\omega}) = \mu_2 \sum_{n=1}^{N} T \log\left(1 + h_2 P_n^{\tilde{\mathcal{A}}}\right). \tag{4.5}$$

Proposition 6. *For an arbitrary energy input sequence $\boldsymbol{\omega} \in \boldsymbol{\Omega}$, the profit obtained by $\mathcal{A}$ is lower bounded by that obtained by $\tilde{\mathcal{A}}$, i.e, for $-\frac{\mu_1}{\mu_2} \leq -1$ and $-1 + \frac{h_1 - h_2}{h_1 + \frac{h_1 h_2 E_{\max}}{T}} \geq -\frac{\mu_1}{\mu_2} > -1$, $B^{\mathcal{A}}(\boldsymbol{\omega}) \geq B^{\tilde{\mathcal{A}}}(\boldsymbol{\omega}) = \mu_1 \sum\limits_{n=1}^{N} T \log\left(1 + h_1 P_n^{\tilde{\mathcal{A}}}\right)$ and for $-\frac{\mu_1}{\mu_2} > -1 + \frac{h_1 - h_2}{h_1 + \frac{h_1 h_2 E_{\max}}{T}}$, $B^{\mathcal{A}}(\boldsymbol{\omega}) \geq B^{\tilde{\mathcal{A}}}(\boldsymbol{\omega}) = \mu_2 \sum\limits_{n=1}^{N} T \log\left(1 + h_2 P_n^{\tilde{\mathcal{A}}}\right)$.*

Proof. For each $n \in \{1, \cdots, N\}$, the rate pair $\left(r_{1,n}^{\mathcal{A}}, r_{2,n}^{\mathcal{A}}\right)$ is the optimal solution to Problem (P3.4n). Hence, no other rate pairs can result in a larger value of $\mu_1 r_{1,n} + \mu_2 r_{2,n}$. □

4.4.2.1 Competitive ratio for $-\frac{\mu_1}{\mu_2} > -1 + \frac{h_1 - h_2}{h_1 + \frac{h_1 h_2 E_{\max}}{T}}$

Note that with the enhanced energy input sequence $\tilde{\boldsymbol{\omega}}$ for $\boldsymbol{\omega} \in \boldsymbol{\Omega}$, the causal EH constraints in (3.17) are inactive and $\mathcal{O}$ will lead to a constant sum power allocation,

$\tilde{P}^{\mathcal{O}} = \left(\sum_{n=1}^{N} E_n\right)/(NT)$, and a constant rate pair $\left(\tilde{r}_1^{\mathcal{O}}, \tilde{r}_2^{\mathcal{O}}\right)$ over all n slots. Partition $\boldsymbol{\Omega}$ into two mutually disjoint subsets, given as

$$\boldsymbol{\Omega}_1 = \left\{ \boldsymbol{\omega} \in \boldsymbol{\Omega} \middle| 0 \leq \left(\sum_{n=1}^{N} E_n\right)/(NT) \leq g\left(R_c, 0\right) \right\},$$

and

$$\boldsymbol{\Omega}_2 = \left\{ \boldsymbol{\omega} \in \boldsymbol{\Omega} \middle| \left(\sum_{n=1}^{N} E_n\right)/(NT) > g\left(R_c, 0\right) \right\}.$$

Note that, the rate profile given by $\mathcal{O}$ for serving the enhanced energy input sequences of the energy input sequences belong to these two subsets have different structures.

For an arbitrary energy input sequence $\boldsymbol{\omega} \in \boldsymbol{\Omega}_1$, the rate pair $\left(\tilde{r}_1^{\mathcal{O}}, \tilde{r}_2^{\mathcal{O}}\right)$ is given as $\left(\tilde{r}_1^{\mathcal{O}}, \tilde{r}_2^{\mathcal{O}}\right) = \left(\log\left(1 + h_1 \tilde{P}^{\mathcal{O}}\right), 0\right)$. Hence, we obtain

$$\begin{aligned}
\left.\frac{B^{\mathcal{O}}(\boldsymbol{\omega})}{B^{\mathcal{A}}(\boldsymbol{\omega})}\right|_{\boldsymbol{\omega}\in\boldsymbol{\Omega}_1} &\overset{(a)}{\leq} \frac{B^{\mathcal{O}}(\tilde{\boldsymbol{\omega}})}{B^{\mathcal{A}}(\boldsymbol{\omega})} \overset{(b)}{<} \frac{\mu_1 NT \log\left(1 + h_1 \frac{\sum_{n=1}^{N} E_n}{NT}\right)}{\mu_2 T \sum_{n=1}^{N} \log\left(1 + h_2 \frac{E_n}{T}\right)} \\
&\overset{(c)}{<} \frac{\mu_1 NT h_1 \frac{\sum_{n=1}^{N} E_n}{NT \ln 2}}{\mu_2 T \sum_{n=1}^{N} h_2 \frac{E_n}{T} \frac{\log\left(1+h_2 \frac{E_{\max}}{T}\right)}{h_2 E_{\max}/T}} = \frac{\mu_1 h_1 E_{\max}/T}{\ln 2 \mu_2 \log\left(1 + h_2 \frac{E_{\max}}{T}\right)} = K_2 \frac{\mu_1 h_1}{\mu_2 \ln 2},
\end{aligned} \tag{4.6}$$

where $K_2 = \frac{\frac{E_{\max}}{T}}{\mathcal{C}\left(h_2 \frac{E_{\max}}{T}\right)}$; (a) and (b) follow from Proposition 5 and 6, respectively; (c) follows from the facts that $\mathcal{C}(x) \leq x/\ln 2, \forall x \geq 0$ [Top04] and $\mathcal{C}\left(x\right) \geq x/\left(h_2 K_2\right), \forall x \in [0, h_2 E_{\max}/T]$, which can be proved from the concavity of log function.

Since (4.6) applies to arbitrary $\boldsymbol{\omega} \in \boldsymbol{\Omega}_1$, it can be concluded that

$$\max_{\boldsymbol{\omega}\in\boldsymbol{\Omega}_1} \frac{B^{\mathcal{O}}(\boldsymbol{\omega})}{B^{\mathcal{A}}(\boldsymbol{\omega})} < K_2 \frac{\mu_1 h_1}{\mu_2 \ln 2}. \tag{4.7}$$

For an arbitrary energy input sequence $\boldsymbol{\omega} \in \boldsymbol{\Omega}_2$, the rate pair $\left(\tilde{r}_1^{\mathcal{O}}, \tilde{r}_2^{\mathcal{O}}\right)$ is given as

$\left(r_{1,n}^{\mathcal{O}}, r_{2,n}^{\mathcal{O}}\right) = \left(R_c, \log\left(\frac{h_1\left(1+h_2 P_n^{\mathcal{O}}\right)}{h_1-h_2+h_2 2^{R_c}}\right)\right)$. Based on Propositions 5 and 6, we obtain

$$\begin{aligned}
\left.\frac{B^{\mathcal{O}}(\boldsymbol{\omega})}{B^{\mathcal{A}}(\boldsymbol{\omega})}\right|_{\boldsymbol{\omega}\in\boldsymbol{\Omega}_2} &\leq \frac{NT\left(\mu_1 R_c + \mu_2 \log\left(\frac{h_1\left(1+h_2\frac{\sum_{n=1}^{N} E_n}{NT}\right)}{h_1-h_2+h_2 2^{R_c}}\right)\right)}{\mu_2 T \sum_{n=1}^{N} \log\left(1+h_2\frac{E_n}{T}\right)} \\
&\quad + \frac{NT\mu_2 \log\left(\frac{h_1\left(1+h_2\frac{\sum_{n=1}^{N} E_n}{NT}\right)}{h_1-h_2+h_2 2^{R_c}}\right)}{\mu_2 T \sum_{n=1}^{N} h_2\frac{E_n}{T}\frac{\log\left(1+h_2\frac{E_{\max}}{T}\right)}{h_2\frac{E_{\max}}{T}}} \\
&< \frac{NT\mu_1 R_c}{\mu_2 T \sum_{n=1}^{N} h_2\frac{E_n}{T}\frac{\log\left(1+h_2\frac{E_{\max}}{T}\right)}{h_2\frac{E_{\max}}{T}}} + \frac{NT\mu_2 \log\left(\frac{h_1\left(1+h_2\frac{\sum_{n=1}^{N} E_n}{NT}\right)}{h_1-h_2+h_2 2^{R_c}}\right)}{\mu_2 T \sum_{n=1}^{N} h_2\frac{E_n}{T}\frac{\log\left(1+h_2\frac{E_{\max}}{T}\right)}{h_2\frac{E_{\max}}{T}}} \\
&< K_2\left(\frac{NT\left(\mu_1 R_c + \mu_2 \log\left(\frac{h_1}{h_1-h_2+h_2 2^{R_c}}\right)\right)}{\mu_2 \sum_{n=1}^{N} E_n} + \frac{\frac{\mu_2 h_2 \sum_{n=1}^{N} E_n}{\ln 2}}{\mu_2 \sum_{n=1}^{N} E_n}\right) \\
&< K_2\left(\frac{\mu_1 R_c + \mu_2 \log\left(\frac{h_1}{h_1-h_2+h_2 2^{R_c}}\right)}{\mu_2 g(R_c, 0)} + \frac{h_2}{\ln 2}\right)
\end{aligned} \tag{4.8}$$

Similarly, since (4.8) applies to arbitrary $\boldsymbol{\omega} \in \boldsymbol{\Omega}_2$, it can be concluded that

$$\max_{\boldsymbol{\omega}\in\boldsymbol{\Omega}_2} \frac{B^{\mathcal{O}}(\boldsymbol{\omega})}{B^{\mathcal{A}}(\boldsymbol{\omega})} < K_2\left(\frac{\mu_1 R_c + \mu_2 \log\left(\frac{h_1}{h_1-h_2+h_2 2^{R_c}}\right)}{\mu_2 g(R_c, 0)} + \frac{h_2}{\ln 2}\right). \tag{4.9}$$

Proposition 7. *The online scheme $\mathcal{A}$ is ρ_1-competitive for $-\frac{\mu_1}{\mu_2} > -1 + \frac{h_1-h_2}{h_1+\frac{h_1 h_2 E_{\max}}{T}}$, where ρ_1 is defined as*

$$\rho_1 \triangleq K_2 \max\left\{\frac{\mu_1 h_1}{\mu_2 \ln 2}, \frac{\mu_1 R_c + \mu_2 \log\left(\frac{h_1}{h_1-h_2+h_2 2^{R_c}}\right)}{\mu_2 g(R_c, 0)} + \frac{h_2}{\ln 2}\right\}. \tag{4.10}$$

Proof. Since $\boldsymbol{\Omega}_1 \cup \boldsymbol{\Omega}_2 = \boldsymbol{\Omega}$, we have

$$\begin{aligned}\rho_1 &> \max\left\{\max_{\boldsymbol{\omega}\in\boldsymbol{\Omega}_1}\frac{B^{\mathcal{O}}(\boldsymbol{\omega})}{B^{\mathcal{A}}(\boldsymbol{\omega})}, \max_{\boldsymbol{\omega}\in\boldsymbol{\Omega}_2}\frac{B^{\mathcal{O}}(\boldsymbol{\omega})}{B^{\mathcal{A}}(\boldsymbol{\omega})}\right\}\\ &= \max_{\boldsymbol{\omega}\in\boldsymbol{\Omega}}\frac{B^{\mathcal{O}}(\boldsymbol{\omega})}{B^{\mathcal{A}}(\boldsymbol{\omega})}.\end{aligned}$$

□

Remark 5. *If* $-\frac{\mu_1}{\mu_2} \geq -\frac{h_2}{h_1}$*, the capping rate* R_c *equals* 0*. In this case,* $\boldsymbol{\Omega}_1$ *is empty. Thus, the corresponding ratio* (4.7) *should be replaced by* 1*.*

4.4.2.2 Competitive ratio for $-1+\frac{h_1-h_2}{h_1+\frac{h_1h_2E_{\max}}{T}} \geq -\frac{\mu_1}{\mu_2} > -1$

For an arbitrary energy input sequence $\boldsymbol{\omega} \in \boldsymbol{\Omega}$, since $\frac{\sum_{n=1}^{N} E_n}{NT} \leq E_{\max}/T < g(R_c, 0)$, the rate pair $\left(\tilde{r}_1^{\mathcal{O}}, \tilde{r}_2^{\mathcal{O}}\right)$ is given as $\left(\tilde{r}_1^{\mathcal{O}}, \tilde{r}_2^{\mathcal{O}}\right) = \left(\log\left(1+h_1\tilde{P}^{\mathcal{O}}\right), 0\right)$. Hence, we obtain

$$\begin{aligned}\left.\frac{B^{\mathcal{O}}(\boldsymbol{\omega})}{B^{\mathcal{A}}(\boldsymbol{\omega})}\right|_{\boldsymbol{\omega}\in\boldsymbol{\Omega}} &\leq \frac{B^{\mathcal{O}}(\tilde{\boldsymbol{\omega}})}{B^{\mathcal{A}}(\boldsymbol{\omega})} < \frac{\mu_1 NT\log\left(1+h_1\frac{\sum_{n=1}^{N}E_n}{NT}\right)}{\mu_1 T\sum_{n=1}^{N}\log\left(1+h_1\frac{E_n}{T}\right)}\\ &< \frac{\mu_1 NTh_1\frac{\sum_{n=1}^{N}E_n}{NT\ln 2}}{\mu_1 T\sum_{n=1}^{N}h_1\frac{E_n}{T}\frac{\log\left(1+h_1\frac{E_{\max}}{T}\right)}{h_1E_{\max}/T}}\\ &= K_1\frac{h_1}{\ln 2},\end{aligned} \tag{4.11}$$

where $K_1 = \frac{\frac{E_{\max}}{T}}{\mathcal{C}\left(h_1\frac{E_{\max}}{T}\right)}$.

Since (4.11) applies to arbitrary $\boldsymbol{\omega} \in \boldsymbol{\Omega}$, it can be concluded that

$$\max_{\boldsymbol{\omega}\in\boldsymbol{\Omega}}\frac{B^{\mathcal{O}}(\boldsymbol{\omega})}{B^{\mathcal{A}}(\boldsymbol{\omega})} < K_1\frac{h_1}{\ln 2}. \tag{4.12}$$

Proposition 8. *The online scheme* $\mathcal{A}$ *is* ρ_2*-competitive for* $-1+\frac{h_1-h_2}{h_1+\frac{h_1h_2E_{\max}}{T}} \geq -\frac{\mu_1}{\mu_2} >$

-1, *where* $\rho_2 = K_1 \frac{h_1}{\ln 2}$.

4.4.2.3 Competitive ratio for $-\frac{\mu_1}{\mu_2} \leq -1$

For an arbitrary energy input sequence $\boldsymbol{\omega} \in \boldsymbol{\Omega}$, the rate pair $\left(\tilde{r}_1^{\mathcal{O}}, \tilde{r}_2^{\mathcal{O}}\right)$ is given as $\left(\tilde{r}_1^{\mathcal{O}}, \tilde{r}_2^{\mathcal{O}}\right) = \left(\log\left(1 + h_1 \tilde{P}^{\mathcal{O}}\right), 0\right)$. Hence, we obtain

$$\begin{aligned}
\left.\frac{B^{\mathcal{O}}(\boldsymbol{\omega})}{B^{\mathcal{A}}(\boldsymbol{\omega})}\right|_{\boldsymbol{\omega}\in\boldsymbol{\Omega}} \leq \frac{B^{\mathcal{O}}(\tilde{\boldsymbol{\omega}})}{B^{\mathcal{A}}(\boldsymbol{\omega})} &< \frac{\mu_1 NT \log\left(1 + h_1 \frac{\sum_{n=1}^{N} E_n}{NT}\right)}{\mu_1 T \sum_{n=1}^{N} \log\left(1 + h_1 \frac{E_n}{T}\right)} \\
&< \frac{\mu_1 NT h_1 \frac{\sum_{n=1}^{N} E_n}{NT \ln 2}}{\mu_1 T \sum_{n=1}^{N} h_1 \frac{E_n}{T} \frac{\log\left(1+h_1 \frac{E_{\max}}{T}\right)}{h_1 E_{\max}/T}} \\
&= K_1 \frac{h_1}{\ln 2}. \qquad (4.13)
\end{aligned}$$

Since (4.13) applies to arbitrary $\boldsymbol{\omega} \in \boldsymbol{\Omega}$, it can be concluded that

$$\max_{\boldsymbol{\omega}\in\boldsymbol{\Omega}} \frac{B^{\mathcal{O}}(\boldsymbol{\omega})}{B^{\mathcal{A}}(\boldsymbol{\omega})} < K_1 \frac{h_1}{\ln 2}. \qquad (4.14)$$

Proposition 9. *The online scheme* $\mathcal{A}$ *is* ρ_3*-competitive for* $-\frac{\mu_1}{\mu_2} \leq -1$, *where* $\rho_3 = K_1 \frac{h_1}{\ln 2}$.

Remark 6. *The competitive ratios given in Proposition 7∼9 also hold for the case of finite battery capacity if* $E_{\max}$ *is truncated at* $\mathcal{E}$ *(which is equivalent to truncating* E_n, $n = 1, \cdots, N$, *at* $\mathcal{E}$*). This can be easily verified by the fact that given any input sequence (truncated at* $\mathcal{E}$*), the profit achieved by the optimal offline scheme is upper-bounded by that achieved for the case of infinite battery capacity, whereas the profit achieved by the greedy scheme is the same as that for the case of infinite battery capacity.*

4.4.3 A Numerical Example

We adopt $h_1 = 0.8$, $h_2 = 0.7$, $N = 15$, $E_{\max} = 20$ J, and $T = 10$ s. The competitive ratios of the online greedy scheme against the optimal offline scheme with different $\mu_1 \in [0, 1]$ are plotted in Fig. 4.5. In Fig. 4.5, the ratios between the profits for the optimal offline scheme $\mathcal{O}$ and the online greedy scheme $\mathcal{A}$ for serving energy input sequences $\boldsymbol{\omega}_1$ and $\boldsymbol{\omega}_2$, respectively, with infinite battery capacity[1] are also plotted, where $\boldsymbol{\omega}_1$ and $\boldsymbol{\omega}_2$ are given as

$$\boldsymbol{\omega}_1 = (20, 17.3, 16, 16, 14.7, 16, 10.7, 4, 5.3, 2.7, 10, 13.3, 17.3, 18, 18.7) \text{ J},$$

and

$$\boldsymbol{\omega}_2 = (20, 0, 0, 0, 0, 0, 0, 0, 0, 0, 0, 0, 0, 0, 0) \text{ J}.$$

Note that given $\boldsymbol{\omega}_2$, the optimal offline scheme will spend the 20 J energy which arrives at the beginning of the first slot uniformly in all 15 slots whereas the online greedy scheme will deplete the 20 J energy in the first slot.

With $\boldsymbol{\omega}_1$, the performance of the online greedy scheme is close to that of the optimal offline scheme, which results in ratios close to 1. With $\boldsymbol{\omega}_2$, the power profiles obtained by $\mathcal{O}$ and $\mathcal{A}$ are dramatically different, which result in relatively large ratios, i.e., around 1.6. The ratios with both $\boldsymbol{\omega}_1$ and $\boldsymbol{\omega}_2$ are smaller than the competitive ratios, illustrated by the solid curve in Fig. 4.5, which is in accordance with the fact that the competitive ratios serve as the upper bound of the ratios between the profits of $\mathcal{O}$ and $\mathcal{A}$ for any energy input sequence. Note that the sudden change of the competitive ratio at $\mu_1 = 0.4866$ is due to the discontinuity in the profit function of $\tilde{\mathcal{A}}$ at $-\frac{\mu_1}{\mu_2} = -1 + \frac{h_1 - h_2}{h_1 + \frac{h_1 h_2 E_{\max}}{T}}$, as indicated by (4.4) and (4.5).

[1]For the case of finite battery capacity, the only difference is that the ratio with ω_1 will be slightly smaller.

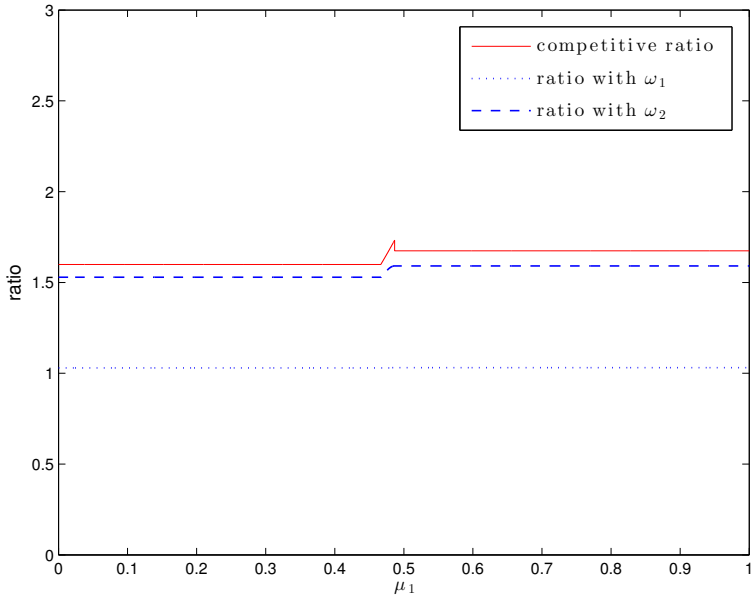

Figure 4.5: The competitive ratios and the ratios obtained with energy input sequence $\boldsymbol{\omega}_1$ and $\boldsymbol{\omega}_2$ in the Gaussian MAC with a shared energy harvester.

4.5 Summary

In this chapter, the online schemes for the Gaussian MAC with a shared renewable energy source were investigated. Three online schemes were proposed which require no/partial statistical information about the energy harvesting process. Simulation results were shown to compare their performance in terms of average weighted sum throughput achieved given some statistical energy harvesting process. It was revealed that the performance of the on-off scheme is influenced by the accuracy of its estimation of the mean energy arrival amount. Moreover, the greedy scheme is recognised to enjoy robustness against the estimation error of the energy arrival process statistics and the battery capacity limitation compared to other online schemes. To further measure the utility of the greedy scheme against the optimal offline scheme, its competitive ratios, which are the maximum ratios between the profits obtained by the offline and online schemes over

arbitrary energy arrival profiles, were derived.

Chapter 5

Optimal Offline Resource Allocation Schemes for Multiple Access Channel with Conferencing Links and a Shared Renewable Source

5.1 Overview

This chapter investigates the offline resource allocation problem for the Gaussian multiple access channel (MAC) with conferencing links, where the two transmitters can talk to each other via wired rate-limited channels. Moreover, the two transmitters are powered by a shared energy harvester which captures energy from the environment. The energy input sequence is assumed to be non-causally known before transmissions start. Resource allocation problems over a finite horizon of N time slots are formulated to characterise

the boundary of the maximum departure regions for both the infinite and finite battery capacity cases. Then, the optimal offline power and rate allocation scheme are developed by exploiting the hidden convexity of the problems. Interestingly, it is shown that there exists a maximum transmission rate (named the capping rate) for one of the transmitters.

5.2 System Model and Problem Formulation

5.2.1 System Model

We consider a two-transmitter Gaussian MAC where the two transmitters are connected by certain wired rate-limited two-way conferencing links, as shown in Fig. 5.1. Via the conferencing links, transmitter 1 can talk to transmitter 2 with a rate up to C_{12}, similar for the opposite direction with a rate up to C_{21}. The benefits of introducing conferencing links into the system is that the cooperation between the two transmitters via the conferencing links can enlarge the channel capacity region, i.e., under the same power constraint, the achievable data rates of the two transmitters can be enhanced [Wil83]. Compared to the transmissions over wireless links that suffer from heavy path losses, the communications over wired links consume much less energy, which is neglected here for the convenience of analysis. Similar assumptions were adopted in [Wil83, BLW08, BLW12, MYK07, SGP$^+$09]. Moreover, it is assumed that the two transmitters share one common EH source (the energy sharing could be enabled via the wired conferencing links). The constant channel power gains from transmitter 1 and transmitter 2 to the receiver are denoted by h_1 and h_2, respectively. Without loss of generality, it is assumed $h_1 \geq h_2$, which indicates that the transmitter 1 link is stronger than or equal to the transmitter 2 link. It is assumed that the additive noise at the receiver is circularly symmetric complex Gaussian (CSCG), with zero mean and unit variance.

Consider a finite time horizon of N slots, each with a duration of T. At the beginning of the n-th slot, $n = 1, \cdots, N$, the EH source receives harvested energy (accu-

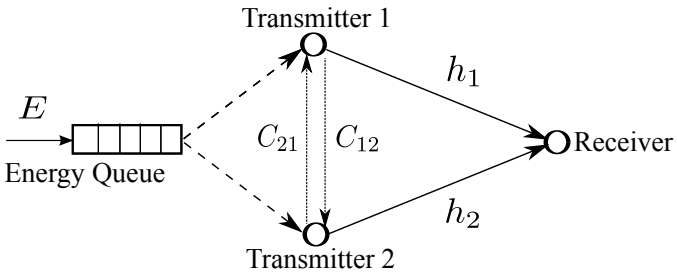

Figure 5.1: MAC channel with conferencing links and a shared renewable energy source

mulated during the previous time slot) with an amount of $E_n \in [0, E_{\max}]$, where $E_{\max}$ denotes the maximum amount from one energy arrival and is assumed to be known. Denote the sequence of N energy arrival amounts as $\boldsymbol{\omega} = (E_1, \cdots, E_N)$ (which is also called the input sequence) and the set of all possible input sequences as $\boldsymbol{\Omega} = \{\boldsymbol{\omega} = (E_1, \cdots, E_N) \,|0 \leq E_n \leq E_{\max}, n = 1, \cdots, N\}$. For the non-causal case, the entire input sequence $\boldsymbol{\omega}$ is known before transmissions. Denote the data rate and the corresponding transmission power for transmitter $i, i = 1, 2$, at the n-th slot, $n = 1, \cdots, N$, as $r_{i,n}$ and $P_{i,n}$, respectively.

Similarly to Section 3.2, the EH constraints for the system model described above could be mathematically modeled as:

$$T \sum_{n=1}^{j} (P_{1,n} + P_{2,n}) \leq \sum_{n=1}^{j} E_n, j = 1, \cdots N. \tag{5.1}$$

5.2.2 Problem Formulation

In this subsection, firstly, the minimum sum power $g(r_{1,n}, r_{2,n})$ required to achieve given data rates $(r_{1,n}, r_{2,n})$ of the two transmitters in the n-th slot is derived. Then, for both the infinite and finite battery cases, the maximum departure regions are defined and optimisation problems are formulated whose optimal solutions give the resource allocation schemes that achieve the boundary points of the maximum departure region, respectively. In the sequel, the index n is omitted whenever it causes no confusion.

5.2.2.1 Minimum Sum Power to Achieve Given Rates

First, the minimum sum power $g(r_1, r_2)$ required to achieve given data rates (r_1, r_2) of the two transmitters is derived.

The coding scheme of the MAC with conferencing links was described in Chapter 2. Denote the power allocated to the private message and the common message of transmitter i, $i = 1, 2$, as P_i^c and $P_i^p = P_i - P_i^c$, respectively, the capacity region of the Gaussian MAC with conferencing links is given as [BLW08]

$$\begin{cases} (r_1 - C_{12})^+ \leq \mathcal{C}(h_1 P_1^p) & (5.2) \\ (r_2 - C_{21})^+ \leq \mathcal{C}(h_2 P_2^p) & (5.3) \\ (r_1 - C_{12})^+ + (r_2 - C_{21})^+ \leq \mathcal{C}(h_1 P_1^p + h_2 P_2^p) & (5.4) \\ r_1 + r_2 \leq \mathcal{C}\left(h_1 P_1 + h_2 P_2 + 2\sqrt{h_1 P_1^c h_2 P_2^c}\right). & (5.5) \end{cases}$$

Then, the sum power function $g(r_1, r_2)$ can be obtained by solving the following sum power minimisation problem:

$$\text{(P5.1)} \quad g(r_1, r_2) = \min_{P_1^c, P_1^p, P_2^c, P_2^p} P_1^c + P_1^p + P_2^c + P_2^p \tag{5.6}$$

$$\text{s.t. } (5.2)\text{–}(5.5),\ P_1^c \geq 0,\ P_1^p \geq 0,\ P_2^c \geq 0,\ P_2^p \geq 0. \tag{5.7}$$

Remark 7. *The Problem (P5.1) is a convex optimisation problem.*

Proof. See Appendix A □

By solving the problem (P5.1), we have the following proposition.

Proposition 10. *For a given rate pair (r_1, r_2), the minimum sum power $g(r_1, r_2)$ is given as*

$$g(r_1, r_2) \triangleq \frac{h_2}{h_1(h_1 + h_2)} 2^{(r_1 - C_{12})^+ + (r_2 - C_{21})^+} + \frac{1}{h_1 + h_2} 2^{r_1 + r_2} + \left(\frac{1}{h_2} - \frac{1}{h_1}\right) 2^{(r_2 - C_{21})^+} - \frac{1}{h_2}, \tag{5.8}$$

and the corresponding power allocation for the messages is given as:

$$P_1^{c*} = \frac{h_1\left(2^{r_1+r_2} - 2^{(r_1-C_{12})^+ + (r_2-C_{21})^+}\right)}{(h_1+h_2)^2}, \tag{5.9}$$

$$P_1^{p*} = \frac{1}{h_1} 2^{(r_2-C_{21})^+}\left(2^{(r_1-C_{12})^+} - 1\right), \tag{5.10}$$

$$P_2^{c*} = \frac{h_2\left(2^{r_1+r_2} - 2^{(r_1-C_{12})^+ + (r_2-C_{21})^+}\right)}{(h_1+h_2)^2}, \tag{5.11}$$

$$P_2^{p*} = \frac{1}{h_2}\left(2^{(r_2-C_{21})^+} - 1\right). \tag{5.12}$$

Proof. Denote the optimal solution of Problem (P5.1) as $P_1^{c*}, P_1^{p*}, P_2^{c*}$ and P_2^{p*}. To solve Problem (P5.1), consider the following four cases:

1) For $r_1 > C_{12}, r_2 > C_{21}$: Let $P^c = P_1^c + P_2^c$ be the total power for common messages from both users and $P_1^c = \alpha P^c$, $P_2^c = (1-\alpha)P^c$, $\alpha \in [0,1]$, the constraint (5.5) can be rewritten as

$$P^c = P_1^c + P_2^c \geq \frac{2^{r_1+r_2} - 1 - h_1 P_1^p - h_2 P_2^p}{h_1\alpha + h_2(1-\alpha) + 2\sqrt{h_1 h_2 \alpha(1-\alpha)}}. \tag{5.13}$$

First, we prove that in the optimal solution, the numerator in the RHS of (5.13) must be non-negative, i.e., $2^{r_1+r_2} - 1 - h_1 P_1^{p*} - h_2 P_2^{p*} \geq 0$. Assuming that

$$2^{r_1+r_2} - 1 - h_1 P_1^{p^*} - h_2 P_2^{p*} < 0$$

(which indicates the constraints (5.4) and (5.5) are both satisfied with strict inequality), to minimize the sum power, we have $P_1^{c*} = 0, P_2^{c*} = 0$. Also notice that at least one of (5.2) and (5.3) must be satisfied with strict inequality as otherwise the constraint (5.4) would be violated. If strict inequality holds for (5.2), i.e., $r_1 < \mathcal{C}\left(h_1 P_1^{p*}\right) + C_{12}$, then there must exist $0 < \delta \leq \min\left\{P_1^{p*} - \frac{2^{r_1-C_{12}}-1}{h_1}, P_1^{p*} - \frac{2^{r_1+r_2}-1-h_2P_2^{p*}}{h_1}\right\}$, such that $r_1 \leq \mathcal{C}\left(h_1(P_1^{p*}-\delta)\right) + C_{12}$ and $2^{r_1+r_2} - 1 - h_1(P_1^{p*}-\delta) - h_2 P_2^{p*} \leq 0$. Define a new power profile as $\tilde{P}_1^p = P_1^{p*} - \delta$, $\tilde{P}_2^p = P_2^{p*}$, $\tilde{P}_1^c = P_1^{c*} = 0$ and $\tilde{P}_2^c = P_2^{c*} = 0$. It is easy to check that the new power allocation satisfies all constraints and leads to a smaller sum power, i.e., $\tilde{P}_1^p + \tilde{P}_2^p + \tilde{P}_1^c + \tilde{P}_2^c < P_1^{p*} + P_1^{c*} + P_2^{p*} + P_2^{c*}$. If equality holds for (5.2), then

strict inequality must hold for (5.3). Similar to the above case, we can always find a new power profile that satisfies all constraints while leading to a smaller sum power. Thus, the optimal power allocation cannot result in $2^{r_1+r_2}-1-h_1P_1^{p^*}-h_2P_2^{p*}<0$ and it can concluded that $2^{r_1+r_2}-1-h_1P_1^{p*}-h_2P_2^{p*}\geq 0$.

Next, we prove that equality must be achieved for (5.13). Notice that constraints (5.2)-(5.4) do not involve P_1^c and P_2^c. Suppose that $P^c > \frac{2^{r_1+r_2}-1-h_1P_1^{p*}-h_2P_2^{p*}}{h_1\alpha+h_2(1-\alpha)+2\sqrt{h_1h_2\alpha(1-\alpha)}}$, since the RHS of (5.13) is non-negative, we can always reduce P^c by an arbitrarily small amount Δ (while keeping P_1^{p*} and P_2^{p*} unchanged) without violating (5.13) such that the sum power is reduced, which contradicts with the optimality of the original power allocation. Hence, in the optimal solution, (5.13) must be satisfied with equality and we have

$$P^c = P_1^c + P_2^c = \frac{2^{r_1+r_2}-1-h_1P_1^p-h_2P_2^p}{h_1\alpha+h_2(1-\alpha)+2\sqrt{h_1h_2\alpha(1-\alpha)}}. \tag{5.14}$$

Since $2^{r_1+r_2}-1-h_1P_1^{p^*}-h_2P_2^{p*}\geq 0$, the denominator in the RHS of (5.13) must be maximised. Define $f(\alpha)=h_1\alpha+h_2(1-\alpha)+2\sqrt{h_1\alpha\cdot h_2(1-\alpha)}$, $\alpha\in[0,1]$. The first order and second order derivatives of $f(\alpha)$ are given as

$$f'(\alpha)=h_1-h_2+\frac{(1-2\alpha)h_1h_2}{\sqrt{(1-\alpha)\alpha h_1h_2}}, \tag{5.15}$$

$$f''(\alpha)=-\frac{h_1^2h_2^2}{2((1-\alpha)\alpha h_1h_2)^{3/2}}<0. \tag{5.16}$$

As indicated by (5.16), $f(\alpha)$ is concave. Therefore, the maximum value of $f(\alpha)$ is achieved when the first order derivative (5.15) is equal to zero, i.e., when $\alpha=\frac{h_1}{h_1+h_2}$. The maximum value of $f(\alpha)$ is given as

$$\hat{f}(\alpha)=\max_{\alpha\in[0,1]} f(\alpha)=f(\frac{h_1}{h_1+h_2})=h_1+h_2. \tag{5.17}$$

Substituting (5.17) into (5.14), we have

$$P_1^{c*} + P_2^{c*} = \frac{2^{r_1+r_2} - 1 - h_1 P_1^{p*} - h_2 P_2^{p*}}{h_1 + h_2}, \tag{5.18}$$

and therefore

$$P_1^{c*} + P_1^{p*} + P_2^{c*} + P_2^{p*} = \frac{2^{r_1+r_2} - 1 + h_2 P_1^{p*} + h_1 P_2^{p*}}{h_1 + h_2}. \tag{5.19}$$

It is easy to see that P_1^{p*} and P_2^{p*} should be the optimal solution of the following problem:

$$\text{(P5.1.1)} \min_{P_1^p, P_2^p} h_2 P_1^p + h_1 P_2^p \tag{5.20}$$

$$\text{s.t. (5.2)}-\text{(5.4)}. \tag{5.21}$$

Note that the Problem (P5.1.1) is convex and its Lagrangian $\mathcal{L}$ is defined as

$$\begin{aligned}
&\mathcal{L}(P_1^p, P_2^p, \lambda_1, \lambda_2, \lambda_3) \\
&= \lambda_1(2^{r_1 - C_{12}} - 1 - h_1 P_1^p) + \lambda_2(2^{r_2 - C_{21}} - 1 - h_2 P_2^p) \\
&+ \lambda_3(2^{r_1 - C_{12} + r_2 - C_{21}} - 1 - h_1 P_1^p - h_2 P_2^p) + h_2 P_1^p + h_1 P_2^p,
\end{aligned}$$

where $\lambda_1 \geq 0$, $\lambda_2 \geq 0$, and $\lambda_3 \geq 0$ are the Lagrangian multipliers.

By letting the partial derivatives of $\mathcal{L}$ with respective to P_1^p and P_2^p be equal to zero, respectively, the first set of optimality conditions is given as

$$h_2 - \lambda_1 h_1 - \lambda_3 h_1 = 0, \tag{5.22}$$

$$h_1 - \lambda_2 h_2 - \lambda_3 h_2 = 0. \tag{5.23}$$

The complementary slackness conditions of this problem are

$$\lambda_1(2^{r_1-C_{12}} - 1 - h_1P_1^p) = 0, \tag{5.24}$$

$$\lambda_2(2^{r_2-C_{21}} - 1 - h_2P_2^p) = 0, \tag{5.25}$$

$$\lambda_3(2^{r_1-C_{12}+r_2-C_{21}} - 1 - h_1P_1^p - h_2P_2^p) = 0. \tag{5.26}$$

1. For $h_1 > h_2$: If $\lambda_2 = 0$, solving (5.22) and (5.23) gives $\lambda_3 = \frac{h_1}{h_2} > 0$ and $\lambda_1 = \frac{h_2^2-h_1^2}{h_2h_1} < 0$, which is infeasible as the condition $\lambda_1 \geq 0$ is violated. If $\lambda_3 = 0$, solving (5.22) and (5.23) gives $\lambda_1 = \frac{h_2}{h_1} > 0$ and $\lambda_2 = \frac{h_1}{h_2} > 0$, which is also infeasible, since it would imply that constraints (5.2) and (5.3) should be achieved with equality, which violates the constraint (5.4). Thus, it can concluded that $\lambda_2 > 0$ and $\lambda_3 > 0$ both hold.

   Therefore, by complementary slackness, we have that the optimal solution of Problem (P5.1.1) is achieved when constraints (5.3) and (5.4) are achieved with equality, while the constraint (5.2) would be inactive since (5.2) and (5.3) cannot be active at the same time as we argued above. Based on this, we have $P_1^{p*} = \frac{1}{h_1}2^{r_2-C_{21}}\left(2^{r_1-C_{12}} - 1\right)$ and $P_2^{p*} = \frac{1}{h_2}\left(2^{r_2-C_{21}} - 1\right)$.

2. For $h_1 = h_2$: From (5.22) and (5.23) we have $\lambda_3 = 1 - \lambda_1 = 1 - \lambda_2$ and hence $\lambda_1 = \lambda_2$. If $\lambda_1 = \lambda_2 > 0$, from (5.24) and (5.25) we have $2^{r_1-C_{12}} - 1 - hP_1^p = 0$ and $2^{r_2-C_{21}} - 1 - hP_2^p = 0$, which violate the constraint (5.4). Therefore, we have $\lambda_1 = \lambda_2 = 0$ and $\lambda_3 = 1$ which indicates that the optimal solution is not unique, any P_1^p, P_2^p that satisfy $r_1 \leq \mathcal{C}\left(h_1P_1^p\right) + C_{12}$, $r_2 \leq \mathcal{C}\left(h_2P_2^p\right) + C_{21}$ and $r_1 + r_2 = \mathcal{C}\left(h_1P_1^p + h_2P_2^p\right) + C_{12} + C_{21}$ is optimal. To keep consistency with the case for $h_1 > h_2$, we use $P_1^{p*} = \frac{1}{h_1}2^{r_2-C_{21}}\left(2^{r_1-C_{12}} - 1\right)$ and $P_2^{p*} = \frac{1}{h_2}\left(2^{r_2-C_{21}} - 1\right)$ as the optimal solution in this thesis.

Hence, the optimal solution of the Problem (P5.1) when $r_1 > C_{12}, r_2 > C_{21}$ can be concluded as $P_1^{c*} = \frac{h_1\left(2^{r_1+r_2} - 2^{r_1-C_{12}+r_2-C_{21}}\right)}{(h_1+h_2)^2}$, $P_1^{p*} = \frac{1}{h_1}2^{r_2-C_{21}}\left(2^{r_1-C_{12}} - 1\right)$, $P_2^{c*} =$

$\frac{h_2\left(2^{r_1+r_2}-2^{r_1-C_{12}+r_2-C_{21}}\right)}{(h_1+h_2)^2}$, $P_2^{p*}=\frac{1}{h_2}\left(2^{r_2-C_{21}}-1\right)$ and

$$\begin{aligned} g\left(r_1,r_2\right) \triangleq & \frac{h_2}{h_1\left(h_1+h_2\right)}2^{r_1-C_{12}+r_2-C_{21}}+\frac{1}{h_1+h_2}2^{r_1+r_2} \\ & +\left(\frac{1}{h_2}-\frac{1}{h_1}\right)2^{r_2-C_{21}}-\frac{1}{h_2}. \end{aligned} \tag{5.27}$$

2) For $r_1 \leq C_{12}, r_2 \leq C_{21}$: The constraints (5.2)-(5.4) are satisfied as long as the other constraints are satisfied. Therefore, the Problem (P5.1) is equivalent to

$$\begin{aligned} &\text{(P5.1.2)} \min_{P_1^p,P_1^c,P_2^p,P_2^c} P_1^p+P_1^c+P_2^p+P_2^c \\ &\text{s.t.} \quad (5.5), P_1^p \geq 0, P_1^c \geq 0, P_2^p \geq 0, P_2^c \geq 0. \end{aligned}$$

First, we prove that $P_1^{c*}>0$ and $P_2^{c*}>0$ in the optimal solution by contradiction.

a) Suppose that $P_1^{c*}=P_2^{c*}=0$ in the optimal solution. In such case, at least one of P_1^{p*} and P_2^{p*} must be nonzero as otherwise the constraint (5.5) would be violated. Suppose that $P_{\bar{i}}^{p*}>0$, $\bar{i}\in\{1,2\}$. Define a new power profile as $\tilde{P}_{\bar{i}}^p=P_{\bar{i}}^{p*}-\delta$, $\tilde{P}_{3-\bar{i}}^p=P_{3-\bar{i}}^{p*}$, $\tilde{P}_1^c=\frac{h_1}{h_1+h_2}\delta$ and $\tilde{P}_2^c=\frac{h_2}{h_1+h_2}\delta$, where $0<\delta\leq P_{\bar{i}}^{p*}$. Obviously, the new power profile results in the same sum power with the original solution, i.e., $\tilde{P}_{\bar{i}}^p+\tilde{P}_{3-\bar{i}}^p+\tilde{P}_1^c+\tilde{P}_2^c=P_{\bar{i}}^{p*}+P_{3-\bar{i}}^{p*}+P_1^{c*}+P_2^{c*}$. Since $r_1+r_2\leq\log\left(1+h_{\bar{i}}P_{\bar{i}}^{p*}+h_{3-\bar{i}}P_{3-\bar{i}}^{p*}\right)$, we have

$$\begin{aligned} &\log\left(1+h_{\bar{i}}\tilde{P}_{\bar{i}}^p+h_{3-\bar{i}}\tilde{P}_{3-\bar{i}}^p+h_1\tilde{P}_1^c+h_2\tilde{P}_2^c+2\sqrt{h_1\tilde{P}_1^ch_2\tilde{P}_2^c}\right) \\ =&\log\left(1+h_{\bar{i}}\left(P_{\bar{i}}^{p*}-\delta\right)+h_{3-\bar{i}}P_{3-\bar{i}}^{p*}+\frac{h_1^2}{h_1+h_2}\delta+\frac{h_2^2}{h_1+h_2}\delta+2\sqrt{\frac{h_1^2h_2^2}{\left(h_1+h_2\right)^2}\delta^2}\right) \\ =&\log\left(1+h_{\bar{i}}P_{\bar{i}}^{p*}+h_{3-\bar{i}}P_{3-\bar{i}}^{p*}-h_{\bar{i}}\delta+\left(h_1+h_2\right)\delta\right) \\ >&r_1+r_2. \end{aligned} \tag{5.28}$$

Since the constraint (5.5) is satisfied with strict inequality under the new power profile as indicated by (5.28), we can always reduce either $\tilde{P}_1^c$ or $\tilde{P}_2^c$ by an arbitrarily small amount

without violating (5.5) such that the sum power is reduced, i.e., becomes smaller than the original power allocation. Thus, this case cannot happen.

b) Suppose that $P_1^{c*} = 0$ and $P_2^{c*} > 0$ in the optimal solution. Define a new power allocation profile as $\tilde{P}_1^p = P_1^{p*}$, $\tilde{P}_2^p = P_2^{p*}$, $\tilde{P}_1^c = \frac{h_2}{h_1} P_2^{c*}$ and $\tilde{P}_2^c = 0$. It is easy to check the new power allocation satisfies all the constraints of Problem (P1.2) while leading to a smaller sum power, i.e., $\tilde{P}_1^p + \tilde{P}_2^p + \tilde{P}_1^c + \tilde{P}_2^c < P_1^{p*} + P_1^{c*} + P_2^{p*} + P_2^{c*}$. Thus, this case cannot happen.

c) Suppose that $P_1^{c*} > 0$ and $P_2^{c*} = 0$ in the optimal solution. Define a new power allocation profile as $\tilde{P}_1^p = P_1^{p*}$, $\tilde{P}_2^p = P_2^{p*}$, $\tilde{P}_1^c = \frac{h_1}{h_1+h_2} P_1^{c*}$ and $\tilde{P}_2^c = \frac{h_2}{h_1+h_2} P_1^{c*}$. It is easy to check that the new power profile results in the same sum power with the original power pofile. Similar to (5.28), we can prove that under the new power profile, (5.5) is satisfied with strict inequality. Therefore, we can always reduce either $\tilde{P}_1^c$ or $\tilde{P}_2^c$ by an arbitrarily small amount without violating (5.5) such that the sum power is reduced and becomes smaller than the original power allocation. Thus, this case cannot happen.

Since the above three cases cannot happen, it can be concluded that $P_1^{c*} > 0$ and $P_2^{c*} > 0$ in the optimal solution.

Next, we prove that P_1^{p*} and P_2^{p*} must equal 0. Suppose that $P_1^{p*} > 0$ in the optimal solution. Define a new power allocation profile as $\tilde{P}_1^p = P_1^{p*} - \delta$, $\tilde{P}_1^c = P_1^{c*} + \Delta$, $\tilde{P}_2^p = P_2^{p*}$ and $\tilde{P}_2^c = P_2^{c*}$, where $0 < \delta \leq P_1^{p*}$, $\Delta > 0$ and

$$\begin{aligned} &h_1 P_1^p + h_1 P_1^c + 2\sqrt{h_1 P_1^c h_2 P_2^c} = \\ &h_1 \left(P_1^p - \delta\right) + h_1 \left(P_1^c + \Delta\right) + 2\sqrt{h_1 \left(P_1^c + \Delta\right) h_2 P_2^c}, \end{aligned} \tag{5.29}$$

which indicates that the new power allocation does not change the value of the RHS of (5.5).

Notice that from (5.29), we have

$$\delta = \Delta + 2\sqrt{h_2 P_2^c / h_1}\left(\sqrt{P_1^c + \Delta} - \sqrt{P_1^c}\right) > \Delta. \tag{5.30}$$

The new power allocation satisfies all constraints in Problem (P1.2). Meanwhile, it yields a smaller sum power, i.e., $\tilde{P}_1^p + \tilde{P}_2^p + \tilde{P}_1^c + \tilde{P}_2^c < P_1^{p*} + P_1^{c*} + P_2^{p*} + P_2^{c*}$. Therefore, $P_1^{p*} > 0$ cannot happen in this case.

Similarly, we can prove that $P_2^{p*} = 0$.

The constraint (5.5) should be satisfied with equality as otherwise we can always reduce one of P_1^{c*} and P_2^{c*} until (5.5) is satisfied with equality to minimize the sum power.

Now, Problem (P5.1.2) reduces to minimizing $P_1^c + P_2^c$ subject to

$$r_1 + r_2 = \log\left(1 + h_1 P_1^c + h_2 P_2^c + 2\sqrt{h_1 P_1^c h_2 P_2^c}\right),$$

which can be easily solved based on (5.15)-(5.17).

Therefore, the optimal solution of Problem (P5.1) when $r_1 \leq C_{12}, r_2 \leq C_{21}$ can be concluded as $P_1^{c*} = \frac{h_1\left(2^{r_1+r_2}-1\right)}{(h_1+h_2)^2}$, $P_1^{p*} = 0$, $P_2^{c*} = \frac{h_2\left(2^{r_1+r_2}-1\right)}{(h_1+h_2)^2}$, $P_2^{p*} = 0$ and

$$g\left(r_1, r_2\right) = \frac{2^{r_1+r_2} - 1}{h_1 + h_2}. \tag{5.31}$$

3) For $r_1 > C_{12}, r_2 \leq C_{21}$: The constraints (5.3) and (5.4) are satisfied as long as the other constraints are satisfied. Therefore, the Problem (P5.1) is equivalent to

$$\text{(P5.1.3)} \quad \min_{P_1^p, P_1^c, P_2^p, P_2^c} P_1^p + P_1^c + P_2^p + P_2^c \tag{5.32}$$

$$\text{s.t.} \quad (5.2), (5.5), P_1^p \geq 0, P_1^c \geq 0, P_2^p \geq 0, P_2^c \geq 0. \tag{5.33}$$

We can prove that the optimal solution of Problem (P5.1.3) is given as $P_1^{c*} = \frac{h_1}{(h_1+h_2)^2}\left(2^{r_1+r_2}-2^{r_1-C_{12}}\right)$, $P_1^{p*} = \frac{1}{h_1}\left(2^{r_1-C_{12}}-1\right)$, $P_2^{c*} = \frac{h_2}{(h_1+h_2)^2}\left(2^{r_1+r_2}-2^{r_1-C_{12}}\right)$, $P_2^{p*}=0$ and

$$g\left(r_1,r_2\right) = \frac{2^{r_1+r_2}}{h_1+h_2} + \frac{h_2 2^{r_1-C_{12}}}{h_1\left(h_1+h_2\right)} - \frac{1}{h_1}. \tag{5.34}$$

The proof is similar to case 2) and is thus omitted here due to space limitation.

4) For $r_1 \leq C_{12}, r_2 > C_{21}$: The optimal solution in this case is given as $P_1^{c*} = \frac{h_1\left(2^{r_1+r_2}-2^{r_2-C_{21}}\right)}{\left(h_1+h_2\right)^2}$, $P_1^{p*}=0$, $P_2^{c*} = \frac{h_2\left(2^{r_1+r_2}-2^{r_2-C_{21}}\right)}{\left(h_1+h_2\right)^2}$, $P_2^{p*} = \frac{2^{r_2-C_{21}}-1}{h_2}$ and

$$g\left(r_1,r_2\right) = \frac{2^{r_1+r_2}}{h_1+h_2} + \frac{h_1 2^{r_2-C_{21}}}{h_2\left(h_1+h_2\right)} - \frac{1}{h_2}. \tag{5.35}$$

The proof is also similar to case 2) and is thus omitted.

By summarizing the above four cases, we get the optimal solution of Problem (P5.1) as shown by (5.8)-(5.12).

□

Remark 8. *It is worth noting that when $C_{12}=0$ and $C_{21}=0$, the minimum sum power function in* (5.8) *reduces to $g(r_1,r_2) \triangleq \frac{2^{r_1+r_2}-2^{r_2}}{h_1} + \frac{2^{r_2}-1}{h_2}$, which is exactly the same as that in* (3.8)*, which is the sum power function for the traditional MAC without conferencing links.*

Remark 9. *The function $g\left(r_1,r_2\right)$ given in (5.8) is a non-decreasing convex function jointly over (r_1,r_2).*

Proof. It is easy to prove that $2^{r_1+r_2}$ is convex over (r_1,r_2). Due to the fact that the pointwise maximum of convex functions is also convex [BV04] and the convexity of $2^{r_1-C_{12}}$, $2^{r_2-C_{21}}$ and $2^{r_1-C_{12}+r_2-C_{21}}$ over (r_1,r_2), we can conclude that both $2^{(r_1-C_{12})^+ + (r_2-C_{21})^+}$ and $2^{(r_2-C_{21})^+}$ are convex over (r_1,r_2) as $2^{(r_1-C_{12})^+ + (r_2-C_{21})^+} = \max\left(2^{r_1-C_{12}}, 2^{r_2-C_{21}}, 2^{r_1-C_{12}+r_2-C_{21}}, 1\right)$ and $2^{(r_2-C_{21})^+} = \max\left(1, 2^{r_2-C_{21}}\right)$. Then, the convexity of the function $g\left(r_1,r_2\right)$ can be verified readily from the fact that the nonneg-

ative weighted sums of convex function is still convex [BV04]. □

By (5.8), the causal EH constraints defined in (5.1) could be rewritten as:

$$T\sum_{n=1}^{j} g\left(r_{1,n}, r_{2,n}\right) \leq \sum_{n=1}^{j} E_n, j = 1, \cdots, N. \tag{5.36}$$

5.2.2.2 Problem Formulation for Infinite Battery Capaticy Case

Based on the definition of the EH constraints in (5.36), the maximum departure region is defined as follows.

Definition 4. *Given an energy input sequence $\boldsymbol{\omega} \in \boldsymbol{\Omega}$, within the finite time horizon of N slots, the* ***maximum departure region*** $\mathcal{D}(N)$ *of the Gaussian MAC with conferencing links and a shared energy harvester with infinite battery capacity is defined as the union of all achievable bits pair (B_1, B_2) under the EH constraint (5.36), i.e.,*

$$\mathcal{D}(N) = \left\{ (B_1, B_2) \middle| B_i = T\sum_{n=1}^{N} r_{i,n}, i = 1, 2, \ (5.36) \right\}, \tag{5.37}$$

where B_i is the total amount of data transmitted from transmitter i, $i = 1, 2$.

Proposition 11. *The maximum departure region $\mathcal{D}(N)$ defined in* (5.37) *for the MAC with conferencing links and infinite battery capacity is convex.*

The proof for Proposition 11 is similar to that for Proposition 2 and is thus omitted here.

Due to the convexity of this region and its special structure in the first orthant, the boundary of $\mathcal{D}(N)$ can be characterised by solving the following problem,

$$\text{(P5.2)} \max_{\{r_{1,n}, r_{2,n}\}} \quad \mu_1 \sum_{n=1}^{N} r_{1,n}T + \mu_2 \sum_{n=1}^{N} r_{2,n}T \tag{5.38}$$

$$\text{s.t.} \quad \sum_{n=1}^{j} g\left(r_{1,n}, r_{2,n}\right) T \leq \sum_{n=1}^{j} E_n, \quad j = 1, \cdots, N, \tag{5.39}$$

where $\mu_1 + \mu_2 = 1$, $\mu_1 \geq 0$, $\mu_2 \geq 0$. By varying the value of μ_1 and μ_2, different points on the boundary of $\mathcal{D}(N)$ can be achieved.

5.2.2.3 Problem Formulation for Finite Battery Capaticy Case

Denote the capacity of the battery as $\mathcal{E}$[1]. Similarly to Section 3.2, the battery non-overflow constraints are mathematically modeled as:

$$\left(\sum_{n=1}^{j+1} E_n\right) - \mathcal{E} \leq T \sum_{n=1}^{j} g\left(r_{1,n}, r_{2,n}\right), j = 1, \cdots, N-1. \tag{5.40}$$

Based on the definition of the EH constraints (5.36) and the battery non-overflow constraints (5.40), the maximum departure region for the case of finite battery capacity is defined as follows.

Definition 5. *Given an energy input sequence $\boldsymbol{\omega} \in \boldsymbol{\Omega}$, within the finite time horizon of N slots, the **maximum departure region** $\mathcal{D}(N)$ of the Gaussian MAC with conferencing links and a shared energy harvester with finite battery capacity is defined as the union of all achievable bits pair (B_1, B_2) under the EH constraint (5.36) and the battery non-overflow constraints* (5.40)*, i.e.,*

$$\mathcal{D}(N) = \left\{ (B_1, B_2) \middle| B_i = T \sum_{n=1}^{N} r_{i,n}, i = 1, 2, \ (5.36), (5.40) \right\}. \tag{5.41}$$

Proposition 12. *The maximum departure region $\mathcal{D}(N)$ defined in* (5.41) *for the MAC with conferencing links and finite battery capacity is convex.*

The proof for Proposition 12 is similar to that for Proposition 3 and thus is omitted here.

Due to the convexity of this region and its special structure in the first orthant, the

[1]In the finite battery case, E_n, $n = 1, \cdots, N$, and thus $E_{\max}$ are truncated at $\mathcal{E}$ since any energy exceeding $\mathcal{E}$ cannot be stored in the battery [TY12a].

boundary of $\mathcal{D}(N)$ can be characterised by solving the following problem,

$$\text{(P5.3)} \quad \max_{\{r_{1,n},r_{2,n}\}} \quad \mu_1 \sum_{n=1}^{N} r_{1,n}T + \mu_2 \sum_{n=1}^{N} r_{2,n}T \tag{5.42}$$

$$\text{s.t.} \quad \sum_{n=1}^{j} g\left(r_{1,n}, r_{2,n}\right) T \leq \sum_{n=1}^{j} E_n, \quad j = 1, \cdots, N, \tag{5.43}$$

$$\left(\sum_{n=1}^{j+1} E_n\right) - \mathcal{E} \leq T \sum_{n=1}^{j} g\left(r_{1,n}, r_{2,n}\right), j = 1, \cdots, N-1. \tag{5.44}$$

5.3 Optimal Offline Resource Allocation Scheme

In this section, the optimal resource allocation schemes are described, denoted by $\mathcal{O}$, for solving the Problem (P5.2) and (P5.3). First, for each problem, the structure of the optimal sum power sequence $g(r_{1,n}, r_{2,n})$, $n = 1, \cdots, N$, is analysed. Then, the optimal rate allocation that achieve the boundary points of the maximum departure region $\mathcal{D}(N)$ is derived.

5.3.1 Optimal Sum Power Allocation

5.3.1.1 Optimal Sum Power Allocation for Infinite Battery Case

As indicated by Remark 2 in Chapter 3.3.1.1, since $g(r_1, r_2)$ in (5.8) is convex over (r_1, r_2), the optimal solution of problem (P5.2) satisfies Lemma 6 and Lemma 7.

Lemma 6. *The optimal solution for problem (P5.3) satisfies* $g(r_{1,n}, r_{2,n}) \leq g(r_{1n+1}, r_{2n+1})$, $\forall n \in \{1, \ldots, N-1\}$,*i.e., the optimal sum power can only stay constant or increase over time.*

Lemma 7. *The optimal solution for problem (P5.3) satisfies that if* $g(r_{1,n}, r_{2,n}) < g(r_{1n+1}, r_{2n+1})$, $\forall n \in \{1, \ldots, N-1\}$, *there is no residual energy at* $t = s_n$, *i.e., when the optimal sum power level changes, all harvested energy must be depleted.*

As indicated by Lemma 6 and 7, the optimal sum power sequence for the Problem

(P5.3) has the same structural properties as that for the single-user channel case discussed in [YU12b]. Given an input sequence $\boldsymbol{\omega}$, the optimal offline sum power sequence $\mathbf{P}^{\mathcal{O}} = [P_1^{\mathcal{O}}, \cdots, P_N^{\mathcal{O}}]^T$, where $P_n^{\mathcal{O}}, n = 1, \cdots, N$, denotes the optimal sum power in the n-th slot, can be obtained as [YU12b]:

$$n_k = \arg \min_{n_{k-1} < n \leq N} \left\{ \frac{\sum_{j=n_{k-1}+1}^{n} E_j}{(n - n_{k-1})\, T} \right\}, \tag{5.45}$$

$$g(r_{1,n}, r_{2,n}) = \frac{\sum_{j=n_{k-1}+1}^{n_k} E_j}{(n_k - n_{k-1})\, T} \doteq P_n^{\mathcal{O}}, \text{for } n_{k-1} < n \leq n_k, \tag{5.46}$$

where $n_0 = 0$.

5.3.1.2 Optimal Sum Power Allocation for Finite Battery Case

As indicated by Remark 3 in Chapter 3.3.1.2, since $g(r_1, r_2)$ in (5.8) is convex over (r_1, r_2), the optimal solution of problem (P5.3) satisfies Lemma 8 and Lemma 9.

Lemma 8. *The optimal solution for problem (P5.3) satisfies that if $g(r_{1,n}, r_{2,n}) \neq g(r_{1,n+1}, r_{2,n+1})$, either the energy is depleted at the end of the n-th slot or the battery is full at the beginning of the $(n+1)$-th slot, $\forall n \in \{1, \cdots, N-1\}$.*

Lemma 9. *The optimal solution for problem (P5.3) satisfies that for $n = 1, \cdots, N-1$, $g(r_{1,n}, r_{2,n}) \leq g(r_{1,n+1}, r_{2,n+1})$ if the battery is depleted at the end of the n-th slot and $g(r_{1,n}, r_{2,n}) \geq g(r_{1,n+1}, r_{2,n+1})$ if the battery is full at the beginning of the $(n+1)$-th slot.*

Therefore, the optimal sum power sequence $\mathbf{P}^{\mathcal{O}} = [P_1^{\mathcal{O}}, \cdots, P_N^{\mathcal{O}}]^T$ could be obtained by using Algorithm 1.

5.3.2 Optimal Resource Allocation between the two Transmitters

In subsection 5.3.1, the optimal sum power profiles for both the infinite and finite battery capacity cases was obtained.

From (5.45), (5.46) and Algorithm 1, it is observed that the optimal sum power

sequence $\mathbf{P}^{\mathcal{O}} = [P_1^{\mathcal{O}}, \cdots, P_N^{\mathcal{O}}]$ only depends on the energy input sequence and is not influenced by the values of μ_1 and μ_2, for both cases. The constraints of Problem (P5.2) and P(5.3) can be rewritten as

$$g\left(r_{1,n}, r_{2,n}\right) = P_n^{\mathcal{O}}, n = 1, \cdots, N \tag{5.47}$$

where $P_n^{\mathcal{O}}$ is the optimal sum power profile obtained by (5.45), (5.46) for the infinite battery capacity case and by Algorithm 1 for the finite battery capacity case.

Therefore, both problem (P5.2) and P(5.3) can be decomposed into N optimisation problems as follows. For $n = 1, \ldots, N$,

$$\text{(P5.4n)} \max_{\{r_{1,n}, r_{2,n}\}} \quad \mu_1 r_{1,n} + \mu_2 r_{2,n} \tag{5.48}$$

$$\text{s.t.} \quad g\left(r_{1,n}, r_{2,n}\right) = P_n^{\mathcal{O}}. \tag{5.49}$$

Before presenting the optimal solution of Problem (P5.4n), some properties of the curve defined by $g(r_{1,n}, r_{2,n}) = P_n^{\mathcal{O}}$ (denoted as $\mathcal{G}$) are shown. Define four possible regions as follows:

$$\begin{aligned}
\mathcal{R}_1 &= \left\{(r_{1,n}, r_{2,n}) \in \mathcal{G} \,|0 < r_{1,n} < C_{12}, 0 < r_{2,n} < C_{21}\right\}, \\
\mathcal{R}_2 &= \left\{(r_{1,n}, r_{2,n}) \in \mathcal{G} \,|r_{1,n} > C_{12}, 0 < r_{2,n} < C_{21}\right\}, \\
\mathcal{R}_3 &= \left\{(r_{1,n}, r_{2,n}) \in \mathcal{G} \,|0 < r_{1,n} < C_{12}, r_{2,n} > C_{21}\right\}, \\
\mathcal{R}_4 &= \left\{(r_{1,n}, r_{2,n}) \in \mathcal{G} \,|r_{1,n} > C_{12}, r_{2,n} > C_{21}\right\}.
\end{aligned}$$

Notice that, for any given $P_n^{\mathcal{O}}$, at most three out of the four regions defined above can be non-empty. For the case of $C_{12} > C_{21}$, Fig. 5.2 to Fig. 5.5 illustrate the curve $\mathcal{G}$ with different $P_n^{\mathcal{O}}$ and $h_1 > h_2$. For the case of $C_{12} < C_{21}$, similar results could be observed and thus is omitted in the following. As will be confirmed later by the tangent line property of $\mathcal{G}$, $\mathcal{R}_1$ is a straight line whereas $\mathcal{R}_2, \mathcal{R}_3$ and $\mathcal{R}_4$ are curves when $h_1 > h_2$

(when $h_1 = h_2$, $\mathcal{R}_1$ and $\mathcal{R}_4$ are straight lines).

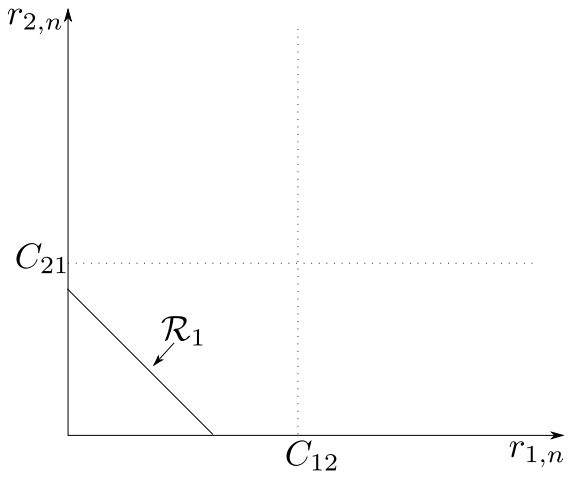

Figure 5.2: Curve $\mathcal{G}$ with non-empty $\mathcal{R}_1$ and empty $\mathcal{R}_2$, $\mathcal{R}_3$, $\mathcal{R}_4$.

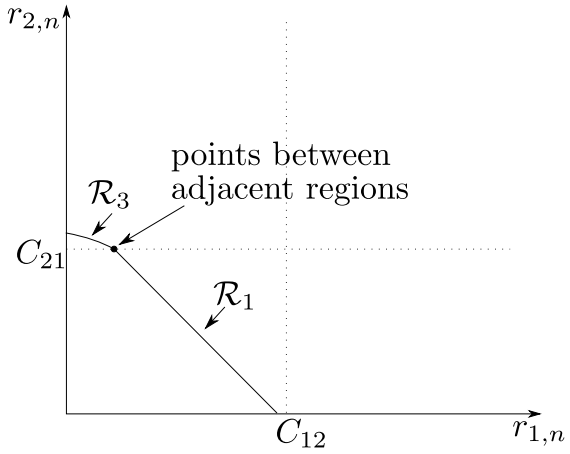

Figure 5.3: Curve $\mathcal{G}$ with non-empty $\mathcal{R}_1$, $\mathcal{R}_3$ and empty $\mathcal{R}_2$, $\mathcal{R}_4$.

As indicated by the shape of $\mathcal{G}$ in Fig. 5.2 to Fig. 5.5, for given μ_1 and μ_2, finding the rate pair $(r_{1,n}, r_{2,n})$ that maximises $\mu_1 r_{1,n} + \mu_2 r_{2,n}$ is equivalent to finding the point $(r_{1,n}, r_{2,n})$ on $\mathcal{G}$, at which the slope of (one of) the tangent line(s) (as will be explained later, the tangent line is unique at most points on $\mathcal{G}$ but not at the others) equals $-\frac{\mu_1}{\mu_2}$. Denote the slope of (one of) the tangent line(s) at point $(r_{1,n}, r_{2,n}) \in \mathcal{G}$ by ϕ. By calculating the first-order derivative of (5.8), it is concluded the properties of ϕ as follows.

Proposition 13. *At the point $(r_{1,n}, r_{2,n})$ in any of the four regions, there exists an*

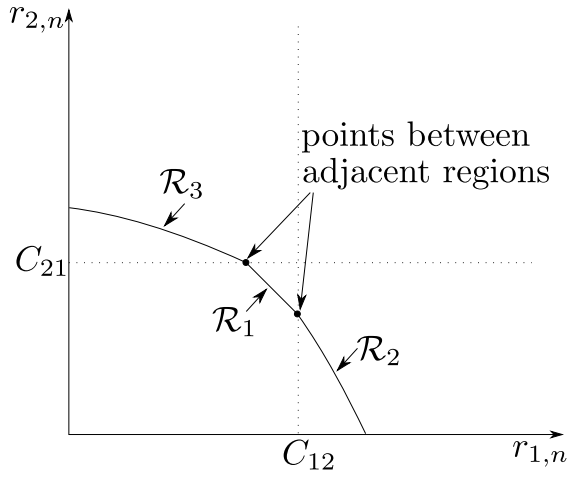

Figure 5.4: Curve $\mathcal{G}$ with non-empty $\mathcal{R}_1$, $\mathcal{R}_2$, $\mathcal{R}_3$ and empty $\mathcal{R}_4$.

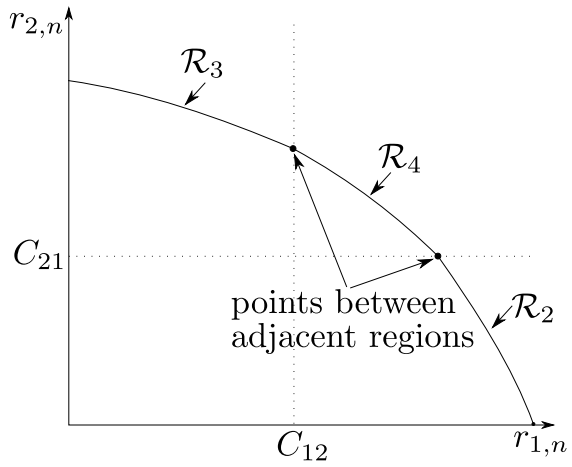

Figure 5.5: Curve $\mathcal{G}$ with non-empty $\mathcal{R}_2$, $\mathcal{R}_3$, $\mathcal{R}_4$ and empty $\mathcal{R}_1$.

unique tangent line and ϕ satisfies

$$\phi = \begin{cases} -1, & \text{if} \quad (r_{1,n}, r_{2,n}) \in \mathcal{R}_1 \\ -1 - \frac{h_2}{h_1 2^{r_{2,n}+C_{12}}} < -1, & \text{if} \quad (r_{1,n}, r_{2,n}) \in \mathcal{R}_2 \\ -1 + \frac{h_1}{h_1 + h_2 2^{r_{1,n}+C_{21}}} > -1, & \text{if} \quad (r_{1,n}, r_{2,n}) \in \mathcal{R}_3 \\ -\left(1 + \frac{(h_1^2 - h_2^2)2^{C_{12}-r_{1,n}}}{h_1 h_2 2^{C_{12}+C_{21}} + h_2^2}\right)^{-1} > -1, & \text{if} \quad (r_{1,n}, r_{2,n}) \in \mathcal{R}_4 \end{cases} . \tag{5.50}$$

At the point $(r_{1,n}, r_{2,n})$ between two adjacent regions, the tangent line is not unique and

ϕ satisfies

$$\phi \in \begin{cases} \left[-1-\frac{h_2}{h_1 2^{r_{2,n}+C_{12}}}, -1\right], & \text{if } (r_{1,n}, r_{2,n}) \text{ is between } \mathcal{R}_1 \text{ and } \mathcal{R}_2 \\ \left[-1, -1+\frac{h_1}{h_1+h_2 2^{r_{1,n}+C_{21}}}\right], & \text{if } (r_{1,n}, r_{2,n}) \text{ is between } \mathcal{R}_1 \text{ and } \mathcal{R}_3 \\ \left[-1+\frac{h_1^2-h_2^2}{h_1^2+h_1 h_2 2^{C_{12}+C_{21}}}, -1+\frac{h_1}{h_1+h_2 2^{C_{12}+C_{21}}}\right], & \text{if } (r_{1,n}, r_{2,n}) \text{ is between } \mathcal{R}_3 \text{ and } \mathcal{R}_4 \\ \left[-1-\frac{h_2}{h_1 2^{C_{21}+C_{12}}}, -\left(1+\frac{(h_1^2-h_2^2)2^{C_{12}-r_{1,n}}}{h_1 h_2 2^{C_{12}+C_{21}}+h_2^2}\right)^{-1}\right], & \text{if } (r_{1,n}, r_{2,n}) \text{ is between } \mathcal{R}_2 \text{ and } \mathcal{R}_4 \end{cases} \tag{5.51}$$

Remark 10. *For $(r_{1,n}, r_{2,n}) \in \mathcal{R}_2$, ϕ is only determined by $r_{2,n}$, i.e., it is independent of $P_n^{\mathcal{O}}$, and increases as $r_{2,n}$ increases. For $(r_{1,n}, r_{2,n}) \in \mathcal{R}_3$, ϕ is only determined by $r_{1,n}$, i.e., it is independent of $P_n^{\mathcal{O}}$, and decreases as $r_{1,n}$ increases. For $(r_{1,n}, r_{2,n}) \in \mathcal{R}_4$, i) if $h_1 > h_2$, ϕ is only determined by $r_{1,n}$, i.e., it is independent of $P_n^{\mathcal{O}}$, and decreases as $r_{1,n}$ increases with $\lim_{r_{1,n}\to\infty} \frac{dr_{2,n}}{dr_{1,n}} = -1$; ii) if $h_1 = h_2$, $\phi = -1$ for any point belongs to $\mathcal{R}_4$.*

Then, the optimal solution of Problem (P5.4n) for $n = 1, \cdots, N$, by finding the point on $\mathcal{G}$ which has a $\phi = -\frac{\mu_1}{\mu_2}$ is obtained. The optimal solution $\left(r_{1,n}^{\mathcal{O}}, r_{2,n}^{\mathcal{O}}\right)$ is concluded as follows; and then by applying (5.9)-(5.12), we complete the whole transmission scheme.

1. If $-\frac{\mu_1}{\mu_2} < -1$, as indicated by (5.50) and (5.51), the optimal point can only possibly be in $\mathcal{R}_2$, between $\mathcal{R}_1$ and $\mathcal{R}_2$, between $\mathcal{R}_2$ and $\mathcal{R}_4$ or on the horizontal axis. Letting $-1-\frac{h_2}{h_1 2^{r_{2,n}+C_{12}}}$ (the second term of (5.50)) equal $-\frac{\mu_1}{\mu_2}$, we have

$$r_{2,n} = \min\left\{\left(\log\frac{h_2\mu_2}{h_1(\mu_1-\mu_2)} - C_{12}\right)^+, C_{21}\right\} \doteq R_2. \tag{5.52}$$

   (a) If $0 \le P_n^{\mathcal{O}} \le g\left(C_{12}, 0\right)$, the optimal rate allocation is given as $r_{2,n}^{\mathcal{O}} = 0$ and $r_{1,n}^{\mathcal{O}} = \mathcal{C}\left(\left(h_1+h_2\right)P_n^{\mathcal{O}}\right)$;

   (b) If $g\left(C_{12}, 0\right) < P_n^{\mathcal{O}} \le g\left(C_{12}, R_2\right)$, the point between $\mathcal{R}_1$ and $\mathcal{R}_2$ satisfies $r_{2,n} < R_2$ and thus has a $\phi = -\frac{\mu_1}{\mu_2}$, which can be easily checked by (5.51) and the

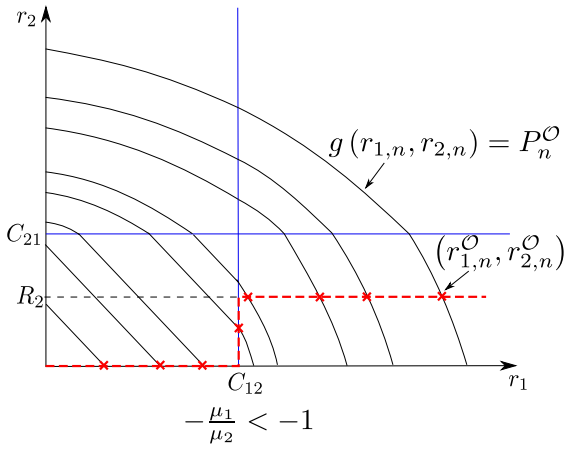

Figure 5.6: An illustration of the optimal offline rate profile when $-\frac{\mu_1}{\mu_2} < -1$

fact that $-1 - \frac{h_2}{h_1 2^{r_{2,n}+C_{12}}}$ decreases as $r_{2,n}$ decreases. Therefore, this point is the optimal solution and the optimal rate allocation is given as $r_{1,n}^{\mathcal{O}} = C_{12}$ and $r_{2,n}^{\mathcal{O}} = \mathcal{C}\left(\left(h_1 + h_2\right) P_n^{\mathcal{O}}\right) - C_{12}$;

(c) If $P_n^{\mathcal{O}} > g\left(C_{12}, R_2\right)$, the optimal rate allocation is given as $r_{2,n}^{\mathcal{O}} = R_2$ and $r_{1,n}^{\mathcal{O}} = \log \frac{\left(h_1+h_2\right)\left(1+h_1 P_n^{\mathcal{O}}\right)}{h_2 2^{-C_{12}} + h_1 2^{R_2}} > C_{12}$, which can be verified directly from the definition of R_2.

It can be seen that R_2 is the maximum possible transmission rate for transmitter 2, regardless of the sum power value $P_n^{\mathcal{O}}$; thus it is named as the capping rate at transmitter 2.

Figure 5.6 shows an illustration of the optimal rate allocation when $-\frac{\mu_1}{\mu_2} < -1$.

2. If $-\frac{\mu_1}{\mu_2} > -1$, similar to the above case, the optimal solution to (P5.4n) can be obtained as follows.

(a) If $0 \leq P_n^{\mathcal{O}} \leq g\left(0, C_{21}\right)$, the optimal rate allocation is given as $r_{1,n}^{\mathcal{O}} = 0$ and $r_{2,n}^{\mathcal{O}} = \mathcal{C}\left(\left(h_1 + h_2\right) P_n^{\mathcal{O}}\right)$;

(b) If $g\left(0, C_{21}\right) < P_n^{\mathcal{O}} \leq g\left(R_1, C_{21}\right)$, where R_1 is defined as

$$R_1 = \begin{cases} \min\left\{\left(\log\left(\frac{h_1}{h_2}\left(\frac{\mu_2}{\mu_2-\mu_1}-1\right)\right)-C_{21}\right)^+, C_{12}\right\}, & \text{if } -\frac{\mu_1}{\mu_2} \geq -1+\frac{h_1^2-h_2^2}{h_1^2+h_1h_2 2^{C_{12}+C_{21}}} \\ \log\left(\frac{\mu_1(h_2^2-h_1^2)}{(\mu_1-\mu_2)h_2(h_1 2^{C_{12}+C_{21}}+h_2)}\right)+C_{12}, & \text{otherwise} \end{cases}, \tag{5.53}$$

the optimal rate allocation is given as:

i. if $-\frac{\mu_1}{\mu_2} \geq -1+\frac{h_1^2-h_2^2}{h_1^2+h_1h_2 2^{C_{12}+C_{21}}}$, $r_{2,n}^{\mathcal{O}} = C_{21}$ and $r_{1,n}^{\mathcal{O}} = \mathcal{C}\left(\left(h_1+h_2\right)P_n^{\mathcal{O}}\right) - C_{21}$;

ii. otherwise, $r_{2,n}^{\mathcal{O}} = C_{21}$ and

$$r_{1,n}^{\mathcal{O}} = \begin{cases} \mathcal{C}\left(\left(h_1+h_2\right)P_n^{\mathcal{O}}\right) - C_{21}, & \text{if } P_n^{\mathcal{O}} \leq g\left(C_{12}, C_{21}\right) \\ \log\frac{\left(h_1+h_2\right)\left(1+h_1P_n^{\mathcal{O}}\right)}{h_2 2^{-C_{12}}+h_1 2^{C_{21}}}, & \text{if } P_n^{\mathcal{O}} > g\left(C_{12}, C_{21}\right) \end{cases};$$

(c) If $P_n^{\mathcal{O}} > g\left(R_1, C_{21}\right)$, the optimal rate allocation is given as

i. if $-\frac{\mu_1}{\mu_2} \geq -1+\frac{h_1^2-h_2^2}{h_1^2+h_1h_2 2^{C_{12}+C_{21}}}$, $r_{1,n}^{\mathcal{O}} = R_1$ and $r_{2,n}^{\mathcal{O}} = \log\frac{\left(1+h_2P_n^{\mathcal{O}}\right)(h_1+h_2)}{h_1 2^{-C_{21}}+h_2 2^{R_1}}$;

ii. otherwise, $r_{1,n}^{\mathcal{O}} = R_1$ and $r_{2,n}^{\mathcal{O}} = \log\frac{\left(h_2P_n^{\mathcal{O}}+1\right)h_1(h_1+h_2)}{h_2^2 2^{R_1-C_{12}-C_{21}}+h_1h_2 2^{R_1}+\left(h_1^2-h_2^2\right)2^{-C_{21}}}$.

Figure 5.7 show illustrations of the optimal rate allocation when $-\frac{\mu_1}{\mu_2} > -1$.

It can be seen that R_1 is the maximum possible transmission rate for transmitter 1, regardless of the sum power value $P_n^{\mathcal{O}}$, thus it is called as the capping transmission rate at transmitter 1.

3. If $-\frac{\mu_1}{\mu_2} = -1$, it follows that:

(a) If $P_n^{\mathcal{O}} \leq g\left(C_{12}, C_{21}\right)$, the optimal rate allocation is not unique, and any rate pair $\left(r_{1,n}^{\mathcal{O}}, r_{2,n}^{\mathcal{O}}\right)$ satisfying $r_{1,n}^{\mathcal{O}} + r_{2,n}^{\mathcal{O}} = \mathcal{C}\left(\left(h_1+h_2\right)P_n^{\mathcal{O}}\right)$, $0 \leq r_{1,n}^{\mathcal{O}} \leq C_{12}$, and $0 \leq r_{2,n}^{\mathcal{O}} \leq C_{21}$, is optimal;

(b) If $P_n^{\mathcal{O}} > g\left(C_{12}, C_{21}\right)$,

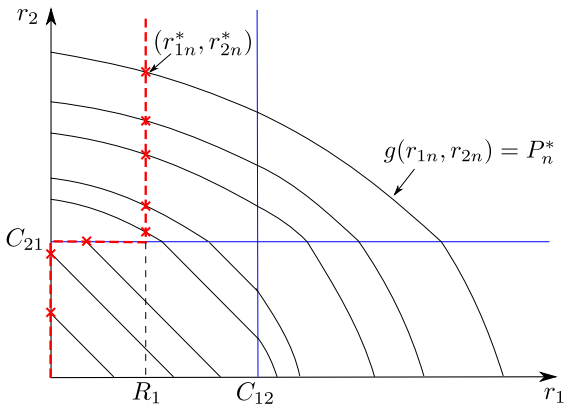

(a) An illustration of the optimal offline rate profile when $-\frac{\mu_1}{\mu_2} > M_1$

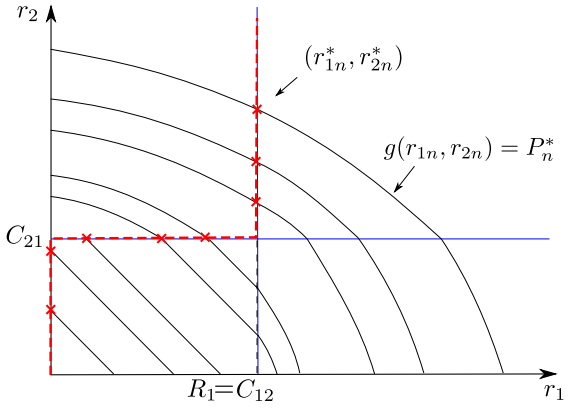

(b) An illustration of the optimal offline rate profile when $M_2 \leq -\frac{\mu_1}{\mu_2} \leq M_1$

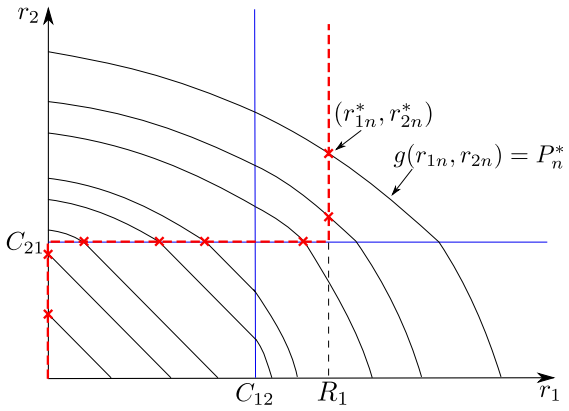

(c) An illustration of the optimal offline rate profile when $-\frac{\mu_1}{\mu_2} < M_2$

Figure 5.7: An illustration of the optimal offline rate profile when $-\frac{\mu_1}{\mu_2} > -1$, $(M_1 = -1 + \frac{h_1}{h_1 + h_2 2^{C_{12}+C_{21}}}$ $M_2 = -1 + \frac{h_1^2 - h_2^2}{h_1^2 + h_1 h_2 2^{C_{12}+C_{21}}})$.

i. when $h_1 > h_2$, the optimal rate allocation is given as $r_{2,n}^{\mathcal{O}} = C_{21}$ and $r_{1,n}^{\mathcal{O}} = \log \frac{(h_1+h_2)\left(1+h_1 P_n^{\mathcal{O}}\right)}{h_2 2^{-C_{12}}+h_1 2^{C_{21}}}$, which is the point between $\mathcal{R}_2$ and $\mathcal{R}_4$. In this case, the capping rate at transmitter 2 is equal to C_{21}.

ii. when $h_1 = h_2$, the optimal rate allocation is not unique, and any rate pair $\left(r_{1,n}^{\mathcal{O}}, r_{2,n}^{\mathcal{O}}\right)$ satisfying $r_{1,n}^{\mathcal{O}} + r_{2,n}^{\mathcal{O}} = \log \frac{2+2h_1 P_n^{\mathcal{O}}}{1+2^{-C_{12}-C_{21}}}$, $r_{1,n}^{\mathcal{O}} \geq C_{12}$, and $r_{2,n}^{\mathcal{O}} \geq C_{21}$, is optimal.

Figure 5.8 shows an illustration of the optimal rate allocation when $-\frac{\mu_1}{\mu_2} = -1$.

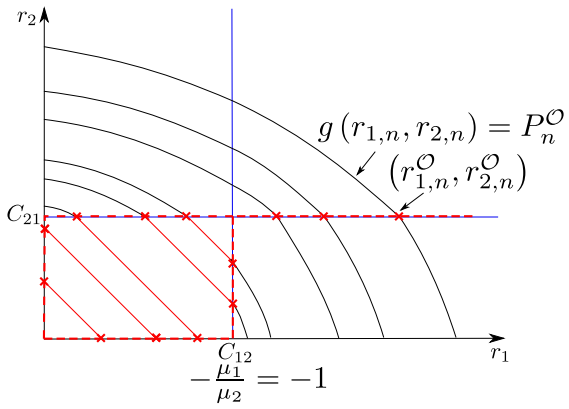

Figure 5.8: An illustration of the optimal offline rate profile when $\mu_1 = \mu_2$

5.4 Numerical Examples

In this section, one energy input sequence is used as an example to illustrate the properties of the optimal offline scheme and the boundary of the maximum departure region. We adopt $C_{12} = 0.5$ bits/s/Hz, $C_{21} = 0.4$ bits/s/Hz, $h_1 = 0.8$, $h_2 = 0.7$, $N = 15$, and $T = 10$ s. For the case of finite battery capacity, it is assumed $\mathcal{E} = 20$ J.

Consider the input sequence

$$\boldsymbol{\omega}_1 = (20, 17.3, 16, 16, 14.7, 16, 10.7, 4, 5.3, 2.7, 10, 13.3, 17.3, 18, 18.7) \text{ J}.$$

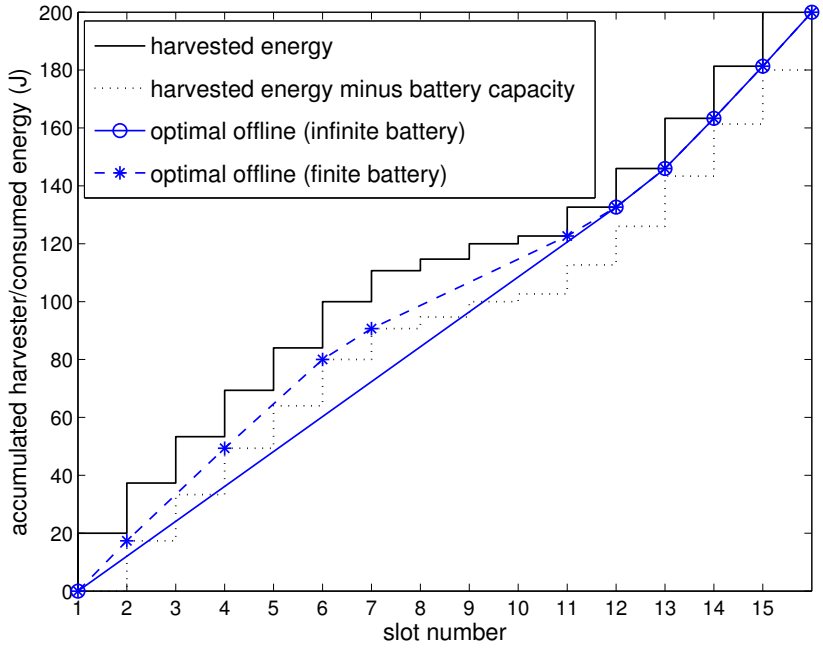

Figure 5.9: The accumulated amounts of harvested energy and energy consumed by the optimal offline scheme with infinite/finite battery capacity given $\boldsymbol{\omega}_1$ in the Gaussian MAC with conferencing links and a shared energy harvester.

Given $\boldsymbol{\omega}_1$, the sum power sequences obtained by the optimal offline scheme with infinite and finite battery capacities are given as

$$\mathbf{P}^{\mathcal{O}} = [1.206, 1.206, 1.206, 1.206, 1.206, 1.206, 1.206, 1.206, 1.206, 1.206, 1.206, 1.33, 1.73, 1.8, 1.87]^T \text{ J/s},$$

and

$$\mathbf{P}_{\mathcal{E}}^{\mathcal{O}} = [1.73, 1.6, 1.6, 1.535, 1.535, 1.07, 0.8, 0.8, 0.8, 0.8, 1, 1.33, 1.73, 1.8, 1.87]^T \text{ J/s},$$

respectively.

Fig. 5.9 illustrates the accumulated amounts of energy harvested (black staircase

curves) and consumed by the schemes (blue curves) during the course of transmissions. The slopes of the blue curves indicate the sum power levels. To satisfy the causal EH constraints, the blue curves must be beneath the black solid curve. For the finite battery case, the blue dash curve must also be above the black dot curve (which represents the accumulated amount of harvested energy minus the battery capacity) to avoid battery overflow.

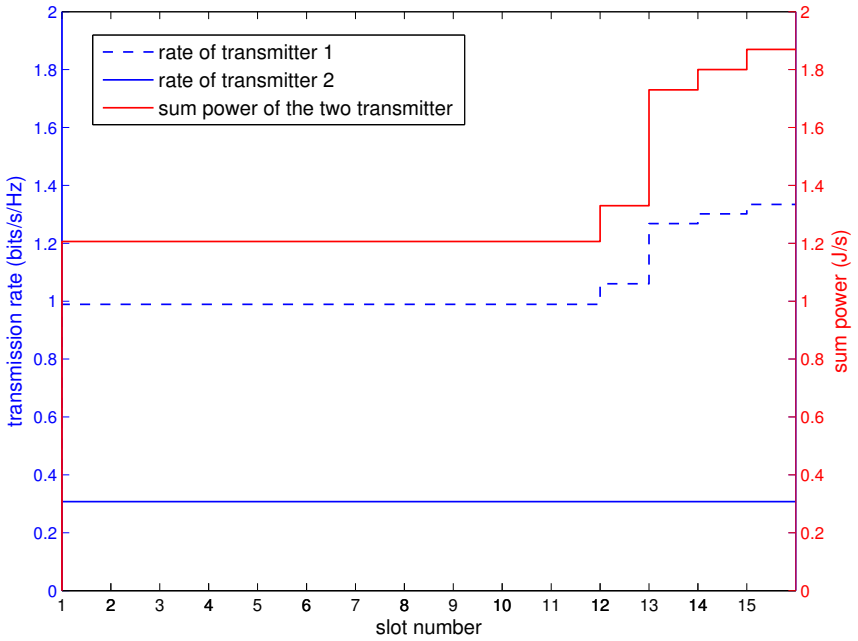

Figure 5.10: Transmission rates of the two transmitters (blue curves, correspond to the left Y axis) when $\mu_1 = 0.6, \mu_2 = 0.4$ and the sum power levels (red curve, corresponds to the right Y axis) during the 15 slots for the Gaussian MAC with conferencing links a shared energy harvester of infinite battery capacity.

Given the energy input sequence $\boldsymbol{\omega}_1$, the sum power levels (which are independent of μ_1, μ_2) and the transmission rates of the two transmitters for the optimal offline scheme $\mathcal{O}$ (with infinite battery capacity) when $\mu_1 = 0.6$ and $\mu_2 = 0.4$ is illustrated in Fig. 5.10. Based on the optimal rate allocation, when $\mu_1 = 0.6$, there exists a capping

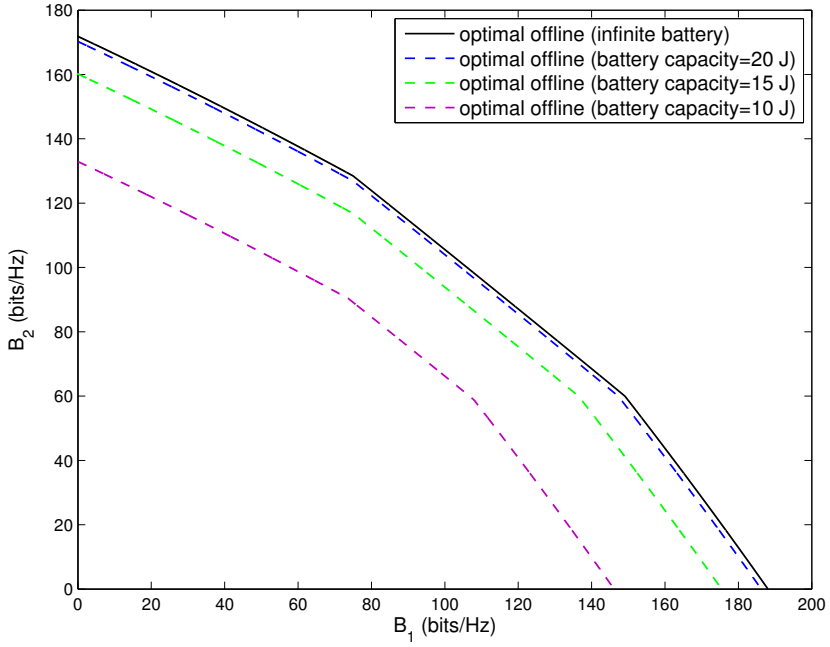

Figure 5.11: The performance achieved by the optimal offline scheme with infinite and finite battery capacities given $\boldsymbol{\omega}_1$ for the Gaussian MAC with conferencing links a shared energy harvester over 15 slots (150s).

rate $R_2 = \min\left\{\left(\log\frac{h_2\mu_2}{h_1(\mu_1-\mu_2)} - C_{12}\right)^+, C_{21}\right\} = 0.307$ bits/s. Since the sum power level $P_n^{\mathcal{O}} > g\left(C_{12}, R_2\right) = 0.5$ J/s, $\forall n \in \{1, \cdots, N\}$, the optimal rate allocation satisfies that the rate of transmitter 2 keeps at the capping rate $R_2 = 0.307$ bits/s all the time while the rate of transmitter 1 increases as the sum power increases.

In Fig. 5.11, the comparison of performance achieved by the optimal offline schemes, i.e., the boundaries of the maximum departure regions, with both infinite and several different finite battery capacities, i.e., $\mathcal{E} = 20, 15, 10$ J, given $\boldsymbol{\omega}_1$, is shown. As expected, the maximum departure region with infinite battery capacity is larger than those with finite battery capacities. Moreover, the smaller the battery capacity, the smaller the maximum departure region.

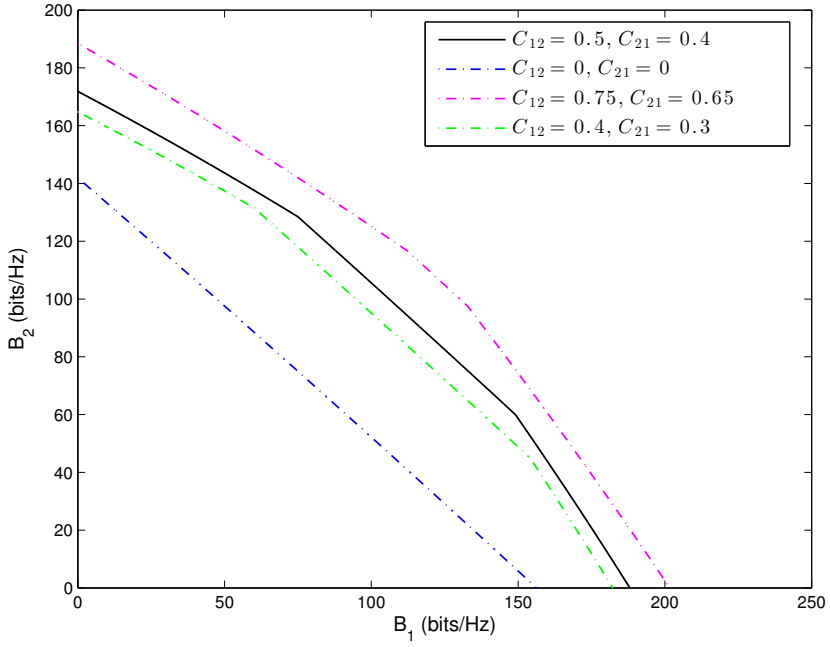

Figure 5.12: The performance achieved by the optimal offline scheme with infinite battery capacity given $\boldsymbol{\omega}_1$ for the Gaussian MAC with conferencing links a shared energy harvester over 15 slots (150s), with different conferencing links capacities.

In Fig. 5.12, the performance achieved by the optimal offline scheme with infinite battery capacity given $\boldsymbol{\omega}_1$ for the Gaussian MAC with conferencing links a shared energy harvester over 15 slots (150s) with different conferencing link capacities is plotted. As can be seen from this figure, the conferencing links can help to improve the performance. With larger conferencing link capacities, larger maximum departure region could be achieved. It is worth noting that, when $C_{12} = 0$ bits/s/Hz and $C_{21} = 0$ bits/s/Hz, the maximum departure region achieved is exactly the same as that achieved in the traditional MAC case in Fig. 3.11. This could be regarded as a verification of the correctness of the derivation.

5.5 Summary

In this chapter, the optimal offline resource allocation schemes for the two-user Gaussian MAC with a shared energy harvester and conferencing links was studied. Both the infinite battery capacity case and the finite battery capacity case were considered. The optimal offline scheme that achieves the boundary of the maximum departure region were developed by investigating the structure of the optimal sum power allocation and then deriving the optimal rate scheduling over the two transmitters. In particular, it was shown that there exists a capping rate at one of the two transmitters in various scenarios. Numerical examples were shown to illustrate the properties of the optimal offline schemes.

Chapter 6

Online Resource Allocation Schemes for Multiple Access Channels with Conferencing Links and a Shared Renewable Source

6.1 Overview

In the previous chapter, the optimal offline resource allocation schemes for the Gaussian MAC with conferencing links, where the two transmitters are powered by a shared energy harvester, were investigated, assuming the energy energy input sequence is known before the transmissions start. In this chapter, the online schemes for the MAC with conferencing links are considered, assuming only causal information of the input energy sequence is known, i.e., at any moment, only the amount of energy arrival in the previous slots are known. First, several online schemes assuming no/partial statistical information about the EH process are described. Then, numerical results are used to evaluate these schemes' average performance given some stochastic energy arrivals. At last, the worst

case performance of the online greedy scheme is evaluated by competitive analysis.

6.2 The Online Schemes

In this section, we consider three online schemes that are similar to the ones in Section 4.2.

1. *Online greedy scheme:* Given an arbitrary energy input sequence $\boldsymbol{\omega} \in \boldsymbol{\Omega}$, the sum power allocated to slot n, $n = 1, \cdots, N$, is $\frac{E_n}{T}$. The rate scheduling of the two transmitters follows the optimal solution of problem (P5.4n).

   This scheme requires no statistical information about the EH process.

2. *Online on-off scheme:* The two transmitters transmit with a sum power of $\frac{\tilde{E}}{T}$, where $\tilde{E}$ is the transmitters' estimation of the average energy arrival amount, whenever there is energy available; otherwise, the transmission is suspended. The rate scheduling of the two transmitters follows the optimal solution of problem (P5.4n).

3. *Online passive scheme:* In this scheme, the sum power allocated in the n-th slot is given as $\frac{1}{T}\sum_{i=1}^{n}\frac{E_i}{N+1-i}$. Similarly, the rate scheduling of the two transmitters follows the optimal solution of problem (P5.4n).

For the case of finite battery capacity, any energy exceeding the battery capacity will be discarded by the online on-off scheme and the online passive scheme. For online greedy scheme, there will be no energy left by the end of each slot. Therefore, battery overflow would never happen in the greedy scheme.

Note that both the online greedy scheme and the online passive scheme require no information about the energy harvesting process while the online on-off scheme requires the partial statistical information, i.e., the average energy arrival amount.

6.3 Simulation Results

In this section, the average performance of the three online schemes described in the previous section is investigated with some stochastic energy arrivals for both the infinite and finite battery cases. We adopt $h_1 = 0.8$, $h_2 = 0.7$, $C_{12} = 0.5$ bits/s/Hz, $C_{21} = 0.4$ bits/s/Hz, $N = 15$, and $T = 10$ s. For the case of finite battery capacity, it is assumed $\mathcal{E} = 20$ J.

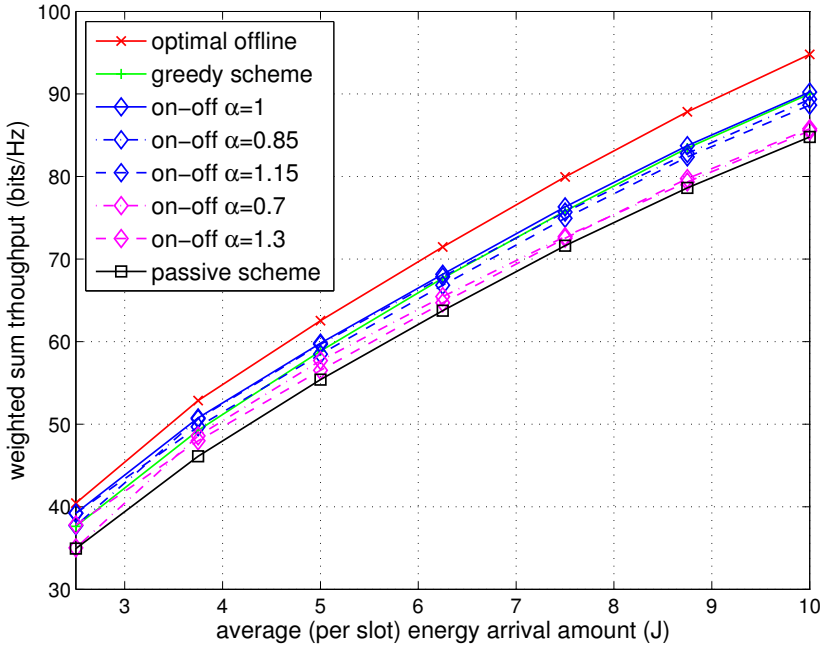

Figure 6.1: Weighted sum throughput versus average energy arrival amounts with infinite battery capacity for Gaussian MAC with conferencing links when $\mu_1 = 0.6, \mu_2 = 0.4$.

For the purpose of exposition, it is assumed that the energy arrival amount, i.e., the amount of harvested energy that arrives at the beginning of a slot, follows a uniform distribution over $[0, E_{\max}]$. The average (per slot) energy arrival amount, denoted by $\bar{E}$, is thus given by $\bar{E} = \frac{E_{\max}}{2}$. For the online on-off scheme, $\alpha = \tilde{E}/\bar{E}$ indicates the estimation accuracy for the average energy arrival amount (i.e., when $\alpha = 1$, the estimation is accurate; otherwise, the average energy arrival amount is either overestimated or

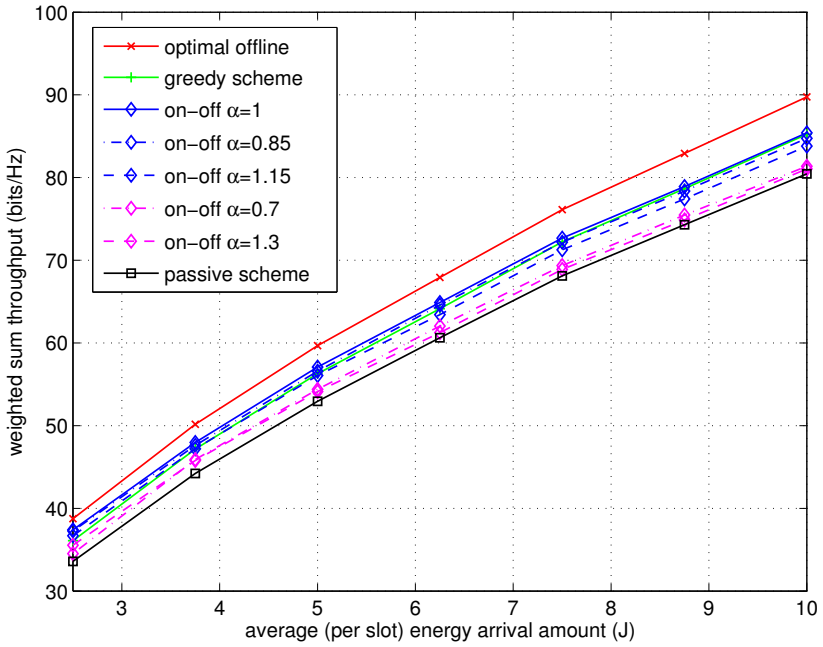

Figure 6.2: Weighted sum throughput versus average energy arrival amounts with infinite battery capacity for Gaussian MAC with conferencing links when $\mu_1 = 0.4, \mu_2 = 0.6$.

underestimated).

Fig. 6.1 and Fig. 6.3 show the performance of the schemes for different average energy arrival amounts with infinite and finite battery capacities, respectively, with weighting factors $\mu_1 = 0.6$ and $\mu_2 = 0.4$. Fig. 6.2 and Fig. 6.4 show the performance of the schemes for different average energy arrival amounts with infinite and finite battery capacities, respectively, with weighting factors $\mu_1 = 0.4$ and $\mu_2 = 0.6$. It is worth noting that the weighted sum throughputs in Fig. 6.1 and Fig. 6.3 are higher than those in Fig. 6.2 and Fig. 6.4, respectively. This is because that with larger μ_1, higher priority is assigned to transmitter 1, who enjoys better channel conditions.

For the case of infinite battery capacity, as seen from Fig. 6.1 and Fig. 6.2, the greedy scheme, whose weighted sum throughput is around 5% less than that of the optimal offline scheme for different average energy arrival amounts, is outperformed by the on-off

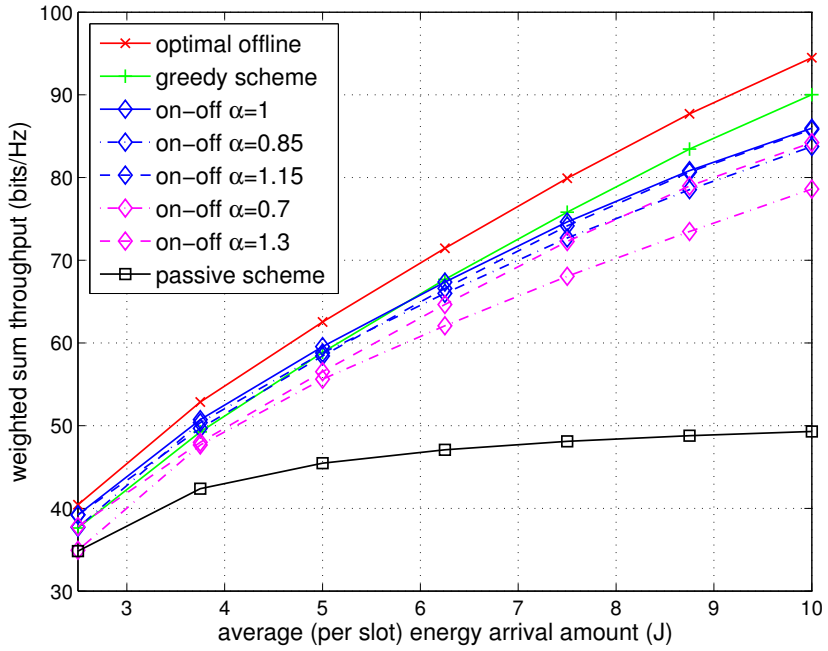

Figure 6.3: Weighted sum throughput versus average energy arrival amounts with finite battery capacity for Gaussian MAC with conferencing links when $\mu_1 = 0.6, \mu_2 = 0.4$.

scheme with accurate estimation, i.e., $\alpha = 1$. However, the performance of the on-off scheme degrades as the estimation becomes inaccurate. In particular, the performance of the on-off scheme is worse than the greedy scheme when $\alpha = 1.3$ or 0.7. The passive scheme performs the worse among all considered schemes.

For the case of finite battery capacity, it can be observed from Fig. 6.3 and Fig. 6.4 that the on-off scheme with accurate estimation has comparable performance with the greedy scheme in the low average energy arrival amount regime. However, the greedy scheme performs significantly better than the on-off scheme in the high average energy arrival amount regime. Unlike the greedy scheme that never causes battery overflow, the on-off scheme and the passive scheme may cause battery overflow since the stored energy may not be depleted before the next energy arrival. The passive scheme performs dramatically worse than all other schemes. It is worth noting that the influence of the

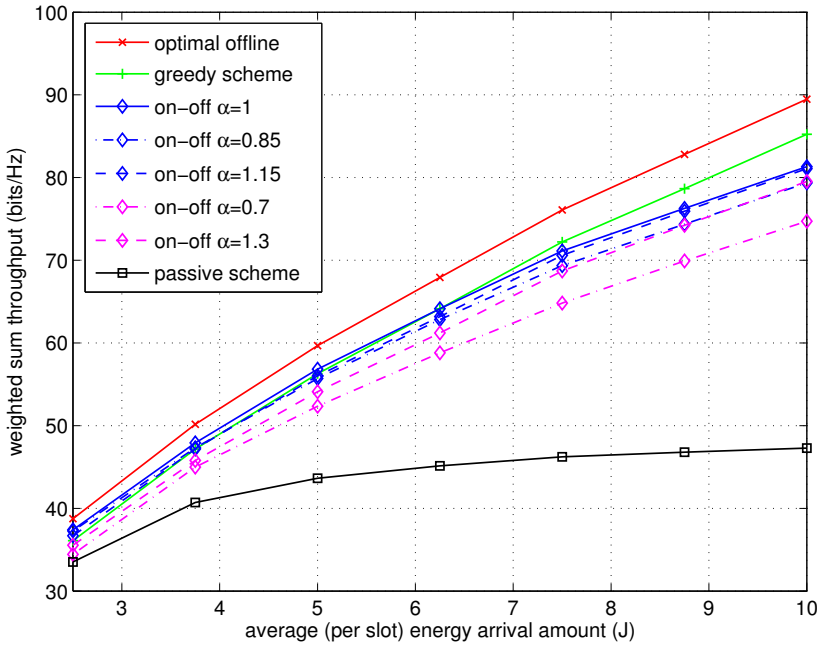

Figure 6.4: Weighted sum throughput versus average energy arrival amounts with finite battery capacity for Gaussian MAC with conferencing links when $\mu_1 = 0.4, \mu_2 = 0.6$.

finite battery capacity on the performance of both the on-off scheme and the passive scheme is more significant in the high average energy arrival amount regime than that in the low average energy arrival amount regime. This is due to the fact that battery overflow is more likely to happen when the energy arrival amount is large.

The greedy scheme is thus recognized to enjoy robustness against the estimation error of the energy arrival process statistics and the battery capacity limitation compared to other schemes.

6.4 Competitive Analysis

In the previous section, the average performance of several online schemes was studied and it is observed that the online greedy scheme enjoy robustness against the estimation

error of the energy arrival process statistics and the battery capacity limitation compared to other schemes. In this section, the performance of the online greedy scheme is further investigated terms of its worst case performance by using competitive analysis. In the sequel, $\mathcal{A}$ is used to denote the online greedy scheme and superscript $^{\mathcal{A}}$ is used to denote quantities related to the greedy scheme. We consider the infinite battery case first. Later, it will be shown the finite battery case could be solved similarly.

6.4.1 Definition of Competitive analysis

Given the input sequence $\boldsymbol{\omega}$ and weighting factors μ_1, μ_2, the profits obtained by the optimal offline scheme $\mathcal{O}$ and the online greedy scheme $\mathcal{A}$ are defined as

$$B^{\mathcal{O}}(\boldsymbol{\omega}) = \mu_1 \sum_{n=1}^{N} r_{1,n}^{\mathcal{O}} T + \mu_2 \sum_{n=1}^{N} r_{2,n}^{\mathcal{O}} T, \tag{6.1}$$

and

$$B^{\mathcal{A}}(\boldsymbol{\omega}) = \mu_1 \sum_{n=1}^{N} r_{1,n}^{\mathcal{A}} T + \mu_2 \sum_{n=1}^{N} r_{2,n}^{\mathcal{A}} T, \tag{6.2}$$

respectively.

Definition 6. *The online greedy scheme $\mathcal{A}$ for solving the maximization problem (P5.2) is called ρ-competitive or has a competitive ratio of ρ if for all possible input sequences $\boldsymbol{\omega} \in \boldsymbol{\Omega}$,*

$$\max_{\boldsymbol{\omega} \in \boldsymbol{\Omega}} \frac{B^{\mathcal{O}}(\boldsymbol{\omega})}{B^{\mathcal{A}}(\boldsymbol{\omega})} \leq \rho, \tag{6.3}$$

where ρ is a constant independent of the input sequence.

6.4.2 Derivation of the Competitive Ratios

Before deriving the competitive ratios of the greedy scheme, two preliminary results are presented, which give the upper bound of the profit obtained by $\mathcal{O}$ and the lower bound of the profit obtained by $\mathcal{A}$, respectively.

Lemma 10. *For an arbitrary input sequence $\boldsymbol{\omega} \in \boldsymbol{\Omega}$, define its corresponding enhanced input sequence as $\tilde{\boldsymbol{\omega}} = \left(\sum_{n=1}^{N} E_n, \underbrace{0, \cdots, 0}_{N-1} \right)$. The profit obtained by $\mathcal{O}$ for serving $\boldsymbol{\omega}$ is upper-bounded by that for serving $\tilde{\boldsymbol{\omega}}$, i.e., $B^{\mathcal{O}}(\boldsymbol{\omega}) \leq B^{\mathcal{O}}(\tilde{\boldsymbol{\omega}})$.*

The proof is the same as that of Lemma 5.

Remark 11. *With the enhanced input sequence $\tilde{\boldsymbol{\omega}}$ for $\boldsymbol{\omega} \in \boldsymbol{\Omega}$, the EH constraints* (5.36) *are inactive and $\mathcal{O}$ leads to constant sum power and rate profiles over all n slots, i.e., $\tilde{P}_1^{\mathcal{O}} = \cdots = \tilde{P}_N^{\mathcal{O}} = \tilde{P}^{\mathcal{O}} \doteq \left(\sum_{n=1}^{N} E_n \right) / (NT)$ and $\left(\tilde{r}_{1,1}^{\mathcal{O}}, \tilde{r}_{2,1}^{\mathcal{O}} \right) = \cdots = \left(\tilde{r}_{1,N}^{\mathcal{O}}, \tilde{r}_{2,N}^{\mathcal{O}} \right) = \left(\tilde{r}_1^{\mathcal{O}}, \tilde{r}_2^{\mathcal{O}} \right)$, where $\tilde{P}_n^{\mathcal{O}}$ and $\tilde{r}_{i,n}^{\mathcal{O}}, i = 1, 2$, represent the sum power and rate of transmitter i in the n-th slot when $\mathcal{O}$ serves $\tilde{\boldsymbol{\omega}}$, respectively.*

As indicated by the solution of Problem (P5.4n) in Chapter 5, with $\mathcal{A}$, the rate profile may have different structures over the transmission period (for example, if $-\frac{\mu_1}{\mu_2} < -1$, only transmitter 1 has non-zero rate when the sum power is small whereas both transmitters can have non-zero rates when the sum power is larger than certain value). Consider a "lazy" version of $\mathcal{A}$, denoted as $\tilde{\mathcal{A}}$, with which the rate profile has a unified structure for all sum power levels. For an arbitrary input sequence $\boldsymbol{\omega} \in \boldsymbol{\Omega}$, $\tilde{\mathcal{A}}$ determines the sum power allocation $P_n^{\tilde{\mathcal{A}}}$ at slot $n, n = 1, \cdots, N$, as $P_n^{\tilde{\mathcal{A}}} = P_n^{\mathcal{A}} = \frac{E_n}{T}$, where the rate pair $\left(r_{1,n}^{\tilde{\mathcal{A}}}, r_{2,n}^{\tilde{\mathcal{A}}} \right)$ determined by $\tilde{\mathcal{A}}$ satisfies: 1) if $-\frac{\mu_1}{\mu_2} \leq -1$, we have $r_{2,n}^{\tilde{\mathcal{A}}} = 0$ and $g\left(r_{1,n}^{\tilde{\mathcal{A}}}, 0 \right) = P_n^{\tilde{\mathcal{A}}}$; 2) otherwise, we have $r_{1,n}^{\tilde{\mathcal{A}}} = 0$ and $g\left(0, r_{2,n}^{\tilde{\mathcal{A}}} \right) = P_n^{\tilde{\mathcal{A}}}$. Denote the profit obtained by $\tilde{\mathcal{A}}$ for serving $\boldsymbol{\omega}$ by $B^{\tilde{\mathcal{A}}}(\boldsymbol{\omega})$. Notice that with $\tilde{\mathcal{A}}$, only one of the two transmitters has non-zero rate during the transmission period, regardless of the sum power levels. From (5.8), we can derive that if $-\frac{\mu_1}{\mu_2} \leq -1$,

$$\begin{aligned} B^{\tilde{\mathcal{A}}}(\boldsymbol{\omega}) &= \mu_1 T \sum_{n=1}^{N} \begin{cases} \mathcal{C}\left((h_1 + h_2) P_n^{\mathcal{A}} \right), & \text{if } P_n^{\mathcal{A}} \leq g\left(C_{12}, 0 \right) \\ \log \frac{(h_1+h_2)\left(1+h_1 P_n^{\mathcal{A}}\right)}{h_2 2^{-C_{12}} + h_1}, & \text{otherwise} \end{cases} \\ &> \mu_1 T \sum\nolimits_{n=1}^{N} \mathcal{C}\left(h_1 P_n^{\mathcal{A}} \right); \end{aligned} \tag{6.4}$$

otherwise,

$$B^{\tilde{\mathcal{A}}}(\boldsymbol{\omega}) = \mu_2 T \sum_{n=1}^{N} \begin{cases} \mathcal{C}\left((h_1+h_2)P_n^{\mathcal{A}}\right), & \text{if } P_n^{\mathcal{A}} \le g\left(0, C_{21}\right) \\ \log \frac{(h_1+h_2)\left(1+h_2 P_n^{\mathcal{A}}\right)}{h_1 2^{-C_{21}}+h_2}, & \text{otherwise} \end{cases}$$
$$> \mu_2 T \sum\nolimits_{n=1}^{N} \mathcal{C}\left(h_2 P_n^{\mathcal{A}}\right). \tag{6.5}$$

Lemma 11. *For an arbitrary input sequence $\boldsymbol{\omega} \in \boldsymbol{\Omega}$, the profit obtained by $\mathcal{A}$ is lower-bounded by that obtained with $\tilde{\mathcal{A}}$. Hence, based on* (6.4) *and* (6.5)*, we obtain: if $-\frac{\mu_1}{\mu_2} \le -1$, we have $B^{\mathcal{A}}(\boldsymbol{\omega}) \ge B^{\tilde{\mathcal{A}}}(\boldsymbol{\omega}) > \mu_1 T \sum_{n=1}^{N} \mathcal{C}\left(h_1 P_n^{\mathcal{A}}\right)$; otherwise, we have $B^{\mathcal{A}}(\boldsymbol{\omega}) \ge B^{\tilde{\mathcal{A}}}(\boldsymbol{\omega}) > \mu_2 T \sum_{n=1}^{N} \mathcal{C}\left(h_2 P_n^{\mathcal{A}}\right)$.*

Proof. For each $n \in \{1, \cdots, N\}$, it is easy to check that $\mu_1 r_{1,n}^{\mathcal{A}} + \mu_2 r_{2,n}^{\mathcal{A}} \ge \mu_1 r_{1,n}^{\tilde{\mathcal{A}}} + \mu_2 r_{2,n}^{\tilde{\mathcal{A}}}$. Hence, the summation over n slots indicates $B^{\mathcal{A}}(\boldsymbol{\omega}) \ge B^{\tilde{\mathcal{A}}}(\boldsymbol{\omega})$. □

With the upper bound of $B^{\mathcal{O}}(\boldsymbol{\omega})$ and the lower bound of $B^{\mathcal{A}}(\boldsymbol{\omega})$ obtained by Lemmas 10 and 11, we can upper-bound $\frac{B^{\mathcal{O}}(\boldsymbol{\omega})}{B^{\mathcal{A}}(\boldsymbol{\omega})}$ by $\frac{B^{\mathcal{O}}(\tilde{\boldsymbol{\omega}})}{B^{\tilde{\mathcal{A}}}(\boldsymbol{\omega})}$, with which an input-independent upper bound can be found by applying certain approximation. Then, the competitive ratios of $\mathcal{A}$ are obtained as follow.

6.4.2.1 Competittive ratio for $-\frac{\mu_1}{\mu_2} < -1$

Partition $\boldsymbol{\Omega}$ into three mutually disjoint subsets, given as

$$\boldsymbol{\Omega}_1 = \left\{ \boldsymbol{\omega} \in \boldsymbol{\Omega} \,\middle|\, 0 \le \frac{\sum_{n=1}^{N} E_n}{NT} \le g\left(C_{12}, 0\right) \right\},$$

$$\boldsymbol{\Omega}_2 = \left\{ \boldsymbol{\omega} \in \boldsymbol{\Omega} \,\middle|\, g(C_{12}, 0) < \frac{\sum_{n=1}^{N} E_n}{NT} \le g(C_{12}, R_2) \right\},$$

and

$$\mathbf{\Omega}_3 = \left\{ \boldsymbol{\omega} \in \mathbf{\Omega} \left| \frac{\sum_{n=1}^{N} E_n}{NT} > g(C_{12}, R_2) \right. \right\}.$$

Note that the rate profile $\left(\tilde{r}_1^{\mathcal{O}}, \tilde{r}_2^{\mathcal{O}}\right)$'s given the input sequences belonging to these three subsets have different structures.

1. For an arbitrary input sequence $\boldsymbol{\omega} \in \mathbf{\Omega}_1$, the rate pair $\left(\tilde{r}_1^{\mathcal{O}}, \tilde{r}_2^{\mathcal{O}}\right)$ is given as $\left(\tilde{r}_1^{\mathcal{O}}, \tilde{r}_2^{\mathcal{O}}\right) = \left(\mathcal{C}\left(\left(h_1+h_2\right)\tilde{P}^{\mathcal{O}}\right), 0\right)$. Hence, we obtain

$$\begin{aligned}
\left.\frac{B^{\mathcal{O}}(\boldsymbol{\omega})}{B^{\mathcal{A}}(\boldsymbol{\omega})}\right|_{\boldsymbol{\omega}\in\mathbf{\Omega}_1} &\overset{(a)}{\leq} \frac{B^{\mathcal{O}}(\tilde{\boldsymbol{\omega}})}{B^{\mathcal{A}}(\boldsymbol{\omega})} \\
&\overset{(b)}{<} \frac{\mu_1 NT\mathcal{C}\left(\left(h_1+h_2\right)\frac{\sum_{n=1}^{N} E_n}{NT}\right)}{\mu_1 T\sum_{n=1}^{N}\mathcal{C}\left(h_1\frac{E_n}{T}\right)} \\
&\overset{(c)}{<} \frac{\mu_1 NT\left(h_1+h_2\right)\frac{\sum_{n=1}^{N} E_n}{NT\ln 2}}{\mu_1 T\sum_{n=1}^{N} h_1\frac{E_n}{T}\frac{\mathcal{C}\left(h_1\frac{E_{\max}}{T}\right)}{h_1 E_{\max}/T}} \\
&= k_1\frac{(h_1+h_2)}{\ln 2},
\end{aligned} \tag{6.6}$$

where (a) and (b) follow from Lemmas 10 and 11, respectively; (c) follows from the facts that $\mathcal{C}(x) \leq x/\ln 2, \forall x \geq 0$ [Top04] and $\mathcal{C}(x) \geq x/\left(h_1 k_1\right), \forall x \in [0, h_1 E_{\max}/T]$, which can be proved from the concavity of log function; and $k_1 = \frac{\frac{E_{\max}}{T}}{\mathcal{C}\left(h_1\frac{E_{\max}}{T}\right)}$.

Since (6.6) applies to an arbitrary $\boldsymbol{\omega} \in \mathbf{\Omega}_1$, it can be concluded that

$$\max_{\boldsymbol{\omega}\in\mathbf{\Omega}_1}\frac{B^{\mathcal{O}}(\boldsymbol{\omega})}{B^{\mathcal{A}}(\boldsymbol{\omega})} < k_1\frac{(h_1+h_2)}{\ln 2}. \tag{6.7}$$

2. For an arbitrary input sequence $\boldsymbol{\omega} \in \mathbf{\Omega}_2$[1], the rate pair $\left(\tilde{r}_1^{\mathcal{O}}, \tilde{r}_2^{\mathcal{O}}\right)$ is given as

[1]For different values of μ_1, μ_2 and system parameters, $\mathbf{\Omega}_1$ is always nonempty whereas $\mathbf{\Omega}_2$ and $\mathbf{\Omega}_3$ may be empty. If a subset is empty, the maximum $\frac{B^{\mathcal{O}}(\boldsymbol{\omega})}{B^{\mathcal{A}}(\boldsymbol{\omega})}$ over all input sequences belonging to this subset will be replaced by 1.

$\left(\tilde{r}_1^{\mathcal{O}}, \tilde{r}_2^{\mathcal{O}}\right) = \left(C_{12}, \mathcal{C}\left(\left(h_1+h_2\right)\tilde{P}^{\mathcal{O}}\right) - C_{12}\right)$. Based on Lemmas 10 and 11, we have

$$\begin{aligned}
\left.\frac{B^{\mathcal{O}}\left(\boldsymbol{\omega}\right)}{B^{\mathcal{A}}\left(\boldsymbol{\omega}\right)}\right|_{\boldsymbol{\omega}\in\boldsymbol{\Omega}_2} &< \frac{NT\left(\mu_1 C_{12} + \mu_2\left(\mathcal{C}\left(\frac{\left(h_1+h_2\right)\sum_{n=1}^{N} E_n}{NT}\right) - C_{12}\right)\right)}{\mu_1 T \sum_{n=1}^{N} \mathcal{C}\left(h_1 \frac{E_n}{T}\right)} \\
&< \frac{NT\left(\mu_1-\mu_2\right)C_{12} + \mu_2 NT\mathcal{C}\left(\left(h_1+h_2\right)\frac{\sum_{n=1}^{N} E_n}{NT}\right)}{\mu_1 \frac{\mathcal{C}\left(h_1\frac{E_{\max}}{T}\right)}{\frac{E_{\max}}{T}} \sum_{n=1}^{N} E_n} \\
&< k_1\left(\frac{NT\left(\mu_1-\mu_2\right)C_{12}}{\mu_1 NT g\left(C_{12},0\right)} + \frac{\mu_2\left(h_1+h_2\right)}{\mu_1 \ln 2}\right) \\
&< k_1\left(h_1+h_2\right)\left(\frac{\left(\mu_1-\mu_2\right)C_{12}}{\mu_1\left(2^{C_{12}}-1\right)} + \frac{\mu_2}{\mu_1 \ln 2}\right). \qquad (6.8)
\end{aligned}$$

Since (6.8) applies to an arbitrary $\boldsymbol{\omega} \in \boldsymbol{\Omega}_2$, it can be concluded that

$$\max_{\boldsymbol{\omega}\in\boldsymbol{\Omega}_2} \frac{B^{\mathcal{O}}\left(\boldsymbol{\omega}\right)}{B^{\mathcal{A}}\left(\boldsymbol{\omega}\right)} < k_1\left(h_1+h_2\right)\left(\frac{\left(\mu_1-\mu_2\right)C_{12}}{\mu_1\left(2^{C_{12}}-1\right)} + \frac{\mu_2}{\mu_1 \ln 2}\right). \qquad (6.9)$$

3. For an arbitrary input sequence $\boldsymbol{\omega} \in \boldsymbol{\Omega}_3$, the rate pair $\left(\tilde{r}_1^{\mathcal{O}}, \tilde{r}_2^{\mathcal{O}}\right)$ is given as $\left(\tilde{r}_1^{\mathcal{O}}, \tilde{r}_2^{\mathcal{O}}\right) = \left(\log\frac{\left(h_1+h_2\right)\left(1+h_1\tilde{P}^{\mathcal{O}}\right)}{h_2 2^{-C_{12}}+h_1 2^{R_2}}, R_2\right)$. Based on Lemmas 5 and 6, we have

$$\begin{aligned}
\left.\frac{B^{\mathcal{O}}\left(\boldsymbol{\omega}\right)}{B^{\mathcal{A}}\left(\boldsymbol{\omega}\right)}\right|_{\boldsymbol{\omega}\in\boldsymbol{\Omega}_3} &< \frac{NT\left(\mu_1 \log\frac{\left(h_1+h_2\right)\left(1+h_1\sum_{n=1}^{N} E_n/NT\right)}{h_2 2^{-C_{12}}+h_1 2^{R_2}} + \mu_2 R_2\right)}{\mu_1 T \sum_{n=1}^{N} \mathcal{C}\left(h_1\frac{E_n}{T}\right)} \\
&< \frac{NT\left(\mu_1 \log\left(\frac{\left(h_1+h_2\right)}{h_2 2^{-C_{12}}+h_1 2^{R_2}}\right) + \mu_2 R_2 + \mu_1 \log\left(1 + h_1\frac{\sum_{n=1}^{N} E_n}{NT}\right)\right)}{\mu_1 T \sum_{n=1}^{N} h_1\frac{E_n}{T}\frac{\log\left(1+h_1\frac{E_{\max}}{T}\right)}{h_1\frac{E_{\max}}{T}}} \\
&< k_1\left(\frac{\mu_1 \log\frac{h_1+h_2}{h_2 2^{-C_{12}}+h_1 2^{R_2}} + \mu_2 R_2}{\mu_1 g\left(C_{12},R_2\right)} + \frac{h_1}{\ln 2}\right). \qquad (6.10)
\end{aligned}$$

Since (6.10) applies to an arbitrary $\boldsymbol{\omega} \in \boldsymbol{\Omega}_3$, it can be concluded that

$$\max_{\boldsymbol{\omega}\in\boldsymbol{\Omega}_3} \frac{B^{\mathcal{O}}(\boldsymbol{\omega})}{B^{\mathcal{A}}(\boldsymbol{\omega})} < k_1 \left(\frac{\mu_1 \log \frac{h_1+h_2}{h_2 2^{-C_{12}}+h_1 2^{R_2}} + \mu_2 R_2}{\mu_1 g(C_{12}, R_2)} + \frac{h_1}{\ln 2} \right). \tag{6.11}$$

Proposition 14. *The online scheme $\mathcal{A}$ is ρ_1-competitive for $-\frac{\mu_1}{\mu_2} < -1$, where ρ_1 is defined as*

$$\rho_1 \triangleq k_1 \max \left\{ \begin{array}{l} (h_1+h_2)/\ln 2 \\ (h_1+h_2)\left(\frac{(\mu_1-\mu_2)C_{12}}{\mu_1\left(2^{C_{12}}-1\right)} + \frac{\mu_2}{\mu_1 \ln 2} \right) \\ \frac{\mu_1 \log \frac{h_1+h_2}{h_2 2^{-C_{12}}+h_1 2^{R_2}} + \mu_2 R_2}{\mu_1 g(C_{12},R_2)} + \frac{h_1}{\ln 2} \end{array} \right\}, \tag{6.12}$$

where $k_1 = \frac{\frac{E_{\max}}{T}}{\mathcal{C}\left(h_1 \frac{E_{\max}}{T}\right)}$.

Proof. Since $\boldsymbol{\Omega}_1 \cup \boldsymbol{\Omega}_2 \cup \boldsymbol{\Omega}_3 = \boldsymbol{\Omega}$, from (6.7), (6.9) and (6.11) we have

$$\begin{aligned} \rho_1 &\triangleq k_1 \max \left\{ \begin{array}{l} (h_1+h_2)/\ln 2, \\ (h_1+h_2)\left(\frac{(\mu_1-\mu_2)C_{12}}{\mu_1\left(2^{C_{12}}-1\right)} + \frac{\mu_2}{\mu_1 \ln 2} \right), \\ \frac{\mu_1 \log \frac{h_1+h_2}{h_2 2^{-C_{12}}+h_1 2^{R_2}} + \mu_2 R_2}{\mu_1 g(C_{12},R_2)} + \frac{h_1}{\ln 2} \end{array} \right\}, \\ &> \max \left\{ \max_{\boldsymbol{\omega}\in\boldsymbol{\Omega}_1} \frac{B^{\mathcal{O}}(\boldsymbol{\omega})}{B^{\mathcal{A}}(\boldsymbol{\omega})}, \max_{\boldsymbol{\omega}\in\boldsymbol{\Omega}_2} \frac{B^{\mathcal{O}}(\boldsymbol{\omega})}{B^{\mathcal{A}}(\boldsymbol{\omega})}, \max_{\boldsymbol{\omega}\in\boldsymbol{\Omega}_3} \frac{B^{\mathcal{O}}(\boldsymbol{\omega})}{B^{\mathcal{A}}(\boldsymbol{\omega})} \right\} \\ &= \max_{\boldsymbol{\omega}\in\boldsymbol{\Omega}} \frac{B^{\mathcal{O}}(\boldsymbol{\omega})}{B^{\mathcal{A}}(\boldsymbol{\omega})}. \end{aligned} \tag{6.13}$$

Based on the definition of competitive ratio (6), it is proved that $\mathcal{A}$ is ρ_1-compeititve when $-\frac{\mu_1}{\mu_2} < -1$.

□

6.4.2.2 Competittive ratio for $-\frac{\mu_1}{\mu_2} = -1$

Similar to the case for $-\frac{\mu_1}{\mu_2} < -1$, we start with partitioning $\boldsymbol{\Omega}$ into disjoint subsets such that the rate profile $\left(\tilde{r}_1^{\mathcal{O}}, \tilde{r}_2^{\mathcal{O}}\right)$'s given the input sequences belonging to different

subsets have different structures. Based on the optimal rate scheduling rules described in Chapter 5, $\boldsymbol{\Omega}$ is partitioned into two disjoint subsets, given as

$$\boldsymbol{\Omega}_1 = \left\{ \boldsymbol{\omega} \in \boldsymbol{\Omega} \left| 0 \leq \frac{\sum_{n=1}^{N} E_n}{NT} \leq g\left(C_{12}, C_{21}\right) \right. \right\}$$

and

$$\boldsymbol{\Omega}_2 = \left\{ \boldsymbol{\omega} \in \boldsymbol{\Omega} \left| \frac{\sum_{n=1}^{N} E_n}{NT} > g\left(C_{12}, C_{21}\right) \right. \right\}.$$

1. For an arbitrary input sequence $\boldsymbol{\omega} \in \boldsymbol{\Omega}_1$, the rate pair $\left(\tilde{r}_1^{\mathcal{O}}, \tilde{r}_2^{\mathcal{O}}\right)$ satisfies $\tilde{r}_1^{\mathcal{O}} + \tilde{r}_2^{\mathcal{O}} = \mathcal{C}\left(\left(h_1 + h_2\right)\tilde{P}^{\mathcal{O}}\right)$ and hence

$$\left.\frac{B^{\mathcal{O}}\left(\boldsymbol{\omega}\right)}{B^{\mathcal{A}}\left(\boldsymbol{\omega}\right)}\right|_{\boldsymbol{\omega}\in\boldsymbol{\Omega}_1} < \frac{NT\mu_1\mathcal{C}\left(\left(h_1+h_2\right)\tilde{P}^{\mathcal{O}}\right)}{\mu_1 T\sum_{n=1}^{N}\mathcal{C}\left(h_1\frac{E_n}{T}\right)} < k_1\frac{h_1+h_2}{\ln 2}. \tag{6.14}$$

   Since (6.14) applies to an arbitrary $\boldsymbol{\omega} \in \boldsymbol{\Omega}_1$, it can be concluded that

$$\max_{\boldsymbol{\omega}\in\boldsymbol{\Omega}_1}\frac{B^{\mathcal{O}}\left(\boldsymbol{\omega}\right)}{B^{\mathcal{A}}\left(\boldsymbol{\omega}\right)} < k_1\frac{h_1+h_2}{\ln 2}. \tag{6.15}$$

2. For an arbitrary input sequence $\boldsymbol{\omega} \in \boldsymbol{\Omega}_2$, the rate pair $\left(\tilde{r}_1^{\mathcal{O}}, \tilde{r}_2^{\mathcal{O}}\right)$ satisfies $\tilde{r}_1^{\mathcal{O}} + \tilde{r}_2^{\mathcal{O}} = \log\frac{2+2h_1\tilde{P}^{\mathcal{O}}}{1+2^{-C_{12}-C_{21}}}$ when $h_1 = h_2$, and $\left(\tilde{r}_1^{\mathcal{O}}, \tilde{r}_2^{\mathcal{O}}\right) = \left(\log\frac{\left(h_1+h_2\right)\left(1+h_1\tilde{P}^{\mathcal{O}}\right)}{h_2 2^{-C_{12}}+h_1 2^{C_{21}}}, C_{21}\right)$ when $h_1 > h_2$. It is easy to check that for both $h_1 > h_2$ and $h_1 = h_2$, we have

$\frac{B^{\mathcal{O}}(\boldsymbol{\omega})}{B^{\mathcal{A}}(\boldsymbol{\omega})}\Big|_{\boldsymbol{\omega}\in\boldsymbol{\Omega}_2} < \frac{NT\mu_1\left(\log\frac{(h_1+h_2)\left(1+h_1\tilde{P}^{\mathcal{O}}\right)}{h_2 2^{-C_{12}}+h_1 2^{C_{21}}}+C_{21}\right)}{\mu_1 T\sum\limits_{n=1}^{N}\mathcal{C}\left(h_1\frac{E_n}{T}\right)}$. Hence, we obtain

$$\begin{aligned}
\frac{B^{\mathcal{O}}(\boldsymbol{\omega})}{B^{\mathcal{A}}(\boldsymbol{\omega})}\Big|_{\boldsymbol{\omega}\in\boldsymbol{\Omega}_2} &< \frac{NT\left(\log\left(\frac{(h_1+h_2)\left(1+h_1\frac{\sum_{n=1}^{N}E_n}{NL}\right)}{h_2 2^{-C_{12}}+h_1 2^{C_{21}}}\right)+C_{21}\right)}{T\sum\limits_{n=1}^{N}\log\left(1+h_1\frac{E_n}{T}\right)} \\
&< \frac{NT\left(\log\left(\frac{(h_1+h_2)}{h_2 2^{-C_{12}-C_{21}}+h_1}\right)+\log\left(1+h_1\frac{\sum_{n=1}^{N}E_n}{NT}\right)\right)}{\sum\limits_{n=1}^{N}T\log\left(1+h_1\frac{E_n}{T}\right)} \\
&< \frac{NT\log\left(\frac{(h_1+h_2)}{h_2 2^{-C_{12}-C_{21}}+h_1}\right)}{\frac{\log\left(1+h_1\frac{E_{\max}}{T}\right)}{\frac{E_{\max}}{T}}\sum\limits_{n=1}^{N}E_n}+\frac{\frac{h_1}{\ln 2}}{\frac{\log\left(1+h_1\frac{E_{\max}}{T}\right)}{\frac{E_{\max}}{T}}} \\
&< k_1\left(\frac{NT\log\left(\frac{(h_1+h_2)}{h_2 2^{-C_{12}-C_{21}}+h_1}\right)}{NTg\left(C_{12},C_{21}\right)}+\frac{h_1}{\ln 2}\right) \\
&= k_1\left(\frac{\log\left(\frac{(h_1+h_2)}{h_2 2^{-C_{12}-C_{21}}+h_1}\right)}{g\left(C_{12},C_{21}\right)}+\frac{h_1}{\ln 2}\right) \qquad (6.16)
\end{aligned}$$

Since (6.16) applies to an arbitrary $\boldsymbol{\omega}\in\boldsymbol{\Omega}_2$, it can be concluded that

$$\max_{\boldsymbol{\omega}\in\boldsymbol{\Omega}_2}\frac{B^{\mathcal{O}}(\boldsymbol{\omega})}{B^{\mathcal{A}}(\boldsymbol{\omega})} < k_1\left(\frac{\log\left(\frac{(h_1+h_2)}{h_2 2^{-C_{12}-C_{21}}+h_1}\right)}{g\left(C_{12},C_{21}\right)}+\frac{h_1}{\ln 2}\right). \qquad (6.17)$$

Proposition 15. *The online scheme $\mathcal{A}$ is ρ_2-competitive for $-\frac{\mu_1}{\mu_2} < -1$, where ρ_2 is defined as*

$$\rho_2 \triangleq k_1\max\left\{\ \frac{h_1+h_2}{\ln 2},\ \frac{\log\frac{h_1+h_2}{h_2 2^{-C_{12}-C_{21}}+h_1}}{g(C_{12},C_{21})}+\frac{h_1}{\ln 2}\ \right\}. \qquad (6.18)$$

Proof. Since $\boldsymbol{\Omega}_1 \cup \boldsymbol{\Omega}_2 = \boldsymbol{\Omega}$, from (6.15) and (6.17) we have

$$\begin{aligned}\rho_2 &\triangleq k_1 \max\left\{\frac{h_1+h_2}{\ln 2}, \frac{\log\frac{(h_1+h_2)}{h_2 2^{-C_{12}-C_{21}+h_1}}}{g\left(C_{12},C_{21}\right)}+\frac{h_1}{\ln 2}\right\},\\ &> \max\left\{\max_{\boldsymbol{\omega}\in\boldsymbol{\Omega}_1}\frac{B^{\mathcal{O}}\left(\boldsymbol{\omega}\right)}{B^{\mathcal{A}}\left(\boldsymbol{\omega}\right)}, \max_{\boldsymbol{\omega}\in\boldsymbol{\Omega}_2}\frac{B^{\mathcal{O}}\left(\boldsymbol{\omega}\right)}{B^{\mathcal{A}}\left(\boldsymbol{\omega}\right)}\right\}\\ &= \max_{\boldsymbol{\omega}\in\boldsymbol{\Omega}}\frac{B^{\mathcal{O}}\left(\boldsymbol{\omega}\right)}{B^{\mathcal{A}}\left(\boldsymbol{\omega}\right)}.\end{aligned} \tag{6.19}$$

Based on the definition of competitive ratio (6.3), it is proved that $\mathcal{A}$ is ρ_2-compeititve when $-\frac{\mu_1}{\mu_2} = -1$. □

6.4.2.3 Competittive ratio for $-\frac{\mu_1}{\mu_2} > -1$

Proposition 16. *For $-\frac{\mu_1}{\mu_2} > -1$, i) if $h_1 > h_2$, $\mathcal{A}$ is ρ_3-competitive when $-1 < -\frac{\mu_1}{\mu_2} < -1+\frac{h_1^2-h_2^2}{h_1^2+h_1h_2 2^{C_{12}+C_{21}}}$ and ρ_4-competitive when $-\frac{\mu_1}{\mu_2} \geq -1+\frac{h_1^2-h_2^2}{h_1^2+h_1h_2 2^{C_{12}+C_{21}}}$; ii) if $h_1 = h_2$, the online scheme $\mathcal{A}$ is ρ_4-competitive for all $-\frac{\mu_1}{\mu_2} > -1$, where*

$$\rho_3 \triangleq k_2 \max\left\{\begin{array}{l}(h_1+h_2)/\ln 2\\ (h_1+h_2)\left(\frac{(\mu_2-\mu_1)C_{21}}{\mu_2\left(2^{C_{21}}-1\right)}+\frac{\mu_1}{\mu_2\ln 2}\right)\\ \frac{\mu_1\log\frac{h_1+h_2}{h_2 2^{-C_{12}+h_1 2^{C_{21}}}}+\mu_2 C_{21}}{\mu_2 g(C_{12},C_{21})}+\frac{\mu_1 h_1}{\mu_2\ln 2}\\ \frac{\mu_2\log\frac{h_1(\mu_2-\mu_1)2^{C_{21}}}{\mu_2(h_1-h_2)}+\mu_1 R_1}{\mu_2 g(R_1,C_{21})}+\frac{h_2}{\ln 2}\end{array}\right\}, \tag{6.20}$$

$$\rho_4 \triangleq k_2 \max\left\{\begin{array}{l}(h_1+h_2)/\ln 2\\ (h_1+h_2)\left(\frac{(\mu_2-\mu_1)C_{21}}{\mu_2\left(2^{C_{21}}-1\right)}+\frac{\mu_1}{\mu_2\ln 2}\right)\\ \frac{\mu_1 R_1+\mu_2\log\frac{h_1+h_2}{h_1 2^{-C_{21}}+h_2 2^{R_1}}}{\mu_2 g(R_1,C_{21})}+\frac{h_2}{\ln 2}\end{array}\right\}, \tag{6.21}$$

and $k_2 = \frac{\frac{E_{\max}}{T}}{\mathcal{C}\left(h_2\frac{E_{\max}}{T}\right)}$.

Proof. Similar to the previous cases, first, partition $\boldsymbol{\Omega}$ into disjoint subsets as follows:

1. If $h_1 > h_2$,

   (a) for $-\frac{\mu_1}{\mu_2} \geq -1 + \frac{h_1^2 - h_2^2}{h_1^2 + h_1 h_2 2^{C_{12}+C_{21}}}$, as indicated by (5.53), the capping rate R_1 satisfies $0 \leq R_1 \leq C_{12}$. The set $\boldsymbol{\Omega}$ is partitioned into three disjoint subsets, given as

$$\boldsymbol{\Omega}_1 = \left\{ \boldsymbol{\omega} \in \boldsymbol{\Omega} \middle| 0 \leq \frac{\sum_{n=1}^{N} E_n}{NT} \leq g\left(0, C_{21}\right) \right\},$$

$$\boldsymbol{\Omega}_2 = \left\{ \boldsymbol{\omega} \in \boldsymbol{\Omega} \middle| g\left(0, C_{21}\right) < \frac{\sum_{n=1}^{N} E_n}{NT} \leq g\left(R_1, C_{21}\right) \right\},$$

   and

$$\boldsymbol{\Omega}_3 = \left\{ \boldsymbol{\omega} \in \boldsymbol{\Omega} \middle| \frac{\sum_{n=1}^{N} E_n}{NT} > g\left(R_1, C_{21}\right) \right\}.$$

   i. For an arbitrary input sequence $\boldsymbol{\omega} \in \boldsymbol{\Omega}_1$, the rate pair $\left(\tilde{r}_1^{\mathcal{O}}, \tilde{r}_2^{\mathcal{O}}\right)$ is given as $\left(0, \mathcal{C}\left(\left(h_1 + h_2\right)\tilde{P}^{\mathcal{O}}\right)\right)$. Hence, we obtain

$$\begin{aligned}
\left.\frac{B^{\mathcal{O}}\left(\boldsymbol{\omega}\right)}{B^{\mathcal{A}}\left(\boldsymbol{\omega}\right)}\right|_{\boldsymbol{\omega}\in\boldsymbol{\Omega}_1} &< \frac{\mu_2 NT \log\left(1 + \left(h_1 + h_2\right)\frac{\sum_{n=1}^{N} E_n}{NT}\right)}{\mu_2 \sum_{n=1}^{N} L \log\left(1 + h_2 \frac{E_n}{L}\right)} \\
&< \frac{\mu_2 NT \log\left(1 + \left(h_1 + h_2\right)\frac{\sum_{n=1}^{N} E_n}{NT}\right)}{\mu_2 \sum_{n=1}^{N} T \log\left(1 + h_2 \frac{E_n}{T}\right)} \\
&< k_2 \frac{h_1 + h_2}{\ln 2}
\end{aligned} \tag{6.22}$$

   Since (6.22) applies to an arbitrary $\boldsymbol{\omega} \in \boldsymbol{\Omega}_1$, it can be concluded that

$$\max_{\boldsymbol{\omega}\in\boldsymbol{\Omega}_1} \frac{B^{\mathcal{O}}\left(\boldsymbol{\omega}\right)}{B^{\mathcal{A}}\left(\boldsymbol{\omega}\right)} < k_2 \frac{h_1 + h_2}{\ln 2}. \tag{6.23}$$

   ii. For an arbitrary input sequence $\boldsymbol{\omega} \in \boldsymbol{\Omega}_2$, the rate pair $\left(\tilde{r}_1^{\mathcal{O}}, \tilde{r}_2^{\mathcal{O}}\right)$ is given

as $\left(\mathcal{C}\left(\left(h_1+h_2\right)\tilde{P}^{\mathcal{O}}\right)-C_{21},C_{21}\right)$. Hence, we obtain

$$\begin{aligned}\left.\frac{B^{\mathcal{O}}\left(\boldsymbol{\omega}\right)}{B^{\mathcal{A}}\left(\boldsymbol{\omega}\right)}\right|_{\boldsymbol{\omega}\in\boldsymbol{\Omega}_2} &< \frac{NT\left(\mu_1\left(\log\left(1+\left(h_1+h_2\right)\frac{\sum_{n=1}^{N}E_n}{NT}\right)-C_{21}\right)+\mu_2 C_{21}\right)}{\mu_2\sum_{n=1}^{N}T\log\left(1+h_2\frac{E_n}{T}\right)}\\ &< k_2\left(\frac{\mu_1\left(h_1+h_2\right)}{\mu_2\ln 2}+\frac{\left(\mu_2-\mu_1\right)C_{21}}{\mu_2 g\left(0,C_{21}\right)}\right)\\ &< k_2\left(h_1+h_2\right)\left(\frac{\mu_1}{\mu_2\ln 2}+\frac{\left(\mu_2-\mu_1\right)C_{21}}{\mu_2\left(2^{C_{21}}-1\right)}\right) \qquad (6.24)\end{aligned}$$

Since (6.24) applies to an arbitrary $\boldsymbol{\omega}\in\boldsymbol{\Omega}_2$, it can be concluded that

$$\max_{\boldsymbol{\omega}\in\boldsymbol{\Omega}_2}\frac{B^{\mathcal{O}}\left(\boldsymbol{\omega}\right)}{B^{\mathcal{A}}\left(\boldsymbol{\omega}\right)} < k_2\left(h_1+h_2\right)\left(\frac{\mu_1}{\mu_2\ln 2}+\frac{\left(\mu_2-\mu_1\right)C_{21}}{\mu_2\left(2^{C_{21}}-1\right)}\right). \qquad (6.25)$$

iii. For an arbitrary input sequence $\boldsymbol{\omega}\in\boldsymbol{\Omega}_3$, the rate pair $\left(\tilde{r}_1^{\mathcal{O}},\tilde{r}_2^{\mathcal{O}}\right)$ is given as $\left(R_1,\log\left(\frac{\left(h_2\tilde{P}^{\mathcal{O}}+1\right)\left(h_1+h_2\right)}{h_1 2^{-C_{21}}+h_2 2^{R_1}}\right)\right)$. Hence, we obtain

$$\begin{aligned}\left.\frac{B^{\mathcal{O}}\left(\boldsymbol{\omega}\right)}{B^{\mathcal{A}}\left(\boldsymbol{\omega}\right)}\right|_{\boldsymbol{\omega}\in\boldsymbol{\Omega}_3} &< \frac{NT\left(\mu_1 R_1+\mu_2\log\left(\frac{\left(h_2\frac{\sum_{n=1}^{N}E_n}{NT}+1\right)\left(h_1+h_2\right)}{h_1 2^{-C_{21}}+h_2 2^{R_1}}\right)\right)}{\mu_2\sum_{n=1}^{N}T\log\left(1+h_2\frac{E_n}{T}\right)}\\ &< k_2\frac{NT\left(\mu_1 R_1+\mu_2\log\left(h_2\frac{\sum_{n=1}^{N}E_n}{NT}+1\right)+\mu_2\log\left(\frac{\left(h_1+h_2\right)}{h_1 2^{-C_{21}}+h_2 2^{R_1}}\right)\right)}{\mu_2\sum_{n=1}^{N}E_n}\\ &< k_2\left(\frac{\mu_1 R_1+\mu_2\log\frac{h_1+h_2}{h_1 2^{-C_{21}}+h_2 2^{R_1}}}{\mu_2 g\left(R_1,C_{21}\right)}+\frac{h_2}{\ln 2}\right) \qquad (6.26)\end{aligned}$$

Since (6.26) applies to an arbitrary $\boldsymbol{\omega} \in \boldsymbol{\Omega}_3$, it can be concluded that

$$\max_{\boldsymbol{\omega}\in\boldsymbol{\Omega}_2} \frac{B^{\mathcal{O}}(\boldsymbol{\omega})}{B^{\mathcal{A}}(\boldsymbol{\omega})} < k_2 \left(\frac{\mu_1 R_1 + \mu_2 \log \frac{h_1+h_2}{h_1 2^{-C_{21}} + h_2 2^{R_1}}}{\mu_2 g(R_1, C_{21})} + \frac{h_2}{\ln 2} \right). \tag{6.27}$$

Since $\boldsymbol{\Omega}_1 \cup \boldsymbol{\Omega}_2 \cup \boldsymbol{\Omega}_3 = \boldsymbol{\Omega}$, from (6.23), (6.25) and (6.27) we have

$$\begin{aligned}
\rho_4 &\triangleq k_4 \max \left\{ \begin{array}{l} (h_1+h_2)/\ln 2, \\ (h_1+h_2)\left(\frac{\mu_1}{\mu_2 \ln 2} + \frac{(\mu_2-\mu_1)C_{21}}{\mu_2\left(2^{C_{21}}-1\right)} \right), \\ \frac{\mu_1 R_1 + \mu_2 \log \frac{h_1+h_2}{h_1 2^{-C_{21}} + h_2 2^{R_1}}}{\mu_2 g(R_1, C_{21})} + \frac{h_2}{\ln 2} \end{array} \right\} \\
&> \max \left\{ \max_{\boldsymbol{\omega}\in\boldsymbol{\Omega}_1} \frac{B^{\mathcal{O}}(\boldsymbol{\omega})}{B^{\mathcal{A}}(\boldsymbol{\omega})}, \max_{\boldsymbol{\omega}\in\boldsymbol{\Omega}_2} \frac{B^{\mathcal{O}}(\boldsymbol{\omega})}{B^{\mathcal{A}}(\boldsymbol{\omega})}, \max_{\boldsymbol{\omega}\in\boldsymbol{\Omega}_3} \frac{B^{\mathcal{O}}(\boldsymbol{\omega})}{B^{\mathcal{A}}(\boldsymbol{\omega})} \right\} \\
&= \max_{\boldsymbol{\omega}\in\boldsymbol{\Omega}} \frac{B^{\mathcal{O}}(\boldsymbol{\omega})}{B^{\mathcal{A}}(\boldsymbol{\omega})}.
\end{aligned} \tag{6.28}$$

Based on the definition of competitive ratio (6.3), it is proved that $\mathcal{A}$ is ρ_4-compeititve for this case.

(b) for $-1 < -\frac{\mu_1}{\mu_2} < -1 + \frac{h_1^2 - h_2^2}{h_1^2 + h_1 h_2 2^{C_{12}+C_{21}}}$, as indicated by (5.53), the capping rate R_1 satisfies $R_1 > C_{12}$. The set $\boldsymbol{\Omega}$ is partitioned into four disjoint subsets, given as

$$\boldsymbol{\Omega}_1 = \left\{ \boldsymbol{\omega} \in \boldsymbol{\Omega} \,\middle|\, 0 \le \frac{\sum_{n=1}^{N} E_n}{NT} \le g(0, C_{21}) \right\},$$

$$\boldsymbol{\Omega}_2 = \left\{ \boldsymbol{\omega} \in \boldsymbol{\Omega} \,\middle|\, g(0, C_{21}) < \frac{\sum_{n=1}^{N} E_n}{NT} \le g(C_{12}, C_{21}) \right\},$$

$$\boldsymbol{\Omega}_3 = \left\{ \boldsymbol{\omega} \in \boldsymbol{\Omega} \,\middle|\, g(C_{12}, C_{21}) < \frac{\sum_{n=1}^{N} E_n}{NT} \le g(R_1, C_{21}) \right\},$$

and

$$\boldsymbol{\Omega}_4 = \left\{ \boldsymbol{\omega} \in \boldsymbol{\Omega} \,\middle|\, \frac{\sum_{n=1}^{N} E_n}{NT} > g(R_1, C_{21}) \right\}.$$

i. For an arbitrary input sequence $\boldsymbol{\omega} \in \boldsymbol{\Omega}_1$, the rate pair $\left(\tilde{r}_1^{\mathcal{O}}, \tilde{r}_2^{\mathcal{O}}\right)$ is given

as $\left(0, \mathcal{C}\left(\left(h_1+h_2\right)\tilde{P}^{\mathcal{O}}\right)\right)$. Similar to (6.22) and (6.23), we have

$$\max_{\boldsymbol{\omega}\in\boldsymbol{\Omega}_1}\frac{B^{\mathcal{O}}\left(\boldsymbol{\omega}\right)}{B^{\mathcal{A}}\left(\boldsymbol{\omega}\right)} < k_2\frac{h_1+h_2}{\ln 2}. \tag{6.29}$$

ii. For an arbitrary input sequence $\boldsymbol{\omega}\in\boldsymbol{\Omega}_2$, the rate pair $\left(\tilde{r}_1^{\mathcal{O}}, \tilde{r}_2^{\mathcal{O}}\right)$ is given as $\left(\mathcal{C}\left(\left(h_1+h_2\right)\tilde{P}^{\mathcal{O}}\right)-C_{21}, C_{21}\right)$. Similar to (6.24) and (6.25), we have

$$\max_{\boldsymbol{\omega}\in\boldsymbol{\Omega}_2}\frac{B^{\mathcal{O}}\left(\boldsymbol{\omega}\right)}{B^{\mathcal{A}}\left(\boldsymbol{\omega}\right)} < k_2\left(h_1+h_2\right)\left(\frac{\mu_1}{\mu_2\ln 2}+\frac{\left(\mu_2-\mu_1\right)C_{21}}{\mu_2\left(2^{C_{21}}-1\right)}\right). \tag{6.30}$$

iii. For an arbitrary input sequence $\boldsymbol{\omega}\in\boldsymbol{\Omega}_3$, the rate pair $\left(\tilde{r}_1^{\mathcal{O}}, \tilde{r}_2^{\mathcal{O}}\right)$ is given as $\left(\log\frac{(h_1+h_2)(1+P)}{h_2 2^{-C_{12}}+h_1 2^{C_{21}}}, C_{21}\right)$. Based on Lemmas 10 and 11, we have

$$\begin{aligned}
\left.\frac{B^{\mathcal{O}}\left(\boldsymbol{\omega}\right)}{B^{\mathcal{A}}\left(\boldsymbol{\omega}\right)}\right|_{\boldsymbol{\omega}\in\boldsymbol{\Omega}_3} &< \frac{NT\left(\mu_1\log\left(\frac{(h_1+h_2)\left(1+h_1\left(\sum_{n=1}^{N}E_n\right)/(NT)\right)}{h_2 2^{-C_{12}}+h_1 2^{C_{21}}}\right)+\mu_2 C_{21}\right)}{\mu_2\sum_{n=1}^{N}T\log\left(1+h_2\frac{E_n}{T}\right)} \\
&< k_2\left(\frac{NT\left(\mu_1\log\frac{h_1+h_2}{h_2 2^{-C_{12}}+h_1 2^{C_{21}}}+\mu_2 C_{21}\right)}{\mu_2\sum_{n=1}^{N}E_n}+\frac{NT\mu_1 C\left(h_1\frac{\sum_{n=1}^{N}E_n}{NT}\right)}{\mu_2\sum_{n=1}^{N}E_n}\right) \\
&< k_2\left(\frac{\mu_1\log\frac{h_1+h_2}{h_2 2^{-C_{12}}+h_1 2^{C_{21}}}+\mu_2 C_{21}}{\mu_2 g(C_{12},C_{21})}+\frac{\mu_1 h_1}{\mu_2\ln 2}\right).
\end{aligned} \tag{6.31}$$

Since (6.31) applies to an arbitrary $\boldsymbol{\omega}\in\boldsymbol{\Omega}_3$, it can be concluded that

$$\max_{\boldsymbol{\omega}\in\boldsymbol{\Omega}_3}\frac{B^{\mathcal{O}}\left(\boldsymbol{\omega}\right)}{B^{\mathcal{A}}\left(\boldsymbol{\omega}\right)} < k_2\left(\frac{\mu_1\log\frac{h_1+h_2}{h_2 2^{-C_{12}}+h_1 2^{C_{21}}}+\mu_2 C_{21}}{\mu_2 g(C_{12},C_{21})}+\frac{\mu_1 h_1}{\mu_2\ln 2}\right). \tag{6.32}$$

iv. For an arbitrary input sequence $\boldsymbol{\omega}\in\boldsymbol{\Omega}_4$, the rate pair $\left(\tilde{r}_1^{\mathcal{O}}, \tilde{r}_2^{\mathcal{O}}\right)$ is given as

$\left(R_1, \log \frac{\left(1+h_2\tilde{P}^{\mathcal{O}}\right)h_1(\mu_2-\mu_1)2^{C_{21}}}{\mu_2(h_1-h_2)}\right)$. Based on Lemmas 10 and 11, we have

$$\begin{aligned}\left.\frac{B^{\mathcal{O}}(\boldsymbol{\omega})}{B^{\mathcal{A}}(\boldsymbol{\omega})}\right|_{\boldsymbol{\omega}\in\boldsymbol{\Omega}_4} &< \frac{NT\left(\mu_1 R_1+\mu_2\log\frac{\left(h_2\frac{\sum_{n=1}^{N}E_n}{NT}+1\right)h_1(\mu_2-\mu_1)2^{C_{21}}}{\mu_2(h_1-h_2)}\right)}{\mu_2\sum_{n=1}^{N}T\log\left(1+h_2\frac{E_n}{T}\right)}\\ &< k_2\left(\frac{\mu_2\log\frac{h_1(\mu_2-\mu_1)2^{C_{21}}}{\mu_2(h_1-h_2)}+\mu_1R_1}{\mu_2 g\left(R_1,C_{21}\right)}+\frac{h_2}{\ln 2}\right). \qquad (6.33)\end{aligned}$$

Since (6.33) applies to an arbitrary $\boldsymbol{\omega}\in\boldsymbol{\Omega}_4$, it can be concluded that

$$\max_{\boldsymbol{\omega}\in\boldsymbol{\Omega}_4}\frac{B^{\mathcal{O}}(\boldsymbol{\omega})}{B^{\mathcal{A}}(\boldsymbol{\omega})} < k_2\left(\frac{\mu_2\log\frac{h_1(\mu_2-\mu_1)2^{C_{21}}}{\mu_2(h_1-h_2)}+\mu_1R_1}{\mu_2 g\left(R_1,C_{21}\right)}+\frac{h_2}{\ln 2}\right). \qquad (6.34)$$

Since $\boldsymbol{\Omega}_1\cup\boldsymbol{\Omega}_2\cup\boldsymbol{\Omega}_3\cup\boldsymbol{\Omega}_4=\boldsymbol{\Omega}$, from (6.29), (6.30), (6.32) and (6.34) we have

$$\begin{aligned}\rho_3 &\triangleq k_2\max\left\{\begin{array}{l}(h_1+h_2)/\ln 2\\ (h_1+h_2)\left(\frac{(\mu_2-\mu_1)C_{21}}{\mu_2\left(2^{C_{21}}-1\right)}+\frac{\mu_1}{\mu_2\ln 2}\right)\\ \frac{\mu_1\log\frac{h_1+h_2}{h_2 2^{-C_{12}}+h_1 2^{C_{21}}}+\mu_2C_{21}}{\mu_2 g(C_{12},C_{21})}+\frac{\mu_1 h_1}{\mu_2\ln 2}\\ \frac{\mu_2\log\frac{h_1(\mu_2-\mu_1)2^{C_{21}}}{\mu_2(h_1-h_2)}+\mu_1R_1}{\mu_2 g(R_1,C_{21})}+\frac{h_2}{\ln 2}\end{array}\right\}\\ &> \max\left\{\max_{\boldsymbol{\omega}\in\boldsymbol{\Omega}_1}\frac{B^{\mathcal{O}}(\boldsymbol{\omega})}{B^{\mathcal{A}}(\boldsymbol{\omega})},\max_{\boldsymbol{\omega}\in\boldsymbol{\Omega}_2}\frac{B^{\mathcal{O}}(\boldsymbol{\omega})}{B^{\mathcal{A}}(\boldsymbol{\omega})},\max_{\boldsymbol{\omega}\in\boldsymbol{\Omega}_3}\frac{B^{\mathcal{O}}(\boldsymbol{\omega})}{B^{\mathcal{A}}(\boldsymbol{\omega})},\max_{\boldsymbol{\omega}\in\boldsymbol{\Omega}_4}\frac{B^{\mathcal{O}}(\boldsymbol{\omega})}{B^{\mathcal{A}}(\boldsymbol{\omega})}\right\}\\ &= \max_{\boldsymbol{\omega}\in\boldsymbol{\Omega}}\frac{B^{\mathcal{O}}(\boldsymbol{\omega})}{B^{\mathcal{A}}(\boldsymbol{\omega})}. \qquad (6.35)\end{aligned}$$

Based on the definition of competitive ratio (6.3), it is proved that $\mathcal{A}$ is ρ_3-compeititve for this case.

2. If $h_1=h_2$, as indicated by (5.53), the capping rate R_1 satisfies $0\le R_1\le C_{12}$. The set $\boldsymbol{\Omega}$ is partitioned into three subsets similar as those in case 1) for $h_1>h_2$.

□

Remark 12. *The competitive ratios given in Proposition 14∼16 also hold for the case of finite battery capacity if we truncate $E_{\max}$ at $\mathcal{E}$ (which is equivalent to truncating E_n, $n = 1, \cdots, N$, at $\mathcal{E}$). This can be easily verified by the fact that given any input sequence (truncated at $\mathcal{E}$), the profit achieved by the optimal offline scheme is upper-bounded by that achieved for the case of infinite battery capacity, whereas the profit achieved by the greedy scheme is the same as that for the case of infinite battery capacity.*

6.4.3 A Numerical Example

We adopt $h_1 = 0.8$, $h_2 = 0.7$, $C_{12} = 0.5$ bits/s/Hz, $C_{21} = 0.4$ bits/s/Hz, $N = 15$, $E_{\max} = 20$ J, and $T = 10$ s. The competitive ratios of the online greedy scheme against the optimal offline scheme with different $\mu_1 \in [0, 1]$ are plotted in Fig. 6.5. In Fig. 6.5, the ratios between the profits for the optimal offline scheme $\mathcal{O}$ and the online greedy scheme $\mathcal{A}$ for serving energy input sequences $\boldsymbol{\omega}_1$ and $\boldsymbol{\omega}_2$, respectively, are also plotted with infinite battery capacity[2], where $\boldsymbol{\omega}_1$ and $\boldsymbol{\omega}_2$ are given as

$$\boldsymbol{\omega}_1 = (20, 17.3, 16, 16, 14.7, 16, 10.7, 4, 5.3, 2.7, 10, 13.3, 17.3, 18, 18.7) \text{ J},$$

and

$$\boldsymbol{\omega}_2 = (20, 0, 0, 0, 0, 0, 0, 0, 0, 0, 0, 0, 0, 0, 0) \text{ J}.$$

With $\boldsymbol{\omega}_1$, the performance of the greedy scheme is close to that of the optimal offline ones. However, we may encounter some "malicious" input sequence, like $\boldsymbol{\omega}_2$, with which the performance of the greedy scheme can be significantly worse than that of the optimal offline schemes. Given $\boldsymbol{\omega}_2$, the optimal offline scheme spends the 20 J energy, which is available at the beginning of the first slot, uniformly over all 15 slots (it is easy to check

[2]For the case of finite battery capacity, the only difference is that the ratio with ω_1 will be slightly smaller.

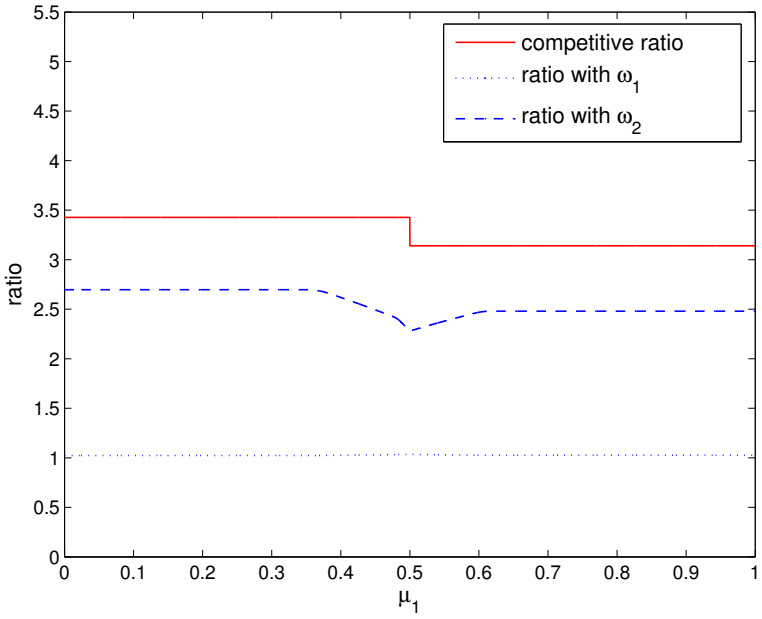

Figure 6.5: The competitive ratios and the ratios obtained with energy input sequence $\boldsymbol{\omega}_1$ and $\boldsymbol{\omega}_2$ in the Gaussian MAC with conferencing links and a shared energy harvester.

such power allocation holds for both infinite and finite battery cases), whereas the greedy scheme depletes all the 20 J energy in the first slot. Note that the sudden change of the competitive ratio is due to the discontinuity in the profit function of $\tilde{\mathcal{A}}$ at $\mu_1 = 0.5$. As expected, $\boldsymbol{\omega}_1$ results in ratios close to 1 whereas $\boldsymbol{\omega}_2$ results in relatively large ratios, i.e., around 2.5, due to the fact that the power profiles given by the optimal offline and the greedy schemes are dramatically different. The competitive ratio, which serves as the theoretical upper bound of the ratios given any possible input sequence, is larger than the ratios with both $\boldsymbol{\omega}_1$ and $\boldsymbol{\omega}_2$.

6.5 Summary

In this chapter, the performance of several online schemes for the Gaussian MAC with conferencing links and a shared renewable energy source was studied . First, their per-

formance in terms of average weighted sum throughput achieved given some statistical energy harvesting process was compared. The simulation results showed that the performance of the on-off scheme is influenced by the accuracy of its estimation of the mean energy arrival amount. Also, the greedy scheme is recognized to enjoy robustness against the estimation error of the energy arrival process statistics and the battery capacity limitation compared to other schemes. Then, the worst case performance of the greedy scheme against the optimal offline scheme was investigated by deriving its competitive ratios, which are the maximum ratio between the profits obtained by the offline and online schemes over arbitrary energy arrival profiles.

Chapter 7

Conclusions and Future Work

7.1 Conclusions

This thesis focuses on the resource allocation schemes for multiuser wireless communication systems powered by renewable energy sources. Both offline schemes and online schemes, which rely on non-causal and causal information about the EH processes, respectively, have been investigated for two system models: 1) the traditional two-user Gaussian MAC; and 2) the two-user Gaussian MAC with conferencing links. The main achievements and insights are summarised as follows.

In Chapter 3, the optimal offline resource allocation schemes were studied for the traditional two-user Gaussian MAC where the two transmitters share a common EH source, aiming at maximising the weighted sum throughput per unit spectrum over a finite time horizon. Both the infinite and finite battery capacity cases were considered. By exploiting the convexity of the problem, the structural properties of the optimal sum power allocation were revealed for both cases, based on which the optimal sum power profiles could be obtained. Then, the optimal power/rate allocation were derived. It was proved that there exists a capping rate at the stronger transmitter: 1) if the sum power is not enough to support the capping rate at the stronger transmitter, all power is

allocated to the stronger transmitter; 2) otherwise, the sum power is allocated to the two transmitters such that the rate of the stronger one equals the capping rate. Moreover, it is shown that the MAC with a shared energy harvester and its dual BC achieve the same maximum departure region.

In Chapter 4, three online schemes for the traditional two-user Gaussian MAC where the two transmitters share a common EH source were studied. First, simulation results showed the performances of the online schemes in terms of average weighted sum throughput achieved under some given statistical EH process. It was revealed that the estimation accuracy influences the performance of online schemes which rely on partial statistical information. Moreover, the greedy scheme, which always consume up all available energy in each slot to maximise the short-term throughput, was recognised to have robustness against estimation error and the battery capacity limitation compared to other schemes. To comprehensively measure the utility of the greedy scheme, competitive analysis was used to quantify its worst-case performance against the optimal offline scheme. To this end, the competitive ratios, i.e., the maximum ratio between the profits obtained by the offline and the greedy schemes over all possible energy input sequences, were derived.

In Chapter 5, the optimal offline resource allocation schemes that maximise the weighted sum throughput in the two-user Gaussian MAC were investigated, where the two transmitters could talk to each other via wired rate-limited channels. First, the optimal sum power profiles for both the infinite and finite battery capacity cases were obtained based on the structural properties revealed in Chapter 3. Then, the rate allocation between the two transmitters was studied. It was shown that there exists a maximum transmission rate (named the capping rate) for one of the transmitters, depending on the weighting factors and system parameters.

In Chapter 6, the performance of three online schemes for the Gaussian MAC with conferencing links and a shared renewable energy source were studied. First, their performance in terms of average weighted sum throughput achieved given some statistical energy harvesting process were compared by simulation results. To further measure the

utility of the greedy scheme, which was considered to enjoy robustness against estimation error and the battery capacity limitation compared to other schemes, its competitive ratios were derived under various weighting factors, which provide the theoretical worst-case performance bound.

7.2 Future Work

In this section, extensions to current work and some future research directions are proposed.

7.2.1 Extension to Current Work

In this thesis, the resource allocation schemes for both the traditional MAC and the MAC with conferencing links were considered. In particular, for both cases, it is assumed that the channel gains are constant, which can be applied to the practical scenario where the locations and the wireless medium between the transmitters and the receiver are relatively fixed. However, in more general scenarios, the channel gains may change during the transmission period. Therefore, new resource allocation schemes designed for fading MAC may be needed. With varying channel gains, the optimal sum power allocation needs to be revised since the convexity approach is no longer valid. One possible alternative is to analysing the KKT conditions of the revised problem to unveil possible structural properties.

Moreover, in this thesis, it is assumed that the data queue for transmitters are always ready before transmissions start. In future work, it could be assumed that the data for transmitters arrives during the transmissions. The resource allocation schemes thus need to be redesigned correspondingly.

7.2.2 Threshold-Based Online Schemes

In this thesis, we mostly focused on the development of the optimal offline schemes and the performance measurement of some simple-to-implement online schemes. In practical applications, smarter online schemes are obviously highly demanding and rewarding research directions. In [HZZC13], the authors investigated the resource allocation problem in a large relay network and proposed threshold-based "save-then-transmit" best effort schemes which have low computational complexity. In these schemes, each transmitter only transmits (with all available energy) when both the forward and backward link channel gains are above certain thresholds simultaneously. Another threshold-based scheduling scheme was studied in [LHCZ14], which considered an adhoc network that contains multiple EH powered transmitter-receiver pairs. Our future work could consider the following topics.

7.2.2.1 Threshold-based constant power transmission scheme in a large relay network

As an extension to the work [HZZC13], instead of the best effort transmission scheme, a threshold-based constant power transmission scheme in a large relay network could be considered. In this scheme, when both the forward and backward link channel gain thresholds are satisfied, the transmitter transmit with a constant power level. Similar to [HZZC13], the battery dynamics of the network could be modeled as a Markov process. The optimal transmission schemes could be obtained by maximising the average throughput at the stationary state of the Markov transmission process. Different from [HZZC13], where the channel gain thresholds are the only optimisation variables, the constant power level also needs to be optimised in the constant power transmission scheme.

7.2.2.2 Threshold-based transmission schemes in a multiple access channel

The threshold-based transmission schemes in a multiple access channel also worth investigating. It is worth noting that the achievable rate for a transmitter in a MAC is influenced by the transmission status of both transmitters since when the receiver decoding the received signal, the signal of one transmitter is treated as interference to the other one. Therefore, the thresholds should be set in the form of achievable rate, instead of channel gains. As a result, the transmission decision of each transmitter depends not only on its own energy and channel status but also the other one's status. Consequently, the battery dynamics of the two transmitters are coupled together. How to analyse the stationary state of the coupled Markov transmission process and find the optimised thresholds are challenging problems. Both the best effort and the constant power transmission schemes worth investigating for this scenario.

Appendix A

Proof of Remark 7

It is obvious that the objective function and the constraints (5.2)-(5.4) are convex, so are the last four constraints. Define $f_1\left(P_1^p, P_2^p, P_1^c, P_2^c\right) = 2^{r_1+r_2} - 1 - h_1 P_1^p - h_1 P_1^c - h_2 P_2^p - h_2 P_2^c - 2\sqrt{h_1 P_1^c h_2 P_2^c}$, the constraint (5.5) can be rewritten as $f_1\left(P_1^p, P_2^p, P_1^c, P_2^c\right) \leq 0$. Now we prove the convexity of $f_1\left(P_1^p, P_2^p, P_1^c, P_2^c\right)$ over $\left(P_1^p, P_1^c, P_2^p, P_2^c\right)$ by the definition of convex function. Let (x_1, y_1, z_1, w_1) and (x_2, y_2, z_2, w_2) be two points in the domain of $f_1\left(P_1^p, P_2^p, P_1^c, P_2^c\right)$. Given any $\theta \in [0, 1]$, let $(\hat{x}, \hat{y}, \hat{z}, \hat{w}) = \theta\left(x_1, y_1, z_1, w_1\right) + (1-\theta)\left(x_2, y_2, z_2, w_2\right) = (\theta x_1 + (1-\theta) x_2, \theta y_1 + (1-\theta) y_2, \theta z_1 + (1-\theta) z_2, \theta w_1 + (1-\theta) w_2)$,

we have

$$
\begin{aligned}
&\theta f_1(x_1,y_1,z_1,w_1)+(1-\theta)f_1(x_2,y_2,z_2,w_2)-f_1(\hat{x},\hat{y},\hat{z},\hat{w})\\
=&\theta\left(2^{r_1+r_2}-1-h_1x_1-h_1y_1-h_2z_1-h_2w_1-2\sqrt{h_1h_2z_1w_1}\right)\\
&+(1-\theta)\left(2^{r_1+r_2}-1-h_1x_2-h_1y_2-h_2z_2-h_2w_2-2\sqrt{h_1h_2z_2w_2}\right)\\
&-\left(2^{r_1+r_2}-1-h_1\bar{x}-h_1\bar{y}-h_2\bar{z}-h_2\bar{w}-2\sqrt{h_1h_2\bar{z}\bar{w}}\right)\\
=&2\sqrt{h_1h_2}\left(\sqrt{(\theta z_1+(1-\theta)z_2)(\theta w_1+(1-\theta)w_2)}-\theta\sqrt{z_1w_1}-(1-\theta)\sqrt{z_2w_2}\right)\\
=&2\sqrt{h_1h_2}\begin{pmatrix}\sqrt{\left(\theta\sqrt{w_1z_1}\right)^2+\left((1-\theta)\sqrt{w_2z_2}\right)^2+(1-\theta)\theta w_2z_1+\theta(1-\theta)w_1z_2}\\-\theta\sqrt{z_1w_1}-(1-\theta)\sqrt{z_2w_2}\end{pmatrix}\\
=&2\sqrt{h_1h_2}\begin{pmatrix}\sqrt{\left(\theta\sqrt{w_1z_1}+(1-\theta)\sqrt{w_2z_2}\right)^2+(1-\theta)\theta\left(w_2z_1-2\sqrt{w_1z_1}\sqrt{w_2z_2}+w_1z_2\right)}\\-\theta\sqrt{z_1w_1}-(1-\theta)\sqrt{z_2w_2}\end{pmatrix}\\
=&2\sqrt{h_1h_2}\begin{pmatrix}\sqrt{\left(\theta\sqrt{w_1z_1}+(1-\theta)\sqrt{w_2z_2}\right)^2+(1-\theta)\theta\left(\sqrt{w_2z_1}-\sqrt{w_1z_2}\right)^2}\\-\theta\sqrt{z_1w_1}-(1-\theta)\sqrt{z_2w_2}\end{pmatrix}\\
\geq&2\sqrt{h_1h_2}\left(\theta\sqrt{w_1z_1}+(1-\theta)\sqrt{w_2z_2}-\theta\sqrt{z_1w_1}-(1-\theta)\sqrt{z_2w_2}\right)=0.
\end{aligned}
$$

That is, $f_1(\hat{x},\hat{y},\hat{z},\hat{w}) \leq \theta f_1(x_1,y_1,z_1,w_1)+(1-\theta)f_1(x_2,y_2,z_2,w_2)$ for any $\theta\in[0,1]$. Therefore, we can say $f_1(P_1^p,P_2^p,P_1^c,P_2^c)$ is convex over $(P_1^p,P_1^c,P_2^p,P_2^c)$. Hence, the Problem (P4.1) is a convex optimization problem.

Note that however, the first order partial derivatives of $f_1(P_1^p,P_2^p,P_1^c,P_2^c)$ is given as $\nabla f_1(P_1^p,P_2^p,P_1^c,P_2^c) = \left\{-h_1,-h_2,-\frac{P_1^ch_1+\sqrt{P_2^cP_1^ch_1h_2}}{P_1^c},-\frac{P_2^ch_2+\sqrt{P_2^cP_1^ch_1h_2}}{P_2^c}\right\}$, which does not exist at the point where $P_1^c=0$ or $P_2^c=0$.

References

[AUBE11] M. A. Antepli, E. Uysal-Biyikoglu, and H. Erkal. Optimal packet scheduling on an energy harvesting broadcast link. *IEEE J. Sel. Areas Commun.*,

29(8):1721–1731, Sep. 2011.

[BEY98] A Borodin and R El-Yaniv. *Online computation and competitive analysis.* Cambridge University Press, New York, NY, USA, 1998.

[BLW08] S.I. Bross, A. Lapidoth, and M.A. Wigger. The Gaussian MAC with conferencing encoders. In *Proc. Int. Symp. Inf. Theory*, Jul. 2008.

[BLW12] S.I. Bross, A. Lapidoth, and M.A. Wigger. Dirty-paper coding for the Gaussian multiaccess channel with conferencing. *IEEE Trans. Inf. Theory*, 58(9), Sept 2012.

[BV04] S. Boyd and L. Vandenberghe. *Convex Optimization.* Cambridge University Press, UK, 2004.

[CSSJ14] S. Chen, P. Sinha, N.B. Shroff, and C. Joo. A simple asymptotically optimal joint energy allocation and routing scheme in rechargeable sensor networks. *IEEE/ACM Trans. Netw.*, 22(4):1325–1336, Aug. 2014.

[CT06] Thomas M. Cover and Joy A. Thomas. *Elements of Information Theory (Wiley Series in Telecommunications and Signal Processing).* Wiley-Interscience, 2006.

[DPEP14] Z. Ding, S.M. Perlaza, I. Esnaola, and H.V. Poor. Power allocation strategies in energy harvesting wireless cooperative networks. *IEEE Tran. Wireless Commun.*, 13(2):846–860, Feb. 2014.

[DZN+15] Z. Ding, C. Zhong, D.W.K. Ng, M. Peng, H.A. Suraweera, R. Schober, and H.V. Poor. Application of smart antenna technologies in simultaneous wireless information and power transfer. *IEEE Commun. Mag.*, 53(4):86–93, Apr. 2015.

[EKM11] M. Erol-Kantarci and H. T. Mouftah. Wireless multimedia sensor and actor networks for the next generation power grid. *Ad Hoc Netw.*, 9(4):542 – 551, Jun. 2011.

[GOJU12] B. Gurakan, O. Ozel, Y. Jing, and S. Ulukus. Two-way and multiple-access energy harvesting systems with energy cooperation. In *Conf. Rec. 46th Asilomar Signals, Syst. Comput.*, pages 58–62, Nov. 2012.

[GOJU13a] B. Gurakan, O. Ozel, Y. Jing, and S. Ulukus. Energy cooperation in energy

harvesting communications. *IEEE Trans. Commun.*, 61(12):4884–4898, Dec. 2013.

[GOJU13b] B. Gurakan, O. Ozel, Y. Jing, and S. Ulukus. Energy cooperation in energy harvesting two-way communications. In *Proc. IEEE ICC*, pages 3126–3130, Jun. 2013.

[GP13] M. Gregori and M. Payaró. Energy-efficient transmission for wireless energy harvesting nodes. *IEEE Trans. Wireless Commun.*, 12(3):1244–1254, Mar. 2013.

[HZ12] C. K. Ho and R. Zhang. Optimal energy allocation for wireless communications with energy harvesting constraints. *IEEE Trans. Sig. Process.*, 60(9):4808–4818, Sep. 2012.

[HZC13] C. Huang, R. Zhang, and S. Cui. Throughput maximization for the Gaussian relay channel with energy harvesting constraints. *IEEE J. Sel. Areas Commun.*, 31(8):1469–1479, Aug. 2013.

[HZZC13] C. Huang, J. Zhang, P. Zhang, and S Cui. Threshold-based transmissions for large relay networks powered by renewable energy. In *Proc. IEEE GLOBECOM*, pages 1921–1926, Dec 2013.

[IGMH05] I.A. Ieropoulos, J. Greenman, C. Melhuish, and J. Hart. Comparative study of three types of microbial fuel cell. *Enzyme and Microbial Technol.*, 37(2):238–245, 2005.

[ISPS12] F. Iannello, O. Simeone, P. Popovski, and U. Spagnolini. Energy group-based dynamic framed aloha for wireless networks with energy harvesting. In *Proc. 46th Annu. Conf. CISS*, pages 1–6, Mar. 2012.

[ISS10] F. Iannello, O. Simeone, and U. Spagnolini. Dynamic framed-aloha for energy-constrained wireless sensor networks with energy harvesting. In *Proc. IEEE Globecom*, pages 1–6, Dec. 2010.

[ISS12] F. Iannello, O. Simeone, and U. Spagnolini. Medium access control protocols for wireless sensor networks with energy harvesting. *IEEE Trans. Commun.*, 60(5):1381–1389, May 2012.

[JSMK09] V. Joseph, V. Sharma, U. Mukherji, and M. Kashyap. Joint power control,

scheduling and routing for multicast in multihop energy harvesting sensor networks. In *Proc. ICUMT*, pages 1–8, Oct. 2009.

[JVG04] N. Jindal, S. Vishwanath, and A. Goldsmith. On the duality of gaussian multiple-access and broadcast channels. *IEEE Trans. Inf. Theory*, 50(5):768–783, May 2004.

[KU06] O. Kaya and Sennur Ulukus. Achieving the capacity region boundary of fading cdma channels via generalized iterative waterfilling. *IEEE Trans. Wireless Commun.*, 5(11):3215–3223, Nov. 2006.

[LHCZ14] H. Li, C. Huang, S. Cui, and J. Zhang. Distributed opportunistic scheduling for wireless networks powered by renewable energy sources. In *Prof. IEEE INFOCOM*, pages 898–906, Apri. 2014.

[LSS07] L. Lin, N.B. Shroff, and R. Srikant. Asymptotically optimal energy-aware routing for multihop wireless networks with renewable energy sources. *IEEE/ACM Trans. Netw.*, 15(5):1021–1034, Oct. 2007.

[LZC13] L. Liu, R. Zhang, and K.C. Chua. Wireless information transfer with opportunistic energy harvesting. *IEEE Trans. Wireless Commun.*, 12(1):288–300, Jan. 2013.

[LZL13] Y. Luo, J. Zhang, and K.B. Letaief. Optimal scheduling and power allocation for two-hop energy harvesting communication systems. *IEEE Trans. Wireless Commun.*, 12(9):4729–4741, Sep. 2013.

[MSPC12] D. Miorandi, S. Sicari, F. D. Pellegrini, and I. Chlamtac. Survey internet of things: Vision, applications and research challenges. *Ad Hoc Netw.*, 10(7):1497 – 1516, Sep. 2012.

[MYK07] I Maric, R.D. Yates, and G. Kramer. Capacity of interference channels with partial transmitter cooperation. *IEEE Trans. Inf. Theory*, 53(10):3536–3548, Oct 2007.

[OE13] O. Orhan and E. Erkip. Throughput maximization for energy harvesting two-hop networks. In *Proc. Int. Symp. Inf. Theory*, Jul. 2013.

[OTY+11] O. Ozel, K. Tutuncuoglu, J. Yang, S. Ulukus, and A. Yener. Transmission with energy harvesting nodes in fading wireless channels: Optimal policies.

IEEE J. Sel. Areas Commun., 29(8):1732–1743, Sep. 2011.

[OYU12a] O. Ozel, J. Yang, and S. Ulukus. Optimal broadcast scheduling for an energy harvesting rechargeable transmitter with a finite capacity battery. *IEEE Trans. Wireless Commun.*, 11(6):2193–2203, Jun. 2012.

[OYU12b] O. Ozel, J. Yang, and S. Ulukus. Optimal broadcast scheduling for an energy harvesting rechargeable transmitter with a finite capacity battery. *IEEE Trans. Wireless Commun.*, 11(6):2193–2203, 2012.

[OYU13] O. Ozel, J. Yang, and S. Ulukus. Optimal transmission schemes for parallel and fading gaussian broadcast channels with an energy harvesting rechargeable transmitter. *Comput. Commun.*, 36(12):1360–1372, 2013.

[PC13] J. Park and B. Clerckx. Joint wireless information and energy transfer in a two-user mimo interference channel. *IEEE Trans. Wireless Commun.*, 12(8):4210–4221, Aug. 2013.

[PFS13] P. Popovski, A.M. Fouladgar, and O. Simeone. Interactive joint transfer of energy and information. *IEEE Trans. Commun.*,, 61(5):2086–2097, May 2013.

[PS05] J.A. Paradiso and T. Starner. Energy scavenging for mobile and wireless electronics. *IEEE Pervasive Comput.*, 4(1):18–27, 2005.

[RAS+00] J. Rabaey, M.J. Ammer, J.L. Silva, D. Patel, and S. Roundy. Picoradio supports ad hoc ultra-low power wireless networking. *IEEE Comput.*, 33(7):42–48, 2000.

[Rou03] S. Roundy. *Energy scavenging for wireless sensor nodes with a focus on vibration to electricity conversion.* PhD thesis, University of California, Berkeley, 2003.

[SET09] W.K.-G. Seah, Zhi Ang Eu, and H. Tan. Wireless sensor networks powered by ambient energy harvesting (wsn-heap) - survey and challenges. In *Wireless Communication, Vehicular Technology, Information Theory and Aerospace Electronic Systems Technology, 2009. Wireless VITAE 2009. 1st International Conference on*, pages 1–5, 2009.

[SGP+09] O. Simeone, D. Gunduz, H.V. Poor, AJ. Goldsmith, and S. Shamai. Com-

pound multiple-access channels with partial cooperation. *IEEE Trans. Inf. Theory*, 55(6):2425–2441, June 2009.

[SK11] S. Sudevalayam and P. Kulkarni. Energy harvesting sensor nodes: Survey and implications. *IEEE Commun. Surveys Tuts.*, 13(3):443–461, 2011.

[SS12] B.R. Singh and O. Singh. *Global trends of fossil fuel reserves and climate change in the 21st century.* INTECH Open Access Publisher, 2012.

[ST08] S. Shahriar and E. TOPAL. An overview of fossil fuel reserve depletion time. In *31st IAEE International Conference*, pages 315–316, 2008.

[ST09] S. Shahriar and E. TOPAL. When will fossil fuel reserves be diminished? *Energy Policy*, 37(1):181 – 189, 2009.

[Top04] F Topsøe. Some bounds for the logarithmic function. *RGMIA Res. Rep. Collection*, 7(2), Article 6, 2004.

[TY12a] K. Tutuncuoglu and A. Yener. Optimum transmission policies for battery limited energy harvesting nodes. *IEEE Trans. Wireless Commun.*, 11(3):1180–1189, Mar. 2012.

[TY12b] K. Tutuncuoglu and A. Yener. Sum-rate optimal power policies for energy harvesting transmitters in an interference channel. *J. Commun. and Networks*, 14(2):151–161, Apr. 2012.

[TY13] K. Tutuncuoglu and A. Yener. Cooperative energy harvesting communications with relaying and energy sharing. In *Proc. IEEE ITW*, pages 1–5, Sep. 2013.

[Wil83] Frans M. J. Willems. The discrete memoryless multiple access channel with partially cooperating encoders. *IEEE Trans. Inf. Theory*, 29(3):441–445, May 1983.

[YOU12] J. Yang, O. Ozel, and S. Ulukus. Broadcasting with an energy harvesting rechargeable transmitter. *IEEE Trans. Wireless Commun.*, 11(2):571–583, Feb. 2012.

[YU12a] J. Yang and S. Ulukus. Optimal packet scheduling in a multiple access channel with energy harvesting transmitters. *J. Commun. and Networks*, 14(2):140–150, Apr. 2012.

[YU12b] J. Yang and S. Ulukus. Optimal packet scheduling in an energy harvesting communication system. *IEEE Trans. Commun.*, 60(1):220–230, Jan. 2012.

[ZZH13] X. Zhou, R. Zhang, and C.K. Ho. Wireless information and power transfer: Architecture design and rate-energy tradeoff. *IEEE Trans. Commun.*, 61(11):4754–4767, Nov. 2013.